DOE/NASA/0048-79/1
NASA CR-159756
TSC 10082-FR

ASSESSMENT AND PRELIMINARY DESIGN OF AN ENERGY BUFFER FOR REGENERATIVE BRAKING IN ELECTRIC VEHICLES

R. Buchholz
A. Mathur
Technology Strategy Center
Honeywell Inc.

December 1979

Prepared for
NATIONAL AERONAUTICS AND SPACE ADMINISTRATION
Lewis Research Center
Under Contract DEN 3-48

for
U.S. DEPARTMENT OF ENERGY
Conservation and Solar Energy
Office of Transportation Programs

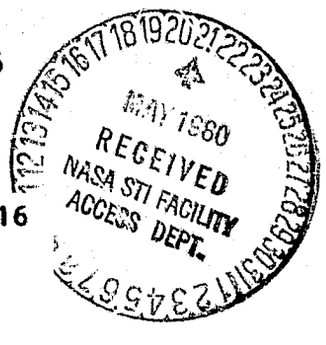

NOTICE

DOE/NASA/0048-79/1
NASA CR-159756
TSC 10082-FR

ASSESSMENT AND PRELIMINARY DESIGN OF AN ENERGY BUFFER FOR REGENERATIVE BRAKING IN ELECTRIC VEHICLES

R. BUCHHOLZ
A. MATHUR
HONEYWELL INC.
TECHNOLOGY STRATEGY CENTER
ST. PAUL, MINNESOTA 55113

DECEMBER 1979

PREPARED FOR
NATIONAL AERONAUTICS & SPACE ADMINISTRATION
LEWIS RESEARCH CENTER
CLEVELAND, OHIO 44135
UNDER CONTRACT DEN3-48

FOR
U.S. DEPARTMENT OF ENERGY
CONSERVATION AND SOLAR ENERGY
OFFICE OF TRANSPORTATION PROGRAMS
WASHINGTON, DC 20545
UNDER INTERAGENCY AGREEMENT EC-77-31-1044

TABLE OF CONTENTS

LIST OF FIGURES

LIST OF FIGURES.-Continued.

LIST OF FIGURES.-Continued.

LIST OF FIGURES.-Concluded.

LIST OF TABLES

LIST OF TABLES.-Continued.

LIST OF TABLES.-Concluded.

ASSESSMENT AND PRELIMINARY DESIGN OF AN ENERGY BUFFER FOR REGENERATIVE BRAKING IN ELECTRIC VEHICLES

Robert Buchholz and Anoop Mathur
Honeywell Inc.
Technology Strategy Center

SUMMARY

An energy buffer is a component within the electric vehicle able to absorb deceleration energy and later release it to provide the peaks of power required for acceleration, thereby resulting in improved vehicle performance and range under stop-and-go driving conditions. The original objectives of the program were to (1) provide an assessment of electric vehicle energy buffers with currently available state of the art, off-the-shelf components, and (2) design, fabricate, and test an engineering model of a selected buffer. The selected buffer was not to include flywheel or electrochemical concepts because of the extensive effort already being devoted to these concepts.

Based on the assessment and subsequent buffer tradeoff evaluation, a hydropneumatic (liquid and gas) buffer concept was recommended and selected for design. The significant components in this buffer are the hydropneumatic accumulator and hydraulic motor/pump. Vehicle energy to provide braking is stored compressing gas in the hydropneumatic accumulator with a hydraulic pump. Energy is provided during acceleration by discharging the stored energy in the accumulator through the hydraulic motor into the drive train.

Detailed analysis of this concept using actual manufacturer-supplied data for weights and efficiencies shows that this concept yields only a 5% improvement in range for the electric vehicle when using commercial, currently available motor/pumps and near-term-available (6 to 9 months) lightweight, fiber-wrapped accumulators. This improvement is over that obtainable with a straight electric vehicle.

Due to an unsatisfactory improvement in range with this concept, the design, fabrication, and test portion of the program was terminated. In its place, a hydraulic motor/pump and accumulator study and buffer design effort was conducted to define to what extent product development was necessary to improve the components sufficiently for a usable concept.

Results show that two motor/pump manufacturers plan to market lighter-weight, improved-performance units in 1980.

Also, lightweight fiber-wrapped pressure vessels can be readily developed.

A final performance analysis shows that the addition to the electric vehicle of the hydropneumatic buffer using these near-term components will result in a 19% improvement in range over a straight electric vehicle.

INTRODUCTION

The electric vehicle offers the potential to significantly shift the transportation energy base from petroleum to other energy sources. An electric vehicle which can bring to reality this potential benefit must overcome current battery limitations on capacity and discharge/charge characteristics. A properly designed energy buffer can improve electric vehicle performance and range by absorbing braking energy for use at times of acceleration, which reduces load demands on the battery pack and extends current battery limitations. A study of buffered automotive propulsion power systems (ref. 1) using hydraulic accumulators was conducted previously for the University of California, Lawrence Livermore Labs. That study resulted in the identification of energy storage requirements for SAE urban and suburban driving schedules, the analysis of accumulator sizing, material requirements and efficiency and the performance predictions for a preliminary buffered vehicle design.

The work described in this report was part of the Department of Energy programs for Electric and Hybrid Vehicles. The objective of this work was to determine to what extent energy buffers improve electric vehicle performance and range using commercially available state-of-the-art components.

The work reported consists of an engineering assessment of electric vehicle energy buffers, tradeoff analysis of those buffers including life cycles costs, a survey to determine the need and extent of buffer component development for near-term application, and a prediction of vehicle range and performance using these near-term-developed components.

Various energy buffer concepts were considered for a 1360-kg (3000-lb) electric vehicle using lead/acid batteries operated repeatedly over the SAE J227a Schedule D driving cycle. They were:

- Electric regeneration (lead/acid battery)
- Hydropneumatic (liquid/gas)
- Pneumatic (gas)

- Mechanical (springs)
- Momentum (flywheel)

For tradeoff purposes, all five concepts were considered initially. However, because significant development effort was already underway with electric regeneration using lead/acid batteries and flywheels, these two concepts were barred from being selected as the recommended buffer for final design analysis.

The hydropneumatic accumulator buffer concept was chosen as a result of the tradeoff and performance analyses. These analyses show a significant improvement in electric vehicle range when using this buffer concept using near-term developed components.

ENERGY BUFFER ASSESSMENT

The objective of this task was to provide an assessment of electric vehicle energy buffers using commercially available components with some refinement of the state of the art but no new applied research and technology. This was done by:

- Determining the requirements for an energy buffer capable of absorbing and delivering energy to a specified electric passenger vehicle operating over a specified SAE driving cycle.
- Identifying and assessing through a quantitative analytic evaluation potential energy buffers applicable to an electric vehicle.
- Developing tradeoff information for each energy buffer considered and evaluating that information with respect to overall improvement of vehicle performance, including initial and life-cycle costs.
- Recommending a buffer, excluding any kind of flywheel or electrochemical (battery) approach, to be designed and developed.
- Making a preliminary conceptual engineering model design.

The buffer requirements for regenerative braking in an electric vehicle are dependent on the vehicle characteristics and the driving cycle over which the vehicle is operated.

Vehicle Characteristics

The vehicle characteristics which determine the energy and power demand necessary to drive a vehicle through a specified cycle are that of mass, frontal area (aerodyramic drag), rolling resistance, and mechanical drive efficiency. These characteristics for the baseline electric vehicle used in the analysis are given in Table 1.

TABLE 1.-ELECTRIC VEHICLE CHARACTERISTICS

Characteristic	Value
Vehicle mass, kg (lb)	1360 (3000)
Frontal area, m^2 (ft^2)	1.8 (20)
Aerodynamic drag coefficient	0.300
Coefficient of rolling resistance	0.008
Mechanical drive efficiency	0.950

Vehicle masses vary as buffers are added and affect the power and energy demand of the vehicle. This in turn affects the energy buffer requirements. Thus, the actual size requirements of the buffer components must be determined by an iterative process in which buffer system component masses and efficiencies are taken into account. However, the analysis presented in this section provides baseline energy and power profiles for the straight electric vehicle as a first step in sizing the buffer components in the subsequent analysis.

Driving Cycle

The driving cycle (vehicle velocity versus time) used in the analysis is the D schedule of the SAE J227a electric vehicle test schedules shown in Figure 1 (ref. 2). The exact configuration of schedule D is shown in Figure 2. This schedule is acceleration to 72 km/h (45 mi/h) in 28 s, cruise for 50 s, coast for 10 s, decelerate in 9 s, and idle for 22 s. This basic driving cycle is used to determine the vehicle power requirements. Deceleration from 88 km/h (55 mi/h) is also shown in Figure 2 and is used later to determine buffer component maximum sizes. Constant acceleration and deceleration was assumed for ease of analytic computation.

J227a schedule		B	C	D
v	Cruise velocity	32 km/h (20 mi/h)	48 km/h (30 mi/h)	72 km/h (45 mi/h)
t	Total time	72 s	80 s	122 s
t_a	Accelerate	19 s	18 s	28 s
t_{cr}	Cruise	19 s	20 s	50 s
t_{co}	Coast	4 s	8 s	10 s
t_b	Brake	5 s	9 s	9 s
t_i	Idle	25 s	25 s	25 s

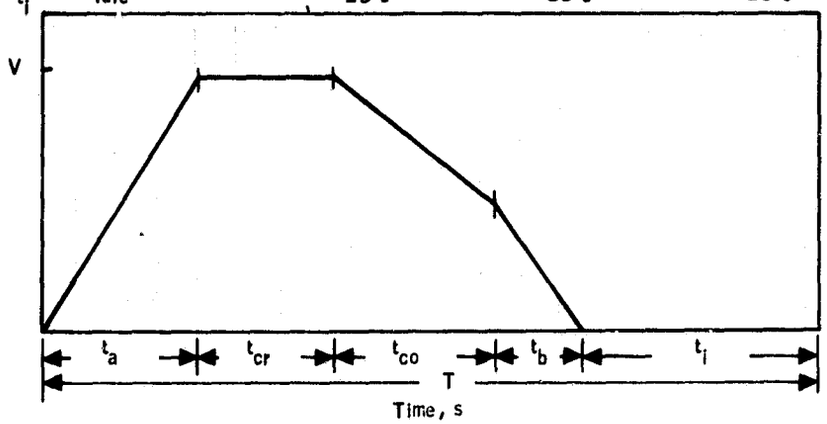

Figure 1.-SAE J227a electric vehicle test schedules B, C, and D.

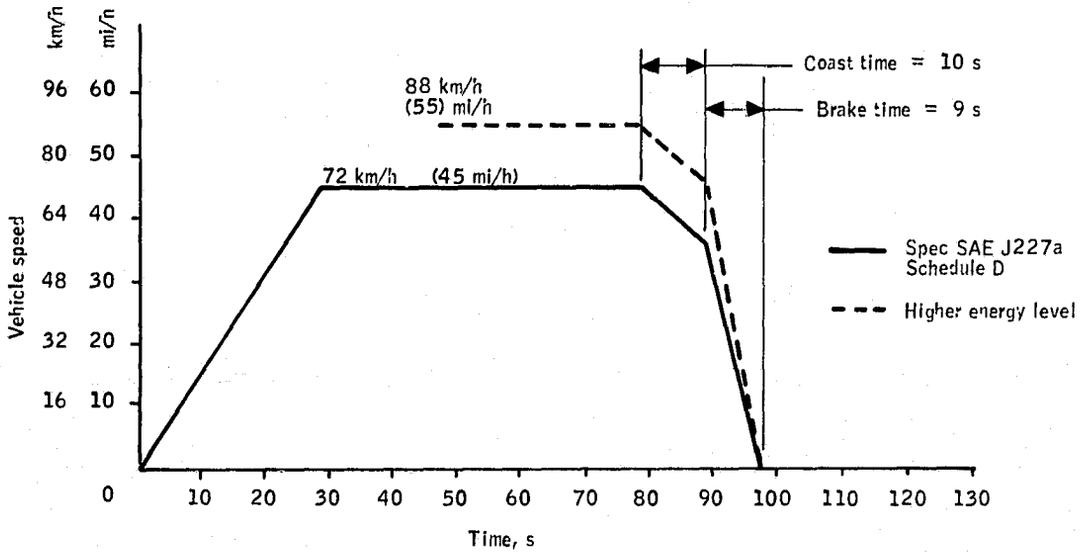

Figure 2.-Driving cycle - SAE J227a schedule D.

Power Analysis

Power demand of the electric vehicle over the J227a Schedule D driving cycle consists of four component elements: inertial power (P_i), rolling resistance power (P_r), aerodynamic drag power (P_d), and terrain gradient power (P_g). Because SAE J227a Schedule D is a level-road cycle, gradient effects are not included but the equations are included here for completeness. The total power (P_T) demand equation can be written as:

$$P_T = P_i + P_r + P_d + P_g \tag{1}$$

where

$$P_i = Mav \quad \text{(inertial power)} \tag{2}$$

$$P_r = R_r Mgv \quad \text{(rolling resistance power)} \tag{3}$$

$$P_d = \frac{1}{2} C_d \rho A v^3 \quad \text{(aerodynamic drag power)} \tag{4}$$

$$P_g = Mgv \sin \theta \quad \text{(terrain gradient power)} \tag{5}$$

where

- M = vehicle mass, kg
- a = vehicle acceleration, m/s^2
- R_r = rolling resistance factor
- C_d = aerodynamic drag coefficient
- ρ = air density, kg/m^3
- A = vehicle frontal area m^2
- v = vehicle velocity, m/s
- g = acceleration of gravity, m/s^2
- θ = road slope angle, deg

These equations are applied to the various segments of the driving cycle to calculate the instantaneous power and total energy that is required or is available at the wheels. The equations are:

$$P_a = P_i + P_r + P_d + P_g \quad \text{(for acceleration)} \tag{6}$$

$$P_{cr} = P_r + P_d \quad \text{(for cruise)} \tag{7}$$

$$P_{co} = 0 \qquad \text{(for coast)} \qquad (8)$$

$$P_b = P_i - P_r - P_d - P_g \qquad \text{(for brake)} \qquad (9)$$

$$P_i = 0 \qquad \text{(for idle)} \qquad (10)$$

Substituting Equations (2) through (5) into Equations (6) through (10) results in the power demand equations for the vehicle. These equations as a function of velocity and time are summarized in Table 2 using the vehicle characteristics shown in Table 1.

TABLE 2.-POWER DEMAND EQUATIONS

Cycle segment	Power form	Power equation
Acceleration	$P_a(v)$	$1078.0v + 0.3350v^3$
$(0 < t \leq 28$ s)	$P_a(t)$	$769.9t + 0.1221t^3$
Cruise	$P_{cr}(v)$	4812
$(28 < t \leq 78$ s)	$P_{cr}(t)$	4812
Coast	$P_{co}(v)$	0
$(78 < t \leq 88$ s)	$P_{co}(t)$	0
Brake	$P_b(t)$	$2659.4v - 0.335v^3$
$(88 < t \leq 97$ s)	$P_b(t)$	$5411.2\,(\Delta t) - 2.821\,(\Delta t)^3$
Idle	$P_i(v)$	0
$(97 < t \leq 122$ s)	$P_i(t)$	0

The velocity at the end of the coast cycle is calculated as follows:

$$a = \frac{dv}{dt} = \frac{-F_r}{M} - \frac{F_D}{M} \qquad (11)$$

where

a = acceleration

F_r = rolling resistance force

F_D = aerodynamic drag force

M = mass of vehicle

and

$$F_r/M = R_r g$$

$$F_D/M = \frac{C_d \rho A v^2}{2M}$$

Substituting these forms in Equation (11) and letting

$$b = R_r g, \quad c = \frac{C_d \rho A}{2M} \tag{12}$$

and integrating yields

$$v(t) = \frac{b}{\sqrt{bc}} \tan \left[\tan^{-1} \left(v_o \frac{\sqrt{bc}}{b} \right) - (t - t_o) \sqrt{bc} \right]$$

Substituting in the following initial conditions

$$v_o = 20.1 \text{ m/s (45 mi/h)}, \quad t = 88 \text{ s}, \quad t_o = 78 \text{ s}$$

results in

$$v_{t=88} = 18.31 \text{ m/s (40.97 mi/h)}$$

for the velocity at the end of the coast cycle (t = 88 s).

Results of Power Analysis

A computer model was developed to simulate the specified vehicle operating over the SAE J227a, Schedule D, driving cycle. The model performs a time integration of the equations in Table 2. The equations are calculated every 0.25 s in the computer program to estimate instantaneous power requirements.

The results of the analysis are presented in Table 3. Shown are the peak power and total energy required or available at the wheels, and at the shaft of the mechanical drive system with a mechanical drive train efficiency of 95%. The power and energy are calculated for the vehicle deceleration from both 88 km/h (55 mi/h) and 72 km/h (45 mi/h). Positive numbers are power and energy required from the electric motor, while negative numbers are power and energy available from braking to an energy buffer system. In addition to the power and energy data provided for the Schedule D driving cycle, results are also presented for a modified Schedule

TABLE 3.-POWER AND ENERGY REQUIRED AT THE WHEELS, AND AT THE SHAFT OF THE MECHANICAL DRIVE SYSTEM[a]

Cycle segement	SAE J227a, schedule D, driving cycle at 72 km/h (45 mi/h) cruise speed				Modified SAE J227a, schedule D, driving cycle at 88 km/h (55 mi/h) cruise speed			
	Peak power, kW		Total energy, kJ		Peak power, kW		Total power, kJ	
	At wheels	At shaft	At wheels	At shaft	At wheels	At shaft	At wheels	At shaft
Acceleration	24.316	25.595	321.229	338.135	36.641	38.569	477.946	503.101
Cruise	4.812	5.065	240.600	253.250	7.611	8.011	380.550	400.550
Coast	0	0	0	0	0	0	0	0
Braking	-45.376	-43.107	-214.232	-203.520	-67.209	-63.848	-318.685	-302.750

[a]95% drive train efficiency.

D cycle having a cruise velocity of 88 km/h (55 mi/h). The final designed buffer will be physically sized to absorb the energy stored during the vehicle braking from 88 km/h (55 mi/h).

The instantaneous power requirements at the wheels necessary to maintain the Schedule D driving cycle are shown in Figure 3. The expended energy from the beginning of the cycle is shown in Figure 4 for the same driving cycle. The deceleration energy is shown as negative due to the intention of recovering this energy in a buffer device. These graphs also include instantaneous power requirements and expended energy for a cruise velocity of 88 km/h (55 mi/h).

The peak acceleration power which must be delivered to the shaft of the drive system by the energy buffer depends on how much of the acceleration energy is to be provided by the electric motor. If it is assumed that the maximum allowable output of the electric motor is to be equal to the 72 km/h (45 mi/h) cruise power requirement plus 10% (i.e., the battery/motor is held to an output of (1.10) times (5.065) = 5.571 kW at the shaft of the drive system), the excess peak acceleration power required above what the electric motor can supply in the 72 km/h (45 mi/h) driving cycle is 20.024 kW (i.e., 25.595 - 5.571 kW).

Therefore, the acceleration energy which must be available in an energy buffer (assuming the battery/motor outputs power at its peak rate of 5.571 kW during the 28-second acceleration phase) is 338.135 - 28 (5.571) = 182.147 kJ. This is less than the requirement of storing the 203.520 kJ of available braking energy, and therefore the braking energy requirement rather than the acceleration requirement will size the energy buffer. This does, however, set a minimum throughput efficiency for the energy buffer of (182.147/203.520) x 100 = 89.5%. If the throughput efficiency of the buffer system is less than 89.5%, the peak battery/motor output will have to be increased above 5.571 kW to be able to meet the 88 km/h (55 mi/h) sizing requirement.

In other words, if 100% of the stored buffer power and 100% of the motor capacity are used to provide acceleration, the buffer must be at least 89.5% efficient to meet the required acceleration rate in the given driving cycle. If the above argument is carried out for several motor sizes, then a curve defining minimum buffer efficiency as a function of motor power can be generated as shown in Figure 5.

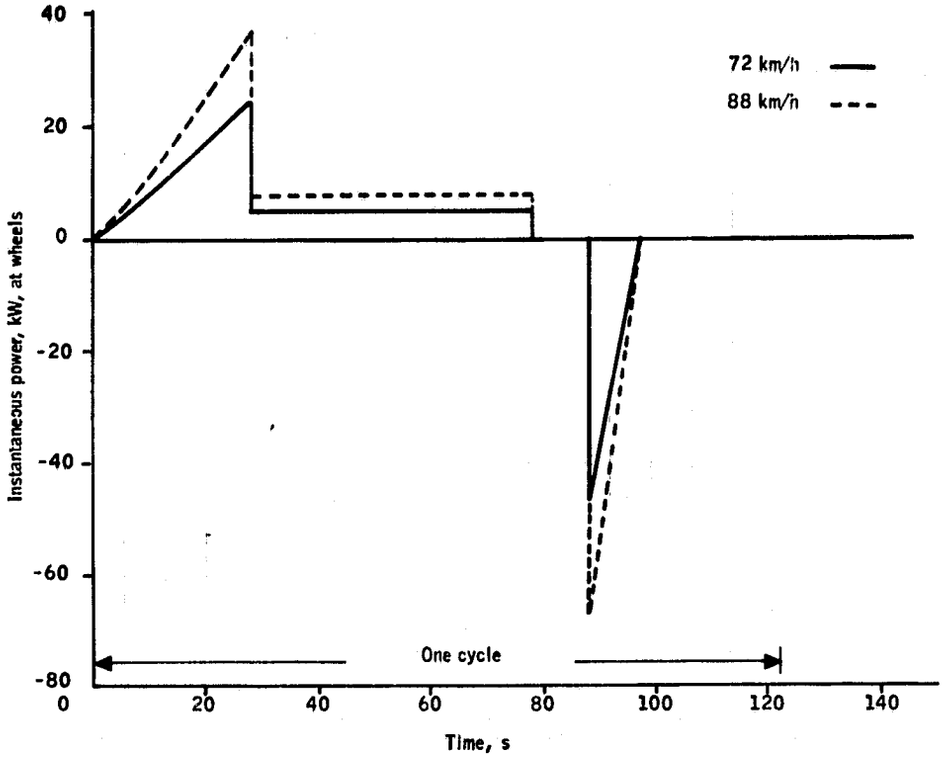

Figure 3.-Instantaneous power profile at the wheels.

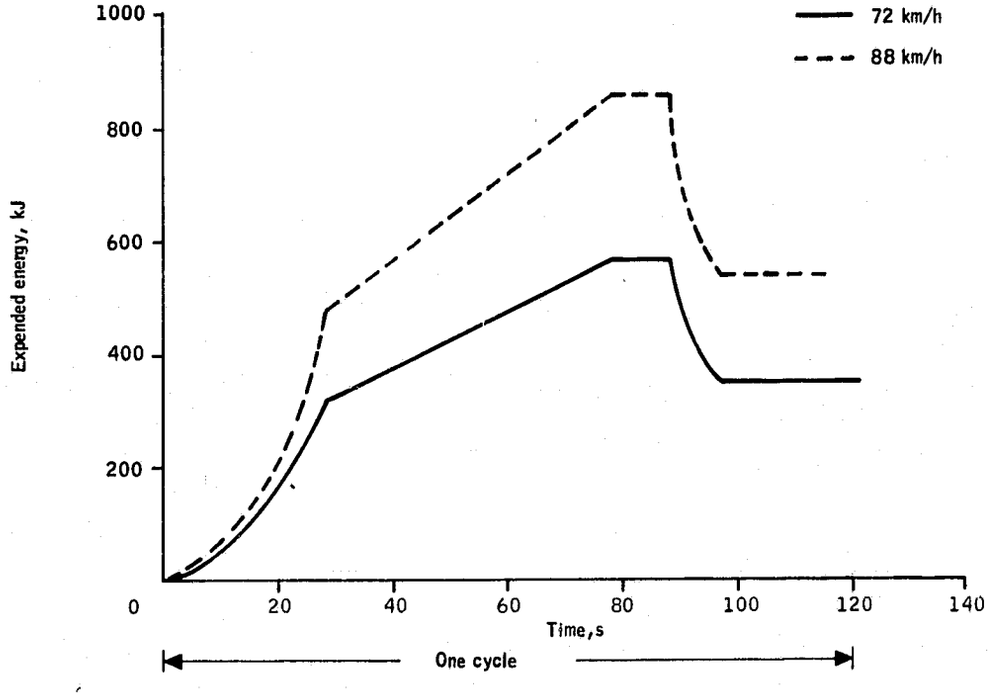

Figure 4.-Expended energy at the wheels.

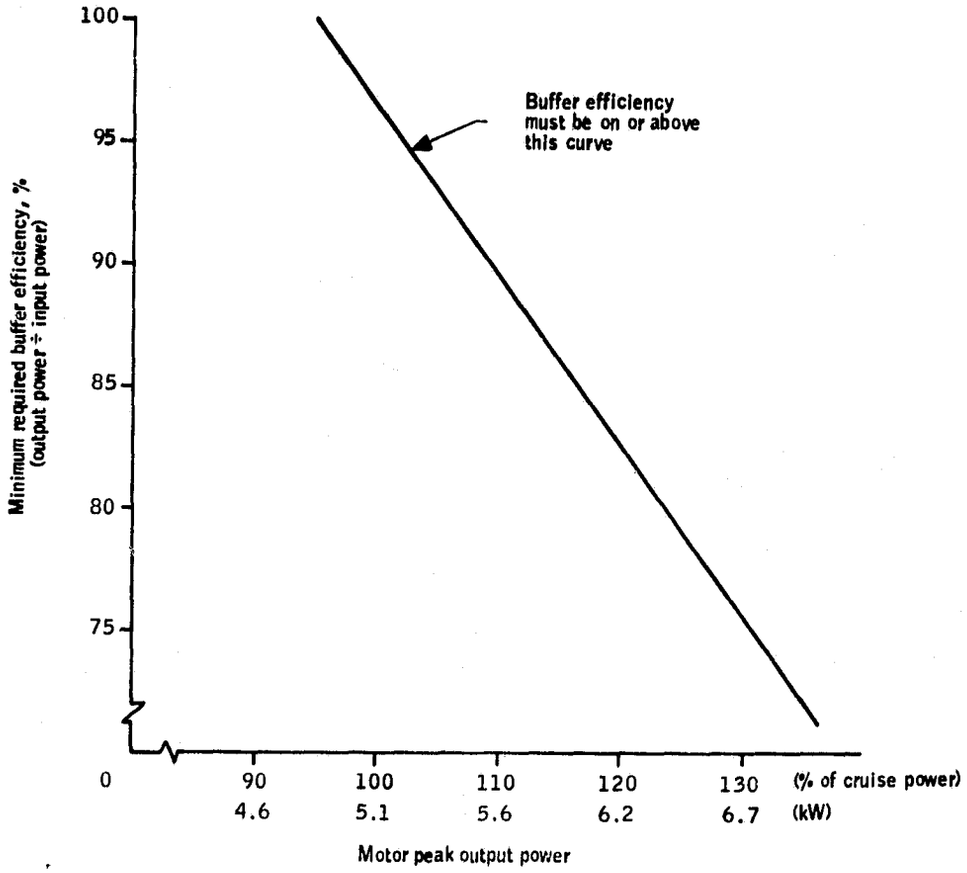

Figure 5.-Required buffer efficiency based on motor sizing and SAE J227a schedule D driving cycle.

Energy Buffer Candidates

An extensive list of energy buffer techniques is given in References 3 through 14. The most significant storage devices used for energy buffers are given in Table 4. Included are numerous types of batteries, mechanical devices, and hydrogen storage methods. The batteries listed, except the lead/acid battery, are all in the research and development stage. Hydrogen storage is also in the research and development stage.

Selected Energy Buffers

Lead/acid batteries and mechanical storage devices are presently being used experimentally with more-or-less state-of-the-art commercially available components. Thus, only lead/acid

battery storage and mechanical storage devices were considered for the buffer system concepts in this study. Four mechanical devices and one lead/acid battery system were selected;

- Lead/acid battery (electrochemical)
- Hydropneumatic accumulator (liquid/gas pressure)
- Pneumatic accumulator (gas pressure)
- Spring (mechanical)
- Flywheel (momentum)

Conceptual schematics of the baseline electric vehicle and the five selected buffer techniques are shown in Figures 6 through 11, respectively.

TABLE 4.-ENERGY BUFFER STORAGE DEVICES

Buffer technique	Device
Batteries	Lead/acid
	Nickel/iron
	Nickel/zinc
	Lithium/iron sulphide
	Sodium/sulphur (ceramic)
	Sodium/sulphur (glass)
	Zinc/chlorine
Metal/air fuel cells	Lithium/air
Mechanical	Pressure
	Momentum
	Spring
Hydrogen	Liquid hydrogen
	Magnesium nickel hydride
	Iron titanium hydride

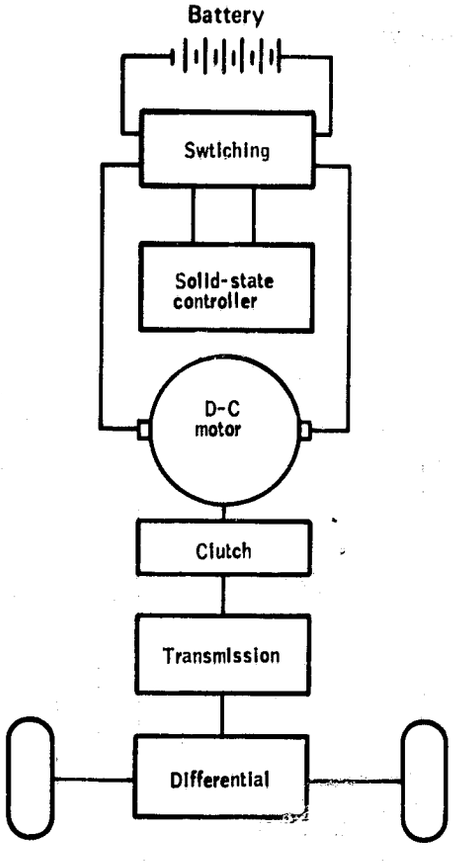

Figure 6.-Baseline electric vehicle concept schematic (without regeneration).

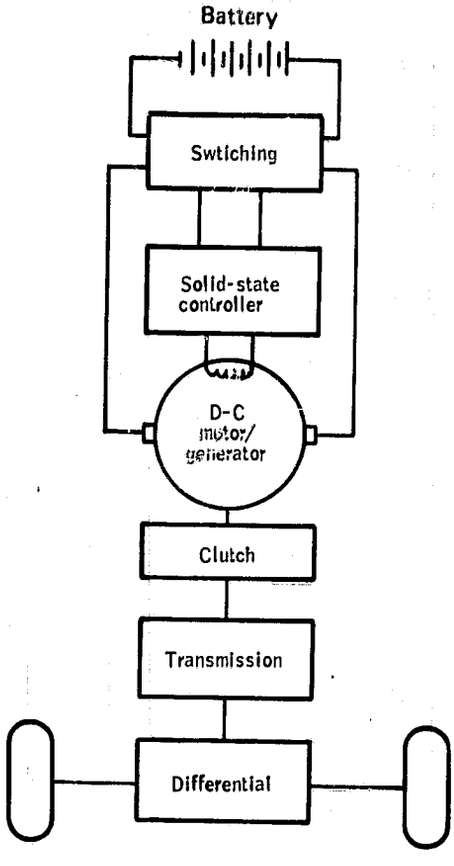

Figure 7.-All-electric, D-C, shunt motor/generator system (with electrical regeneration).

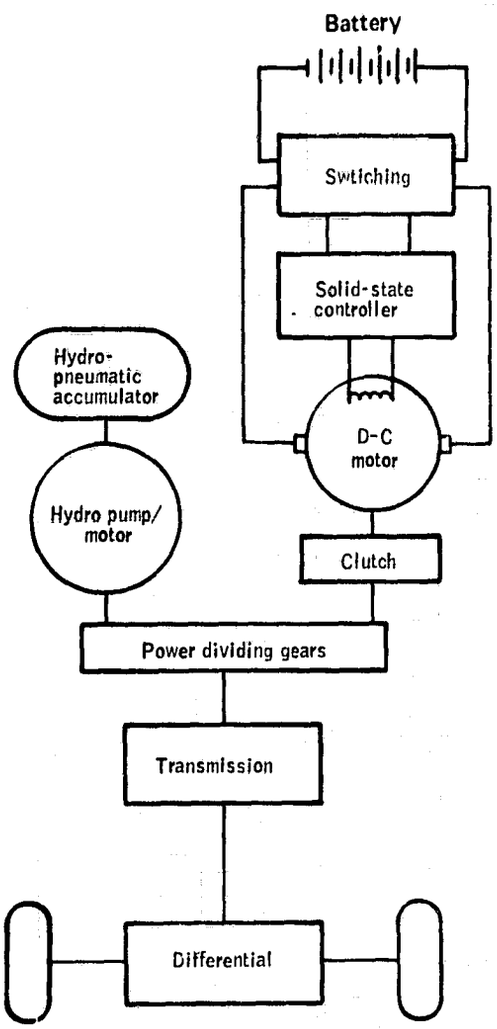

Figure 8.-Hydropneumatic accumulator system.

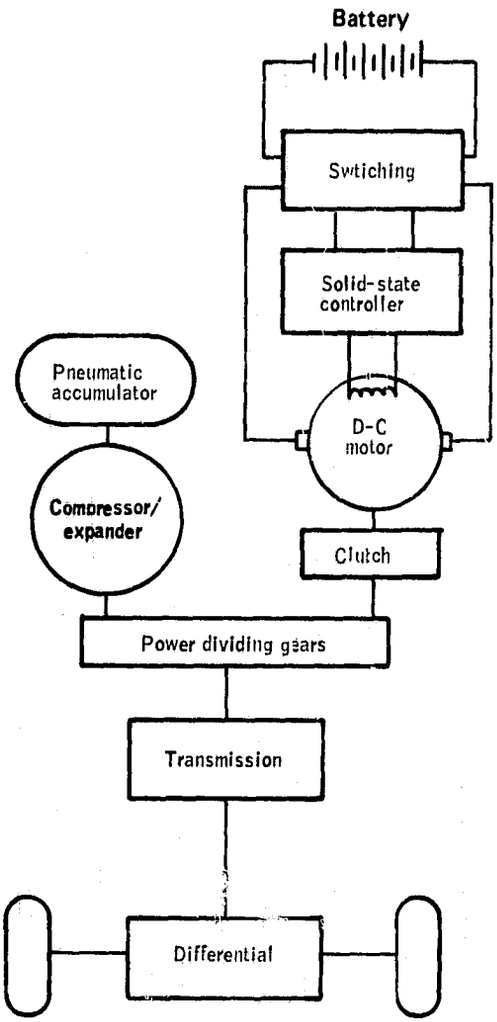

Figure 9.-Pneumatic accumulator system.

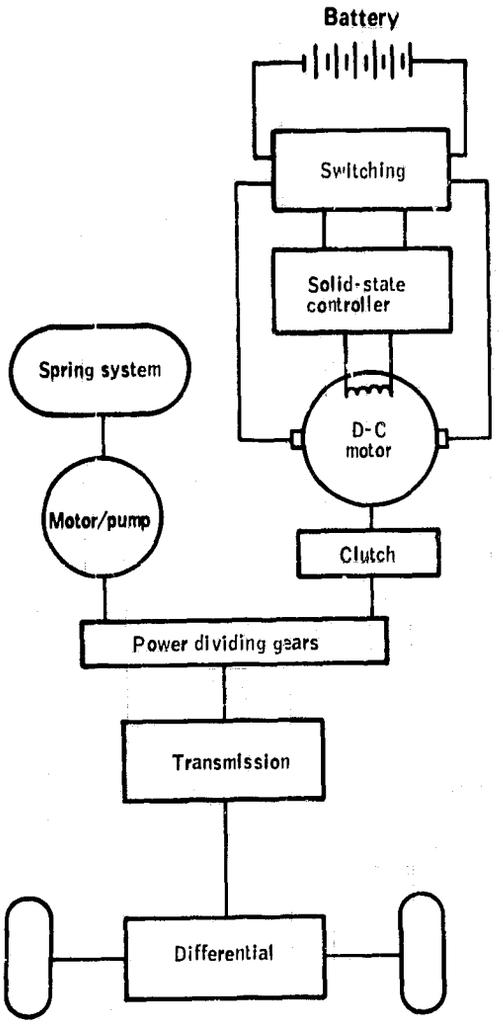

Figure 10.-Spring system.

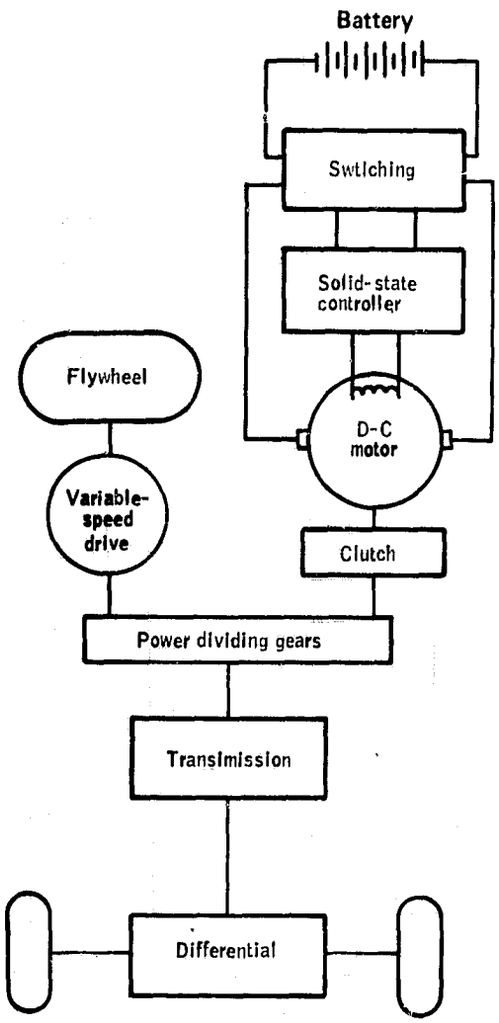

Figure 11.-Flywheel system.

For tradeoff purposes, each of these devices was used in essentially the same parallel drive configuration with the same type drive train and motor. The drive train for a buffered vehicle consists of power dividing gears, transmission, and differential. The efficiency of this driveline system was assumed to be 0.95 for this analysis. Gearing losses and motor drag losses associated with a no-load coast or idle condition were not included in the analysis.

The motor size may change with buffer mass and efficiency but for this preliminary analysis its configuration and size were assumed the same for all buffered vehicles system concepts studied.

Baseline Electric Vehicle

The first model developed was the basic electric vehicle using batteries as the only power source (see Figure 6). The characteristics of the model are shown in Table 5. This list is consistent with the typical electric vehicle found in the literature (ref. 9). The motor size is based on the requirements for acceleration and continuous duty cruise shown in Table 3 (25.6 and 5.1 kW, respectively).

TABLE 5.-BASELINE ELECTRIC VEHICLE ASSUMPTIONS

Table 1. Vehicle characteristics		
Vehicle weight breakdown:	kg	lb
Chassis/shell/drive train	744	1635
Two passengers	135	300
Motor	66	150
Batteries	415	915
	1360	3000
Lead/acid batteries		
D-C motor:		
26 kW peak output		
5.1 kW continuous duty		
95% drive train efficiency		
SCR controller		

The baseline electric vehicle components which were modeled for the simulation are:

- Drive train
- Electric motor
- Chopper/controller
- Battery

These baseline components were sized for the electric unbuffered vehicle and then used for all the candidate buffer systems.

The test data of a representative group of electric vehicles are given in Reference 9. The data for the passenger vehicles from those tests are documented in Table 6 in order to develop representative sizing parameters for the baseline vehicle.

An attempt was made to determine the relationship between motor power, motor weight, and vehicle weight. Because transmission weights and ratios were not included, no particular correlation existed. Thus, the vehicles in Table 6 are simply listed in order of battery weight percentiles.

A direct-drive electric motor with SCR chopper control (with and without regenerative braking) was selected for the vehicle. The battery was sized according to the average battery-to-vehicle weight ratio shown in Table 6, that is, 0.305 x 1360 kg = 415 kg of batteries. The motor with continuous 16-kW output was selected based on allowing a 160% overload condition for short acceleration periods requiring 26-kW of motor output power.

The simulation was done in two parts, the first without regenerative braking (baseline vehicle), and the second with regenerative braking. During each computational iteration, the energy required for propulsion (or recovered from braking) was subtracted from the energy contained in a fully-charged battery, and the SAE J227a (D) driving cycle was repeated until the battery was exhausted.

The energy removed from the battery during the propulsion portion of the driving cycle consisted of the following:

- Propulsive energy required at the wheels, including energy for aerodynamic losses, tire friction, and inertial (acceleration) power
- Losses in the mechanical gearing system

TABLE 6.-TYPICAL ELECTRIC VEHICLE SUMMARY AND AVERAGES

Vehicle	1 Battery wt / curb wt	2 Range, km	3 Range / battery wt ratio	4 Code	5 Vehicle weight, kg	6 Battery wt, kg	7 Peak motor power, kW	8 Vehicle wt / peak motor power, kg/kW	9 (Col 3 ÷ Col 8) (km/%)/(kg/kW)	10 Transmission type	11 Frontal area m^2
EPC Hummingbird	0.245	32	123	P4	1463	359	7.5	195	0.011	4	1.78
EJA Metro Sedan	.277	27	96	P8	1701	472	10.0	170	.055	3	1.86
EVA Contactor	.277	52	186	P3	1701	472	7.5	227	.014	3R	1.86
Zagato Elcor	.286	40	140	P5	653	187	2.0	327	.107	D	1.63
Sebring Citicar	.397	32	106	P10	794	236	4.5	176	.029	D	1.59
EVA Pacer	.304	30	100	P9	2090	636	14.9	140	.003	4R	NA
Waterman DAF	.346	67	193	P1	1365	472	6.7	204	.021	VSB	1.76
Ripp Electric	.396	118	298	P6	1491	590	15.0	99	.013	4R	1.70
Average	.305	49.8	156	-	1407	438	8.5	166	.025	-	-

[a]Note: D = direct-drive, 3 = three-speed, 4 = four-speed, R = regenerative braking, VSB = variable-speed belt.

- Losses in the electric motor
- Losses in the controller
- Internal battery losses

Thus, each component was modeled to determine how much power each consumes due to the losses. A schematic of the vehicle model is shown in Figure 12 which is a simplified version of Figure 6.

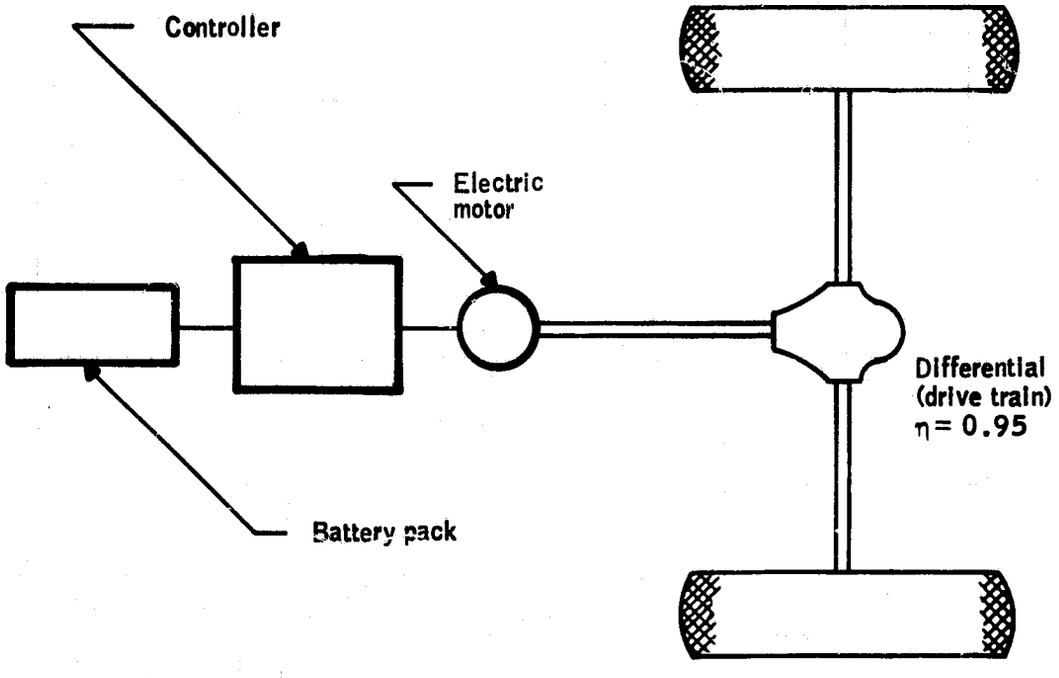

Figure 12.-Electric vehicle model.

Drive train.-The drive train efficiency was 95%. Wheel power divided by 0.95 gives shaft power.

Electric motor.-Power into the motor should be computed as "output power plus losses." This is because the motor will have losses that occur when no output power is being produced (as in the coasting model). At design speed, Reference 5 indicates that a given series-wound motor has the following characteristics:

- Rated power, 21.3 kW
- Rated speed, 3600 rpm
- Maximum speed, 5600 rpm

- Rated current, 221 A
- Maximum overload, 160%
- Maximum overload voltage, 108V
- Efficiency at base power and speed, 89.3%
- Losses at rated power and speed (% of output shaft power):

- Armature	4.8
- Field	3.7
- Eddy current	0.5
- Hysteresis	1.0
- Bearing and brush friction	0.6
- Windage	1.4
- Total losses	12.0

If maximum power requirements have been determined to be 25.595 kW (from simulation), and this motor is capable of 160% overload, then motor rated power should be 16.0 kW (21.44 hp). If the gear ratio is set to give a motor speed of 3600 rpm at 72 km/h (45 mi/h), the motor will have the following characteristics:

- Rated power, 16 kW
- Baseline speed, 3600 rpm - 72 km/h (45 mi/h)
- Maximum speed, 5600 rpm - 112 km/h (70 mi/h)
- Rated current: NA
- Maximum overload: 160%
- Overload voltage: NA
- Efficiency at base power and rpm, 88%

Assuming the percent losses of the 16-kW motor due to armature I^2R losses, field I^2R losses, eddy current losses, hysteresis

losses, friction losses, and windage losses are identical at rated power and speed to the losses for the 21.3-kW motor, the following output and power losses are exhibited by the 16-kW motor when operated at rated conditions (16-kW output, 3600 rpm):

- Output = 16.000 kW
- Armature = 0.768 kW
- Field = 0.592 kW
- Eddy = 0.080 kW
- Hysteresis = 0.160 kW
- Friction = 0.160 kW
- Windage = 0.224 kW

The armature and field power losses are proportional to the square of the power output (at constant voltage), the eddy power is proportional to the power output (at constant voltage), the hysteresis and friction powers are proportional to the motor rpm, and the windage power is proportional to the square of the rpm. Using the above scaling laws and power requirements, the equations defining motor power losses are:

- Armature power $= 3.00 \times 10^{-3} (P_{out})^2$ (13)
- Field power $= 2.31 \times 10^{-3} (P_{out})^2$ (14)
- Eddy current power $= 5.00 \times 10^{-3} (P_{out})$ (15)
- Hysteresis power $= 4.44 \times 10^{-5} (\omega)$ (16)
- Friction power $= 2.67 \times 10^{-5} (\omega)$ (17)
- Windage power $= 1.73 \times 10^{-8} (\omega)^2$ (18)

where P_{out} is the output power of the motor in kW, and ω is the motor rpm. The total input power to the motor under any conditions is the sum of losses plus that required to accelerate the vehicle.

Chopper/controller.-Power into the controller was computed as a function of motor input power. Motor efficiency was reduced by a factor of 1.06 due to the pulse shape out of the chopper (ref. 5). Power into the chopper, then, is:

- Power output, or 1.06 total motor power input requirement
- Steady-state power, 0.015 kW
- Internal resistive losses, 0.02 x motor power.

Battery.-Three battery models were considered. They differ in both the characteristics of the battery modeled (as plotted on a Ragone plot) and the method of interpreting battery performance during the driving cycle.

The battery characteristics of the three different models are summarized in Figure 13. Model 1 battery characteristics are representative of lead/acid battery performance expected in the years 1980 to 1985 (ref. 5). Models 2 and 3 represent the NASA EV-106 battery.

Model 1 interprets the Ragone plot as a "utilization efficiency" and calculates the change in energy capacity of the battery from the maximum battery capacity using this utilization efficiency. The same efficiency is used during regenerative charging of the battery.

Model 2 is the fractional utilization model. It computes the battery time to discharge at a given power density and uses that data to compute how long the battery will last when operated through a given driving cycle. There are no provisions in the model for regenerative charging of the battery. Examination of this fractional utilization model shows it to be conceptually identical to model 1 during battery discharge.

Model 3 uses average discharge battery power requirements during the entire driving cycle to estimate battery capacity from the Ragone plot of the battery. Regenerative braking effects are including by computing the energy available from regenerative braking at the battery terminals, multiplying by a regeneration fraction, and subtracting this energy from the battery energy required per cycle. Two different regeneration fractions were used: 0.70 and 1.067. Results of range increase are shown in Table 7.

Since model no. 1 is based on representative lead/acid battery performance expected in the years 1980 to 1985, and no. 2 contains no provisions for regenerative charging of the battery, it was felt that model no. 3, the NASA EV106 model, was the most representative of lead/acid battery technology today. Thus, this model is used for the final design analysis.

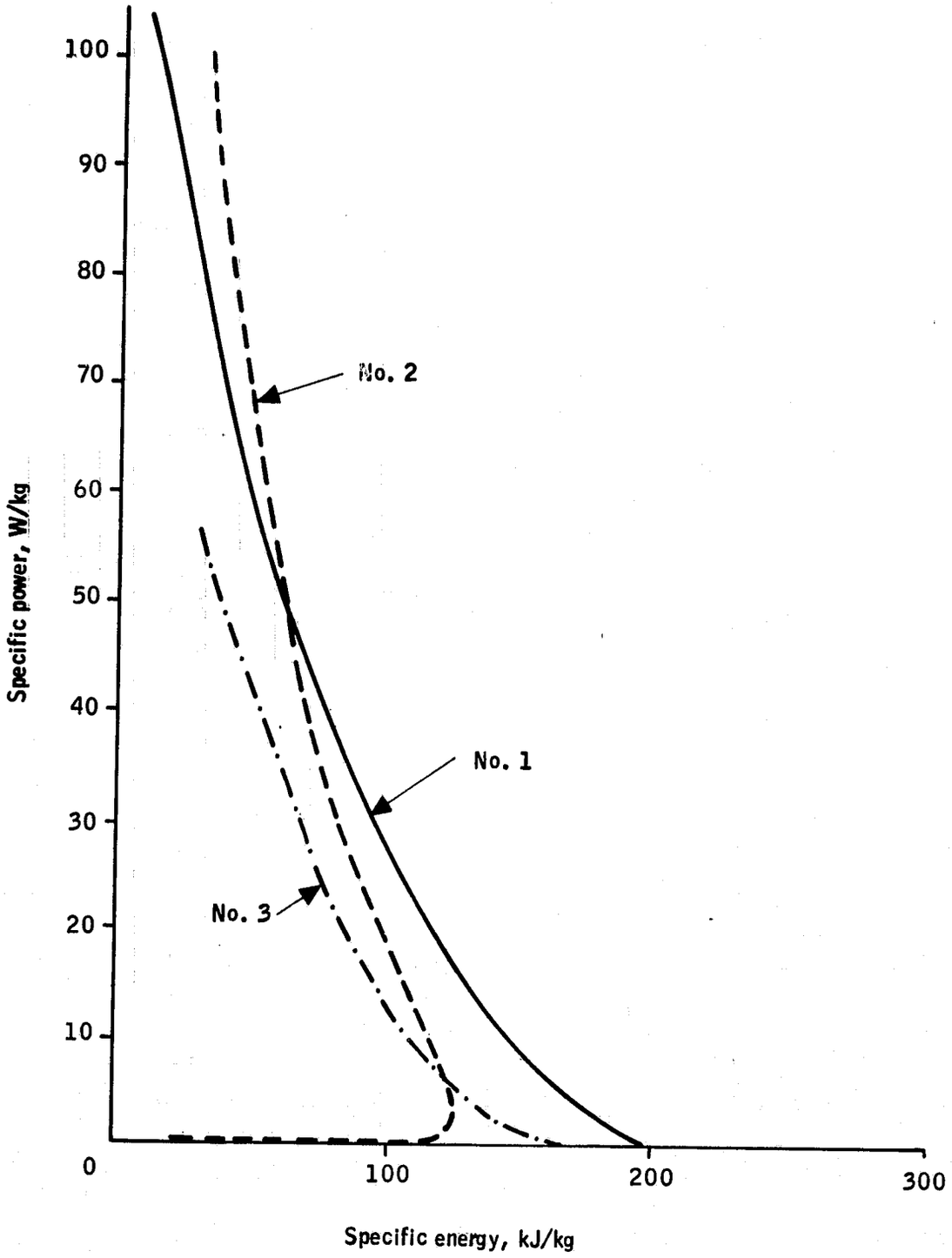

Figure 13.-Ragone plots of lead/acid battery.

TABLE 7.-VEHICLE RANGES FOR ELECTRIC AND MOTOR/GENERATOR VEHICLES

Vehicle	Range (km)		
	Model 1	Model 2	Model 3
Electric	53.1	54.8	68.5
Motor/generator	54.6	-	80.6[a], 89.0[b]

[a]Regeneration fraction = 0.70

[b]Regeneration fraction = 1.067

Electric Vehicle With Regenerative Braking

A schematic of the model is shown in Figure 14, which is a simplified version of Figure 7. Components in this model are essentially the same as the baseline vehicle. However, during the regenerative braking mode the motor must operate as a generator as well. Generator characteristics used in the analysis to calculate losses during power regeneration were the same as those of the motor (ref. 4). The power into the controller in this mode is equal to the shaft power available minus the generator (motor) losses. No weight penalty was added to the vehicle model for the replacement of the motor with a motor/generator unit. Results of the increase in range over the baseline electric vehicle are shown in Table 8.

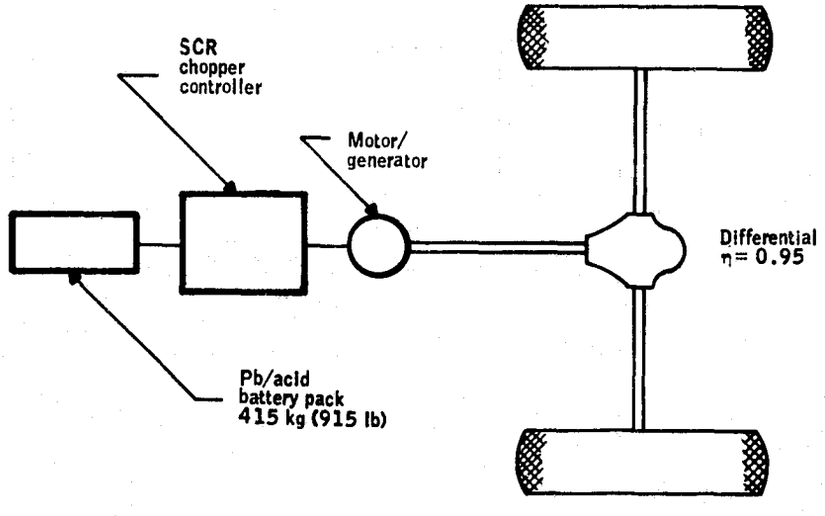

Figure 14.-Electric vehicle model with motor/generator for regenerative braking.

TABLE 8.-BUFFERED VEHICLE PERFORMANCE - REGENERATIVE BRAKING (80% BATTERY DISCHARGE)

Parameter	Electric vehicle with regenerative braking
Range,[a] km	80.6[b], 89.0[c]
Buffer charge rate, kW	66.0
Buffer discharge rate, kW	32.0
Buffer weight, kg	0
Maximum battery discharge, kW	32.0

[a] Straight electric vehicle range = 68.5 km
[b] Regeneration fraction = 0.7
[c] Regeneration fraction = 1.067

Electric Vehicle With Hydropneumatic Buffer

The concept was modeled as shown in Figure 15 which is a simplified version of Figure 8. The two major components of this buffer system are the hydraulic accumulator and the hydraulic motor/pump.

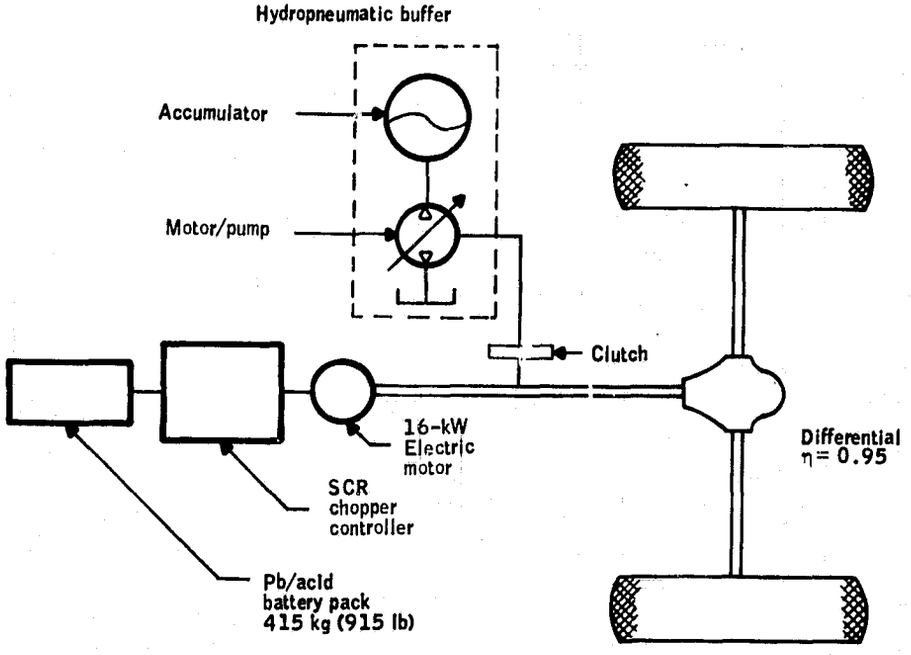

Figure 15.-Electric vehicle with hydropneumatic buffer.

The hydraulic accumulator consists of a shell which is divided into two chambers by a bladder or diaphram. One chamber is filled with hydraulic fluid and the other with inert nitrogen gas. Energy is stored as potential energy by compressing the gas in the bladder gas chamber. When the hydraulic fluid is pumped into the accumulator, the bladder is deformed and the gas volume reduces and the pressure increases, thus storing energy. If this stored energy is needed by the system, hydraulic fluid is discharged from the accumulator through the hydraulic motor to a reservoir maintained at a lower pressure. The gas in the bladder expands resulting in a decrease in pressure.

Various types of hydraulic motors and pumps were considered for this concept including vane, gear, lobe, radial piston, and axial piston. However, because this concept required variable volume flow, the axial piston variable-displacement type was selected. Such a device can either supply shaft horsepower when hydraulic fluid under pressure is supplied to it or it can supply high-pressure hydraulic fluid to an accumulator when shaft horsepower is supplied to it. Thus, it operates as a motor when the electric vehicle accelerates and as a pump when the vehicle is braking.

To determine the range of the electric vehicle using this concept it is necessary to first determine a control strategy by which the energy can be added and removed from the buffer and then to select the correct size for the buffer components. This is to ensure (1) that the accumulator will accept or deliver the required amount of energy when needed, and (2) that the hydraulic motor/pump is capable of transferring the peak power load (occurs the instant the brakes are applied during the braking mode). Control strategy, motor/pump, and accumulator sizing considerations are summarized as follows:

- Control strategy--The accumulator is sized to absorb all the energy of the vehicle decelerating from 88 km/h (55 mi/h) after a 10-s coast. For the 1360 kg (3000 lb) vehicle stopping in 9 s [SAE J227a (D) driving cycle], 302.750 kJ of energy must be stored (Table 1).

  This energy is preprogrammed to be a function of vehicle velocity only, to ensure that the state of the accumulator is driving-cycle independent. For example, if the driver decides to coast to a stop, the electric motor is used to recharge the accumulator, thus assuring that if the driver attempts to reaccelerate, there is adequate energy reserve in the accumulator to assist in the reacceleration.

During an acceleration phase between any two velocities, the energy needed to accelerate the vehicle is the change in the kinetic energy of the vehicle plus the energy required to overcome aerodynamic losses and the rolling resistance losses. During a braking phase between the same two velocities, the recoverable energy is equal to the change in kinetic energy minus the energy required to overcome aerodynamic losses and the rolling resistance losses. In other words, the amount of kinetic energy available from some velocity to any other velocity is less than the amount of kinetic energy necessary to accelerate back to the same velocity by an amount which is twice the aerodynamic and rolling resistance losses. This is shown in Figure 16.

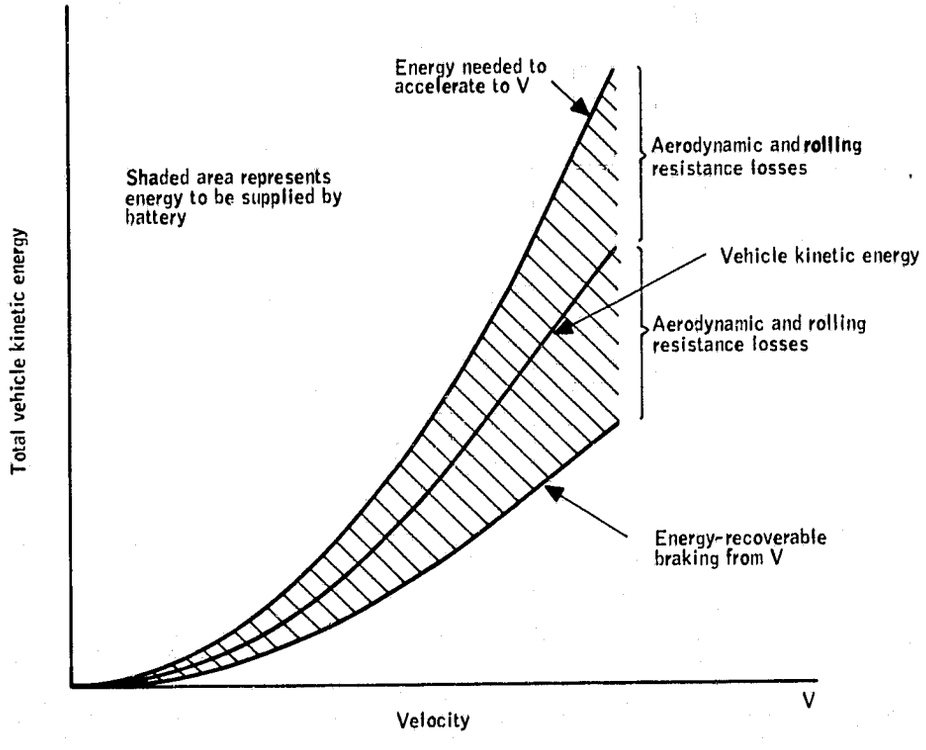

Figure 16.-Kinetic energy distribution.

The preprogrammed pressure schedule for the accumulator was determined by considering the following expression for adiabatic expansion/compression for energy stored in the accumulator between 88 km/h and 0 (55 mi/h and 0):

$$W = \frac{1}{2} Mv^2 \quad \alpha \quad \frac{(p_{88})\ (V_{88})}{n - 1} \left[1 - \left(\frac{p_0}{p_{88}}\right)^{\frac{n - 1}{n}}\right] \text{(ref. 13)} \tag{19}$$

where

W = work of expansion/compression from p_0 to p_{88}

$n = C_p/C_v$ for nitrogen = 1.401 (ratio of specific heat)

p_{88} = accumulator pressure at 88 km/h (55 mi/h)

p_0 = accumulator pressure at zero velocity

V_{88} = accumulator gas volume at 88 km/h (55 mi/h)

M = vehicle mass, kg

The work of expansion/compression between 88 km/h (55 mi/h) and any other velocity, v, is written as

$$W = \frac{1}{2} M\ (v_{88}^2 - v^2) \quad \alpha \quad \frac{p_{88}\ V_{88}}{n - 1} \left[1 - \left(\frac{p}{p_{88}}\right)^{\frac{n - 1}{n}}\right] \tag{20}$$

where

v_{88} = vehicle velocity = 88 km/h (55 mi/h)

Substituting Equation (19) into (20) yields p as a function v:

$$p \quad \alpha \quad p_{88} \left[\left(\frac{p_0}{p_{88}}\right)^{\frac{n - 1}{n}} + \frac{v^2}{v_{88}^2} \left[1 - \left(\frac{p_0}{p_{88}}\right)^{\frac{n - 1}{n}}\right]\right]^{\frac{n}{n - 1}} \tag{21}$$

Given that the maximum pressure in the accumulator will be 20.7 MPa (3000 psi)* when the vehicle is at rest, the pressure schedule over the velocity range can be computed by Equation (21) and is shown graphically in Figure 17.

The maximum storage capacity of the accumulator between 88 km/h (55 mi/h) and 0 as a function of maximum storage

*Typical accumulator maximum pressure rating.

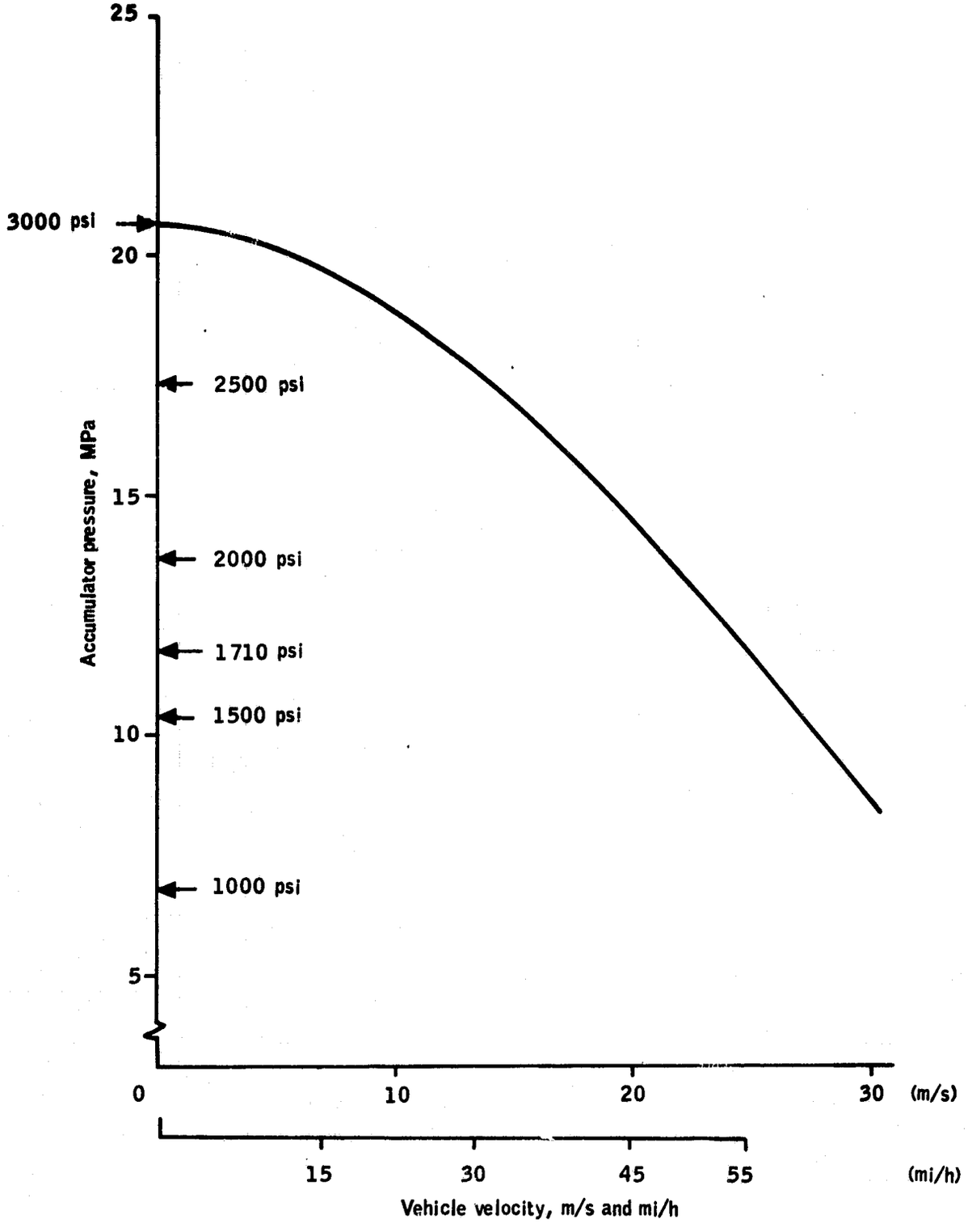

Figure 17.-Hydropneumatic/electric vehicle pressure schedule.

volume (at 88 km/h) is given by Equation (19). This relation is shown graphically in Figure 18.

- Motor/pump--The motor/pump maximum speed was choosen to be 3600 rpm* at a vehicle velocity of 88 km/h (55 mi/h). Maximum motor size and displacement were determined by the peak power handling requirements at that velocity, in this case, the braking power requirement. At lower maximum speeds than 88 km/h (55 mi/h), peak power handling requirements are lower and accumulator pressures are higher, reducing motor/pump displacement and size requirements.

  Losses in a variable-displacement hydraulic motor/pump are caused by four basic factors: internal leakage, friction losses, viscous losses, and compression losses. An initial analysis of typical manufacturer's data for a motor rated at 3600 rpm and 11.8 MPa (1710 psi), the accumulator pressure chosen for 88 km/h (55 mi/h), gives the results (ref. 5) in terms of the following equations:

$$\text{Leakage loss} = 2.204 \times 10^{-6} P_r p_a^{1/2}, \text{ (watts)} \quad (22)$$

$$\text{Friction loss} = 4.148 \times 10^{-13} P_r p_a (\omega), \text{ (watts)} \quad (23)$$

$$\text{Viscous loss} = 2.18 \times 10^{-9} P_r (\omega), \text{ (watts)} \quad (24)$$

$$\text{Compression loss} = 3.708 \times 10^{-12} \text{ rpm}^2 \; p \; (P_o/P_r), \text{ (watts)} \quad (25)$$

  where

  ω = speed of the motor/pump, rpm

  P_r = maximum rated power output of the motor/pump, W

  p_a = accumulator pressure, Pa

  P_o = instantaneous power output of the motor pump, W

  The output power of the hydraulic motor/pump is equal to the input power minus the four loss factors.

*Typical maximum speed of axial piston variable-displacement motor/pumps.

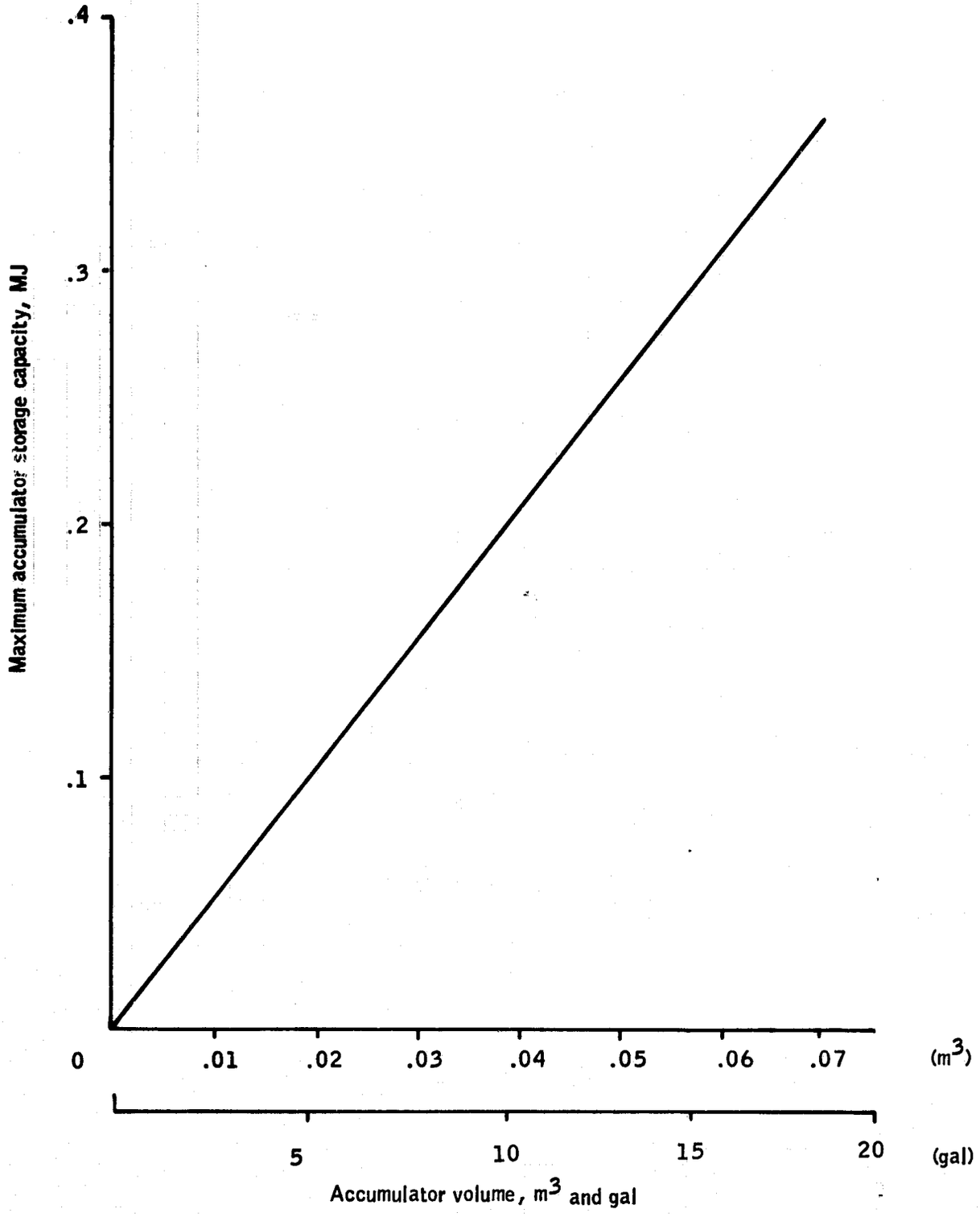

Figure 18.-Maximum accumulator storage capacity as a function of accumulator volume for the hydropneumatic/electric vehicle.

The rated output of the motor/pump depends on both the size of the accumulator storage volume and on the driving cycle requirements. The maximum output of the motor is computed from the following equation:

$$\frac{dW}{dt} = \left(\frac{dW}{dp}\right)\left(\frac{dp}{dv}\right)\left(\frac{dv}{dt}\right) \tag{26}$$

where

$\left(\frac{dW}{dp}\right)$ = the rate of change of accumulator energy content with respect to accumulator pressure - computed from Equation (20) as a function of accumulator volume

$\left(\frac{dp}{dv}\right)$ = the rate of change pressure with respect to velocity - computed from Equation (20)

$\left(\frac{dv}{dt}\right)$ = the rate of change of velocity with respect to time - computed from the driving cycle requirement of stopping in 9 s from a speed of 88 km/h (55 mi/h) after a coast time of 10 s.

The results of this analysis are presented in Figure 19. The rated motor/pump capacity is shown as a function of the accumulator volume.

Using representative manufacturer's catalog data of axial piston motor/pumps and the data from ref. 5 concerning fiber-wrapped pressure vessels, the following empirical equations are used to determine the buffer system mass:

$$\text{Mass (accumulator)} = (727)\text{x}(\text{accumulator volume in } m^3),\ [\text{kg}] \tag{27}$$

$$\text{Mass (reservoir + fluid)} = (190)\text{x}(\text{fluid volume in } m^3)\ [\text{kg}] \tag{28}$$

$$\text{Mass (motor/pump)} = (0.55\ \text{kg})\text{x}(\text{rated power in kW}),\ [\text{kg}] \tag{29}$$

The accumulator system mass as a function of storage volume is given in Figure 20. Thus, choosing an accumulator volume sizes the motor/pump, determines the buffer mass, and thus defines the vehicle for performance estimates.

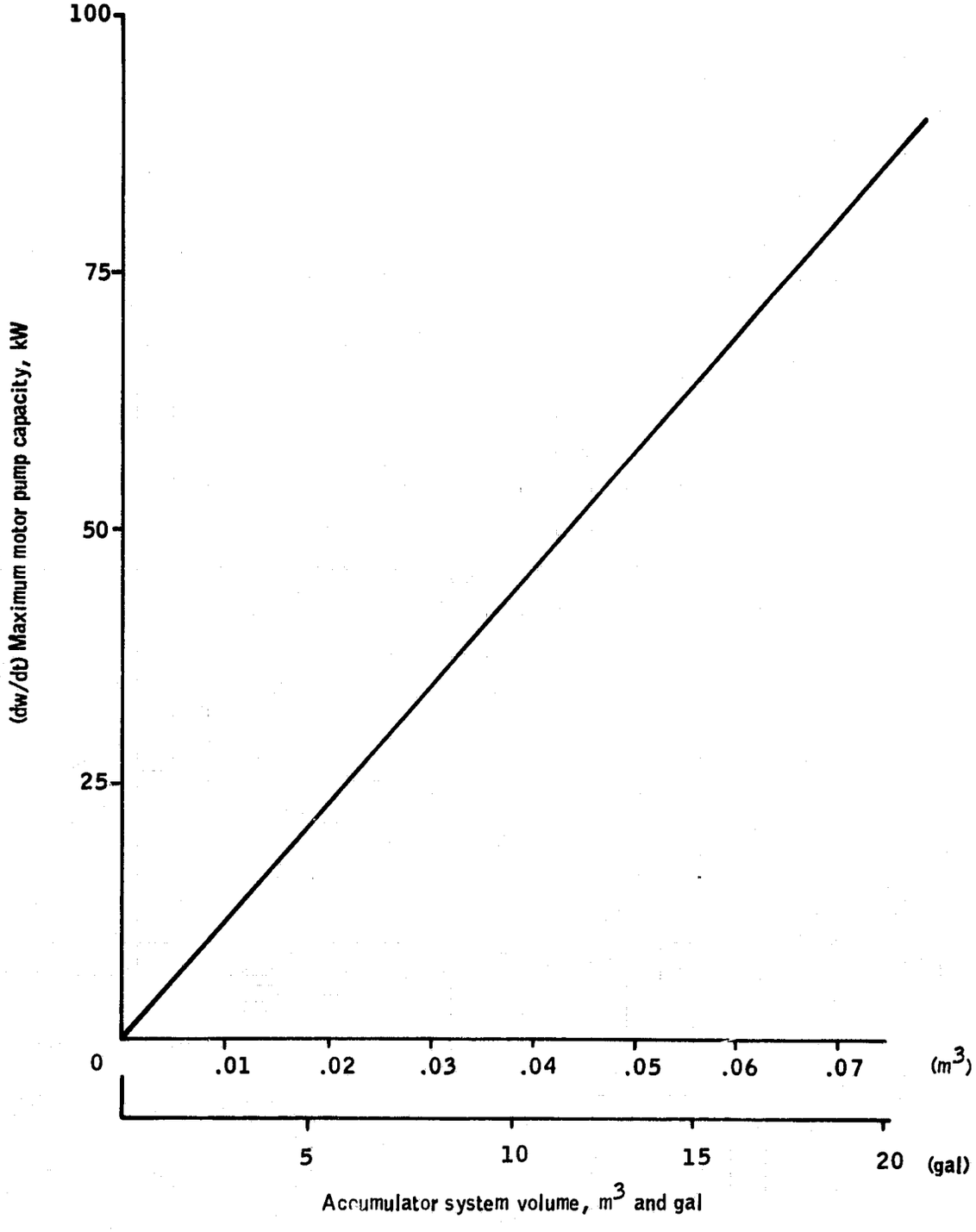

Figure 19.-Maximum hydropneumatic accumulator output rate versus accumulator volume.

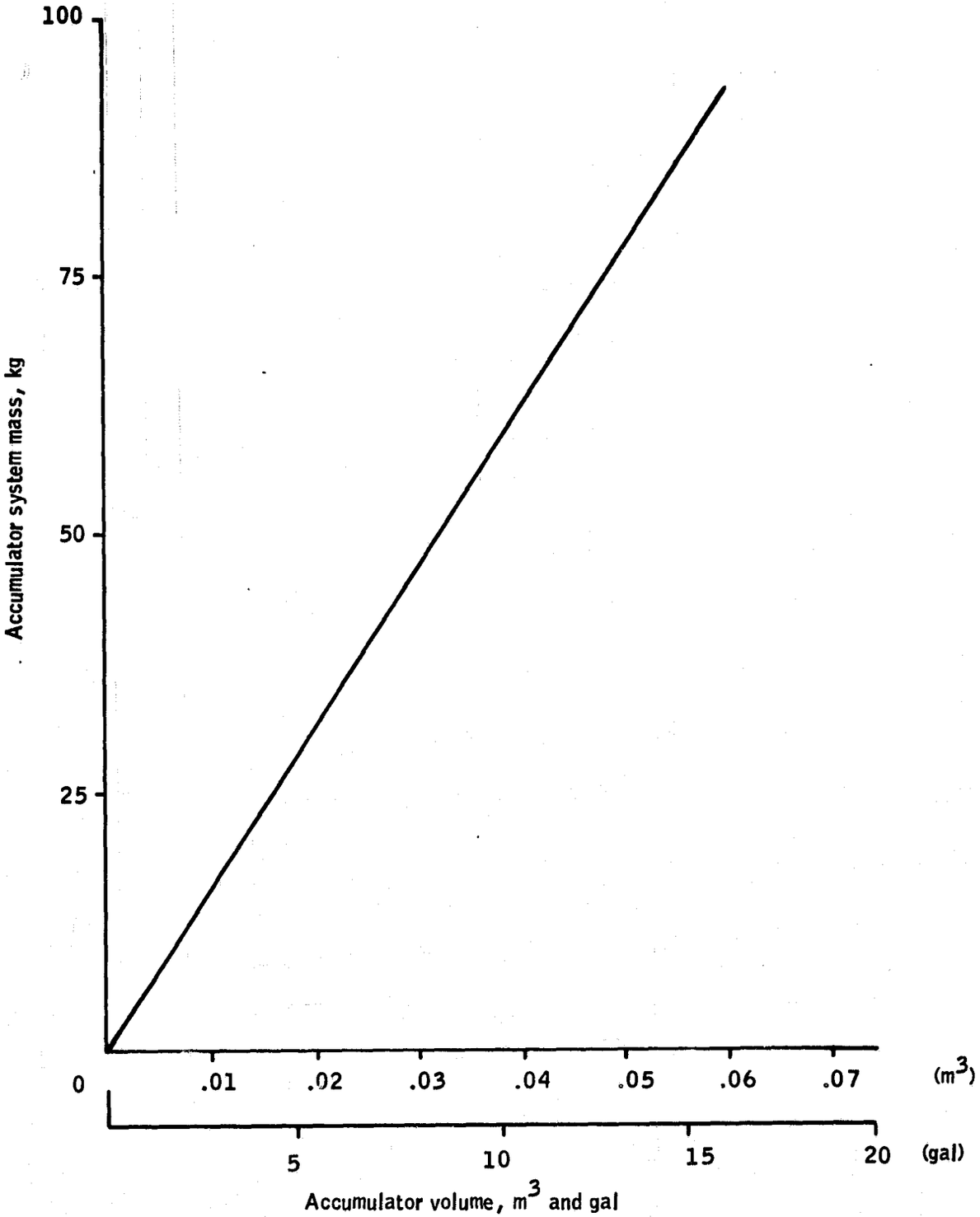

Figure 20.-Hydropneumatic accumulator system mass versus accumulator volume.

- Accumulator sizing--An assumption made was that the accumulator system be capable of accepting all of the braking energy from an 88 km/h (55 mi/h) stop. A plot of the excess braking energy from an 88 km/h (55 mi/h) stop versus accumulator volume is shown in Figure 21. The excess braking energy is defined as the energy available at the inlet shaft to the motor/pump during braking minus the energy required at the shaft to maintain the preprogrammed pressure schedule defined previously. Positive values of excess braking energy require dissipation of some of the braking energy in the brakes; negative values require operation of the electric motor during braking. A value of zero gives the design accumulator volume, in this case 0.072 m^3 (19 gal).

The resulting buffer system weighs 111 kg (244 lb), has a storage capacity of 676 kJ, and a maximum charge rate of 81 kW (corresponding to braking power at 88 km/h). The results of buffered vehicle performance are shown in Table 9.

Electric Vehicle With Pneumatic Buffer

The pneumatic buffer concept is modeled as shown in Figure 22 which is a simplified version of Figure 9. It consists of two major components: a pressurized air storage tank and a variable-displacement compressor/expander. Ambient air is compressed by the compressor/expander during the braking cycle and is expanded through the compressor/expander during the acceleration cycle.

As with the accumulator in the hydropneumatic buffer concept, the pressurized air storage tank is sized to absorb all the energy of the vehicle decelerating from 88 km/h (55 mi/h) after a 10-s coast.

However, unlike the hydropneumatic system, the mass of the gas in the storage tank is constantly changing along with the pressure. The thermo-dynamic defining equation for the storage tank in this system is written as an adiabatic expansion/compression as follows:

$$W = \frac{V_B p_1}{n - 1}\left[1 - \left(\frac{p_a}{p_1}\right)^{\frac{n-1}{n}}\right] - \frac{V_B p_2}{n - 1}\left[1 - \left(\frac{p_a}{p_2}\right)^{\frac{n-1}{n}}\right] \qquad (30)$$

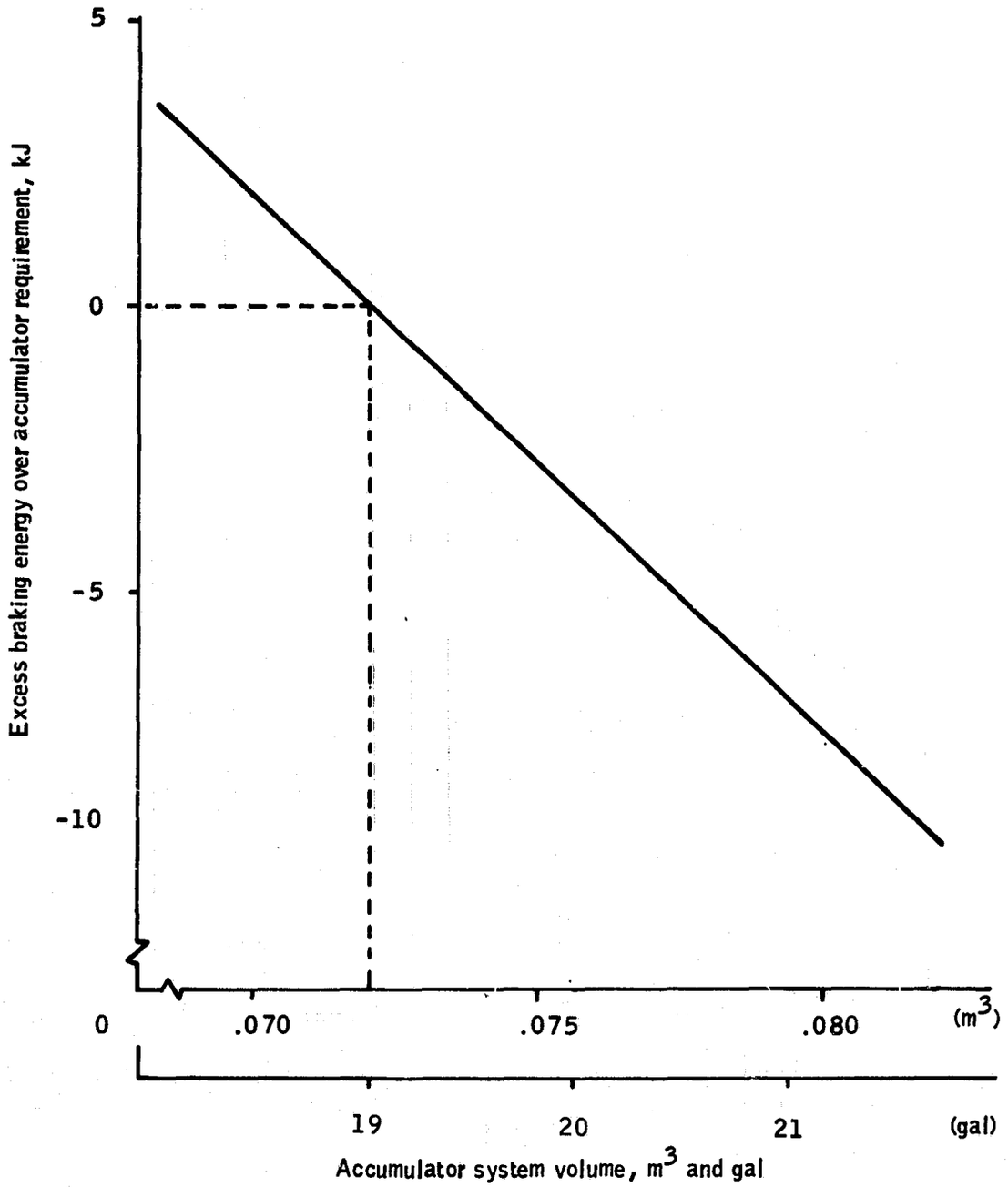

Figure 21.-Excess braking energy versus accumulator storage volume for the hydropneumatic/ electric vehicle.

TABLE 9.-BUFFERED VEHICLE PERFORMANCE - HYDROPNEUMATIC BUFFER (80% BATTERY DISCHARGE)

Parameter	Electric vehicle with regenerative braking	Hydropneumatic buffer vehicle
Range,[a] km	80.6[b], 89.0[c]	83.5
Buffer charge rate, kW	66.0	81.0
Buffer discharge rate, kW	32.0	13.8
Buffer weight, kg	0	111.3
Maximum battery discharge, kW	32.0	16.1

[a] Straight electric vehicle range = 68.5 km
[b] Regeneration fraction = 0.7
[c] Regeneration fraction = 1.067

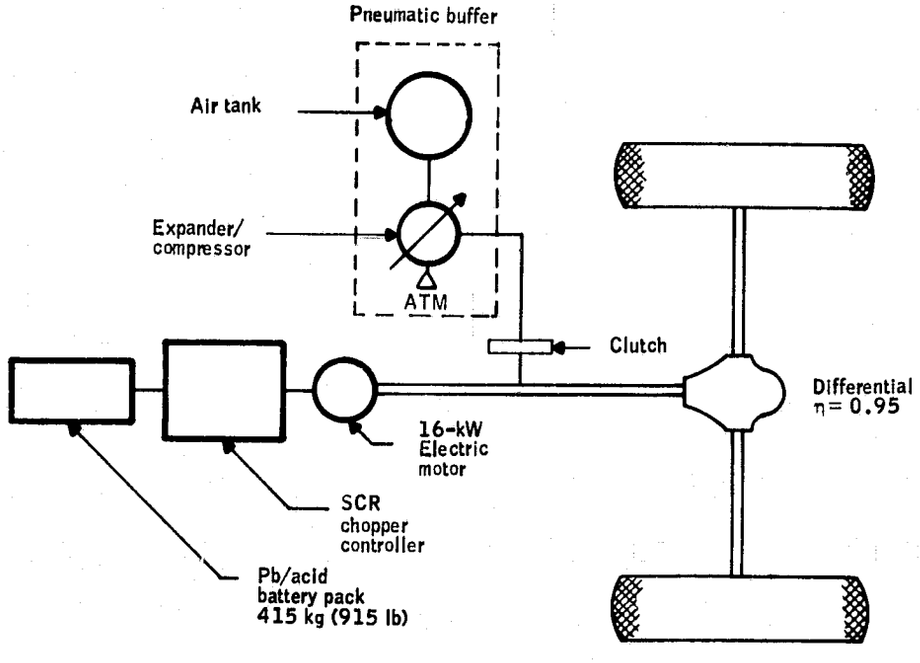

Figure 22.-Model of electric vehicle with pneumatic buffer.

where

W = work of expansion from p_1 to p_2

p_1 = pressure at state 1

p_2 = pressure at state 2

p_a = ambient pressure

V_B = accumulator volume

n = C_p/C_v, ratio of specific heats for air.

As in the hydropneumatic case, the pressure schedule of the accumulator is chosen to be a function of vehicle velocity only and follows the vehicle kinetic energy. The resulting equation for the pressure schedule of the accumulator is:

$$v = \left\{ \frac{v_{88}^2 \left[p_0 - p + p_a \frac{n-1}{n} \left(p^{1/n} - p_0^{1/n} \right) \right]}{p_0 - p_{88} + p_a \frac{n-1}{n} \left(p_{88}^{1/n} - p_0^{1/n} \right)} \right\}^{1/2} \tag{31}$$

where

v = vehicle velocity at accumulator pressure p

v_{88} = maximum vehicle velocity (88 km/h) (55 mi/h)

p_0 = accumulator pressure at zero velocity

p_a = ambient pressure

p = accumulator pressure at velocity v

p_{88} = accumulator pressure at velocity v_{88}

n = C_p/C_v

The maximum displacement of the compressor/expander occurs at a vehicle velocity of 88 km/h (55 mi/h) and can be computed from the following equation (ref. 3):

$$D = \frac{p\,(n-1)}{S\,p_a \left[1 - \left(\frac{p_{88}}{p_a} \right)^{\frac{n-1}{n}} \right]} \tag{32}$$

where

D = compressor/expander displacement

P = braking power at 88 km/h (55 mi/h)

n = C_p/C_v

p_a = ambient pressure

p_{88} = accumulator pressure at 88 km/h (55 mi/h)

S = compressor/expander speed at 88 km/h (55 mi/h)

The maximum accumulator pressure, p_0, is limited by the temperatures available from single-stage compressors and is set at 9.31×10^5 Pa (135 psia). The compressor/expander speed is set at its maximum value of 3600 rpm at 88 km/h (55 mi/h). The power-handling requirement of the compressor/expander at 88 km/h (55 mi/h) is found from the equation (evaluated at 88 km/h) (55 mi/h):

$$P = \left(\frac{dW}{dp}\right)\left(\frac{dp}{dv}\right)\left(\frac{dv}{dt}\right) \qquad (33)$$

where

$\left(\frac{dW}{dp}\right)$ = rate of change in accumulator energy with pressure - computed from Equation (30)

$\left(\frac{dp}{dv}\right)$ = change in accumulator pressure with velocity - computed from Equation (31)

$\left(\frac{dv}{dt}\right)$ = change in vehicle velocity with time, driving cycle - dependent

The power-handling requirement of the compressor/expander is a linear function of the accumulator volume. Therefore, selection of an accumulator volume sizes the compressor/expander, assuming the values of p_0 and p_{88} are known. The value of p_0 is set at 9.31×10^5 Pa (135 psia), the value of p_{88} is a tradeoff between accumulator volume (and therefore accumulator mass) per unit of stored energy and compressor/expander displacement (and therefore compressor/expander mass) per unit of stored energy. Large values of p_{88} decrease compressor/expander displacement but increases the accumulator volume.

Using the value for p_1 of 9.31×10^5 Pa (135 psia) and letting $p_2 = p_{88}$ vary, Equation (30) can be solved for energy storage capacity per unit accumulator volume. Use of Equation (32) and (33) allows calculation of compressor/expander displacement per unit

accumulator volume. Using an accumulator mass of 727 kg per m^3 of accumulator volume, and a compressor/expander mass of 530 kg per m^3 displacement allows computation of the storage capacity of the buffer system per unit system mass. The results are shown in Figure 23. It shows that a choice of 3.9×10^5 Pa (56 psi) maximizes the accumulator storage capacity per unit weight, and is therefore the design value selected.

Using a pressure of 3.9×10^5 Pa (56 psi) at 88 km/h (55 mi/h) and Equation (31) allows computation of the buffer pressure as a function of the vehicle velocity as shown in Figure 24. The accumulator capacity, accumulator maximum charge rate (at 88 km/h), and buffer system mass are plotted as a function of buffer volume for the selected design in Figures 25 through 27. The expander/compressor performance model includes leakage losses, friction losses, inertial losses, and compression losses. These losses are computed with the following equations as:

$$\text{Leakage loss} = 3.08 \times 10^{-6} P_r p^{1/2}, \text{ (watts)} \quad (34)$$

$$\text{Friction loss} = 1.25 \times 10^{-11} P_r(\omega)p, \text{ (watts)} \quad (35)$$

$$\text{Inertial loss} = 3.72 \times 10^{-9} P_r(\omega^2), \text{ (watts)} \quad (36)$$

$$\text{Compression loss} = 1.50 \times 10^{-10} (\omega^2)p\ P/P_r, \text{ (watts)} \quad (37)$$

where

P_r = rated power output of the expander/compressor at 3600 rpm and 3.9×10^5 Pa (56 psi), W

P = instantaneous power output rate of the expander/compressor, W

p = buffer pressure, Pa

ω = expander/compressor speed, rpm

The vehicle is required to accept all of the available braking energy from 88 km/h (55 mi/h) after a 10-s coast. Figures 25 through 27 define a set of possible buffer designs which can be used to determine which design meets the above requirements. Figure 28 shows the results of the analysis, with net excess braking energy plotted versus accumulator volume. The net excess braking energy is the difference between the braking energy available at the driveshaft during braking and what the energy buffer system can accept. The design point is zero net excess braking energy; thus, an accumulator volume of 0.86 m^3 (30.4 ft^3) is required.

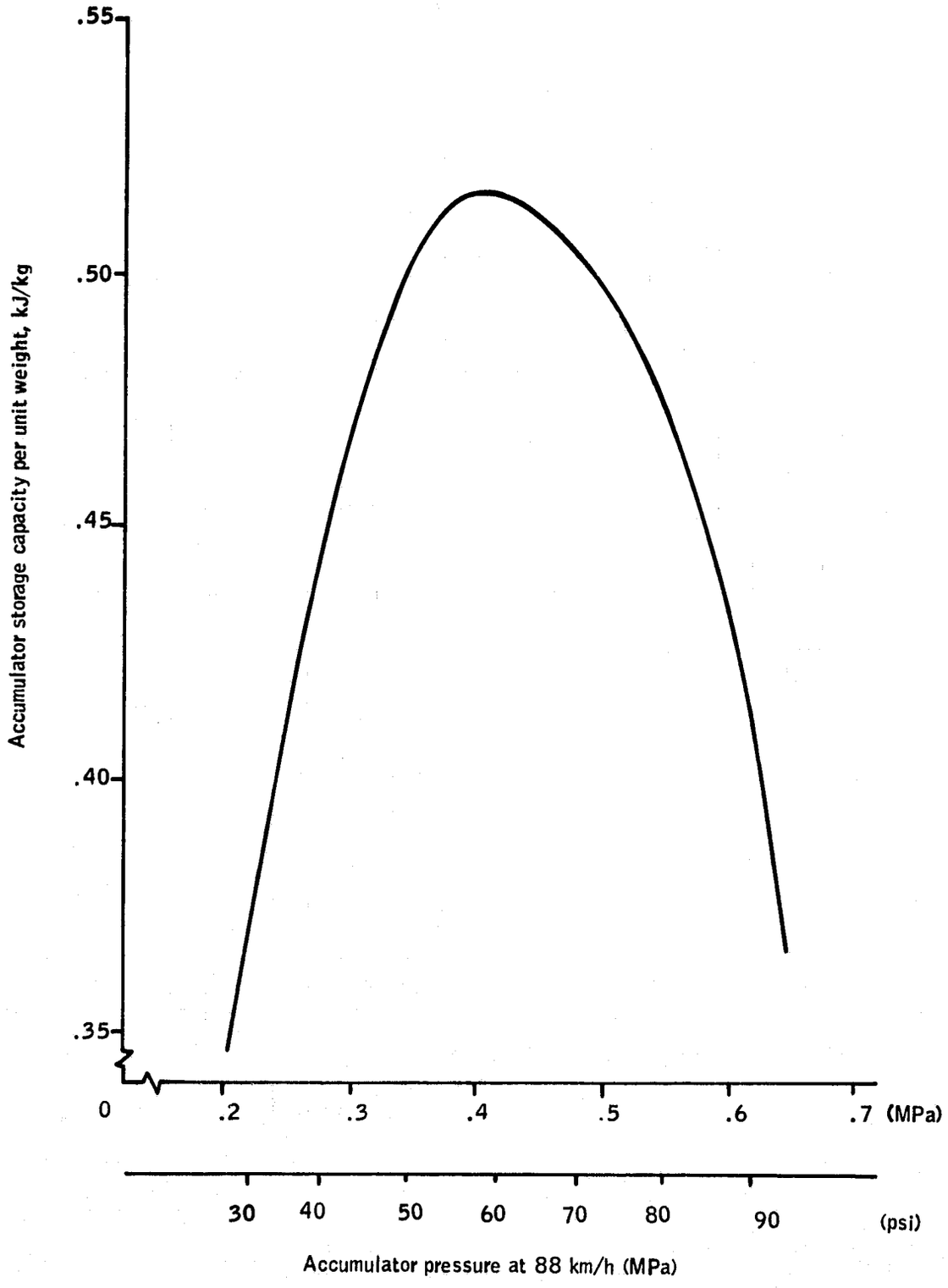

Figure 23.-Pneumatic accumulator specific energy capacity versus minimum accumulator pressure.

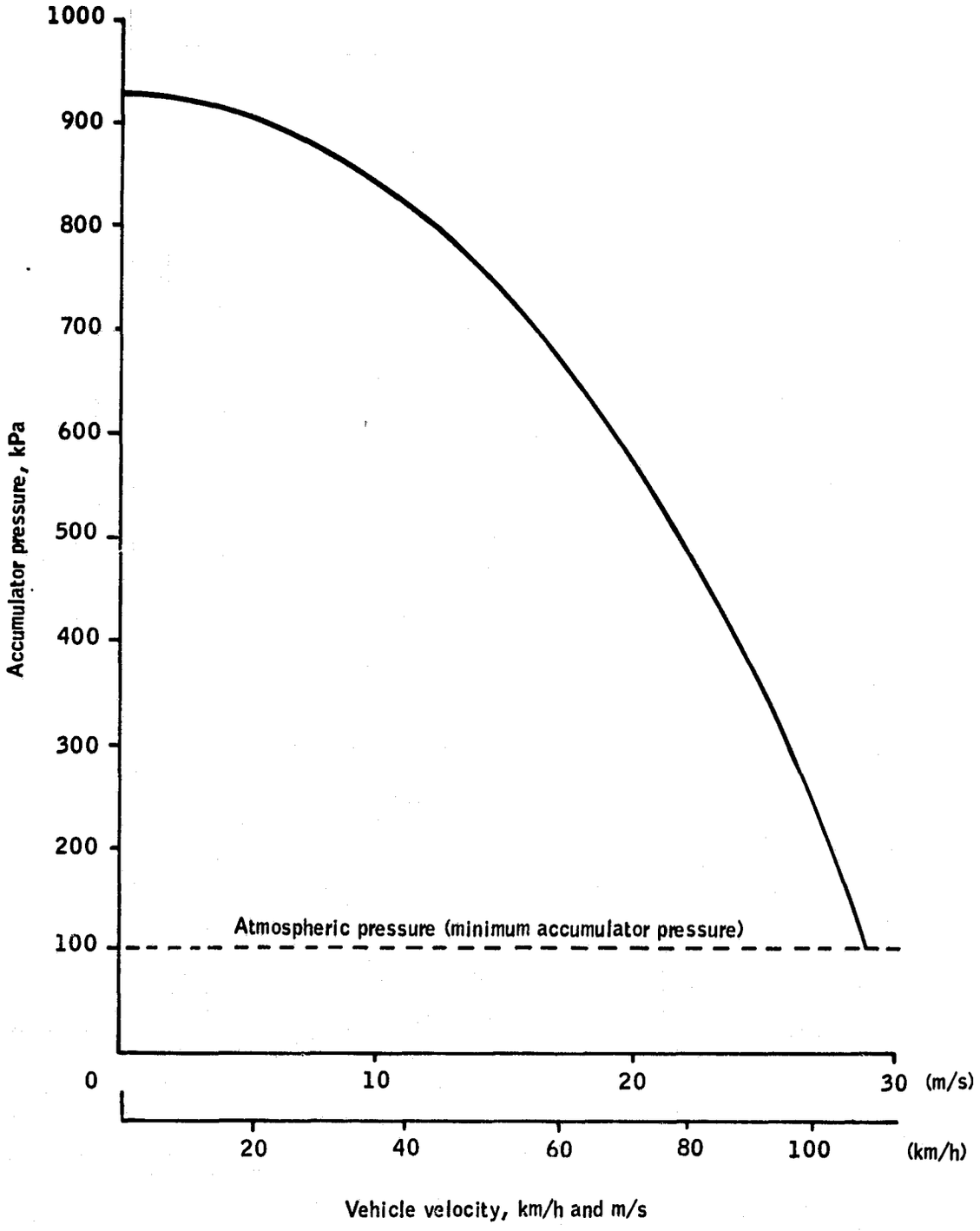

Figure 24.-Pneumatic accumulator system pressure as a function of vehicle velocity.

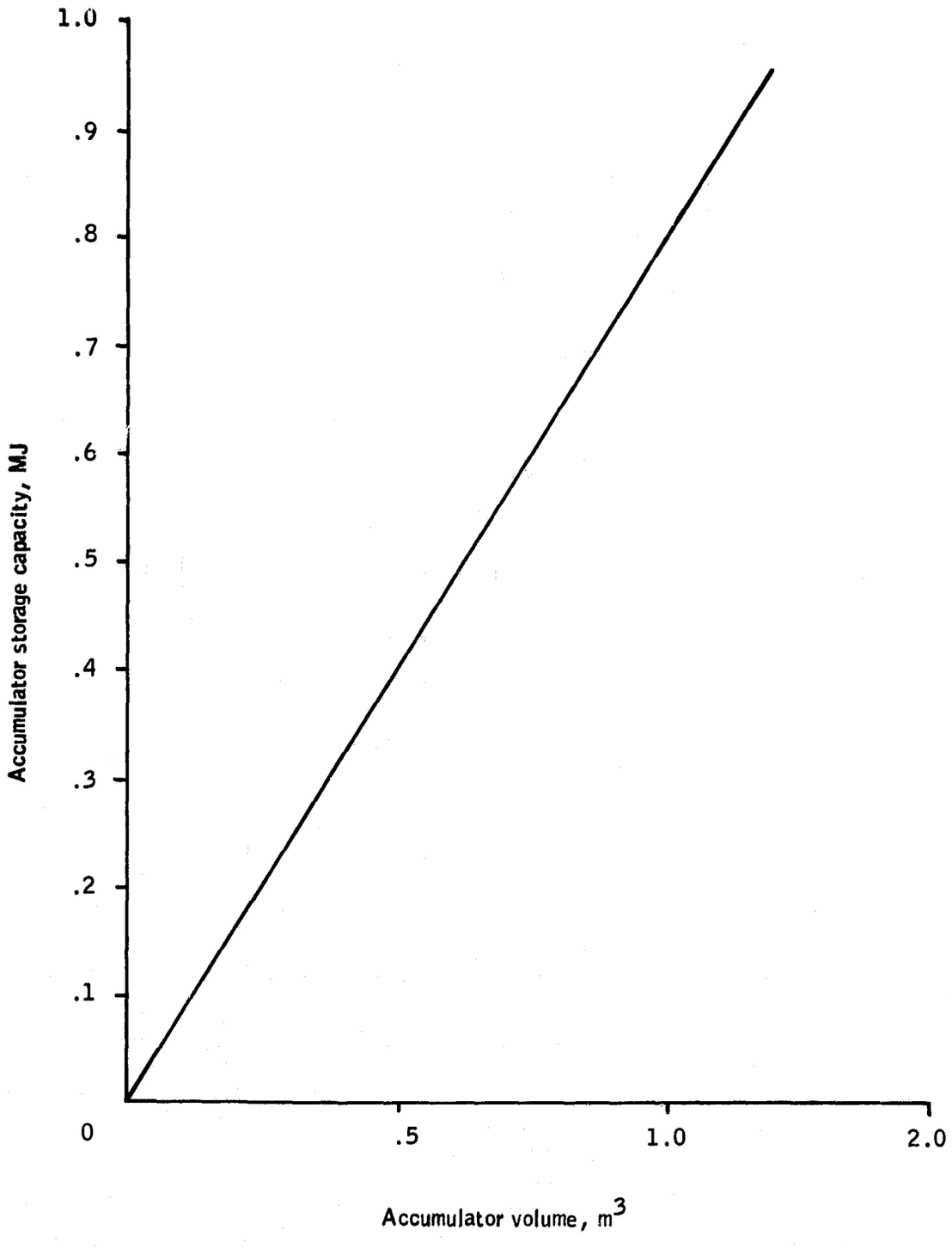

Figure 25.-Pneumatic accumulator storage capacity as a function of accumulator volume.

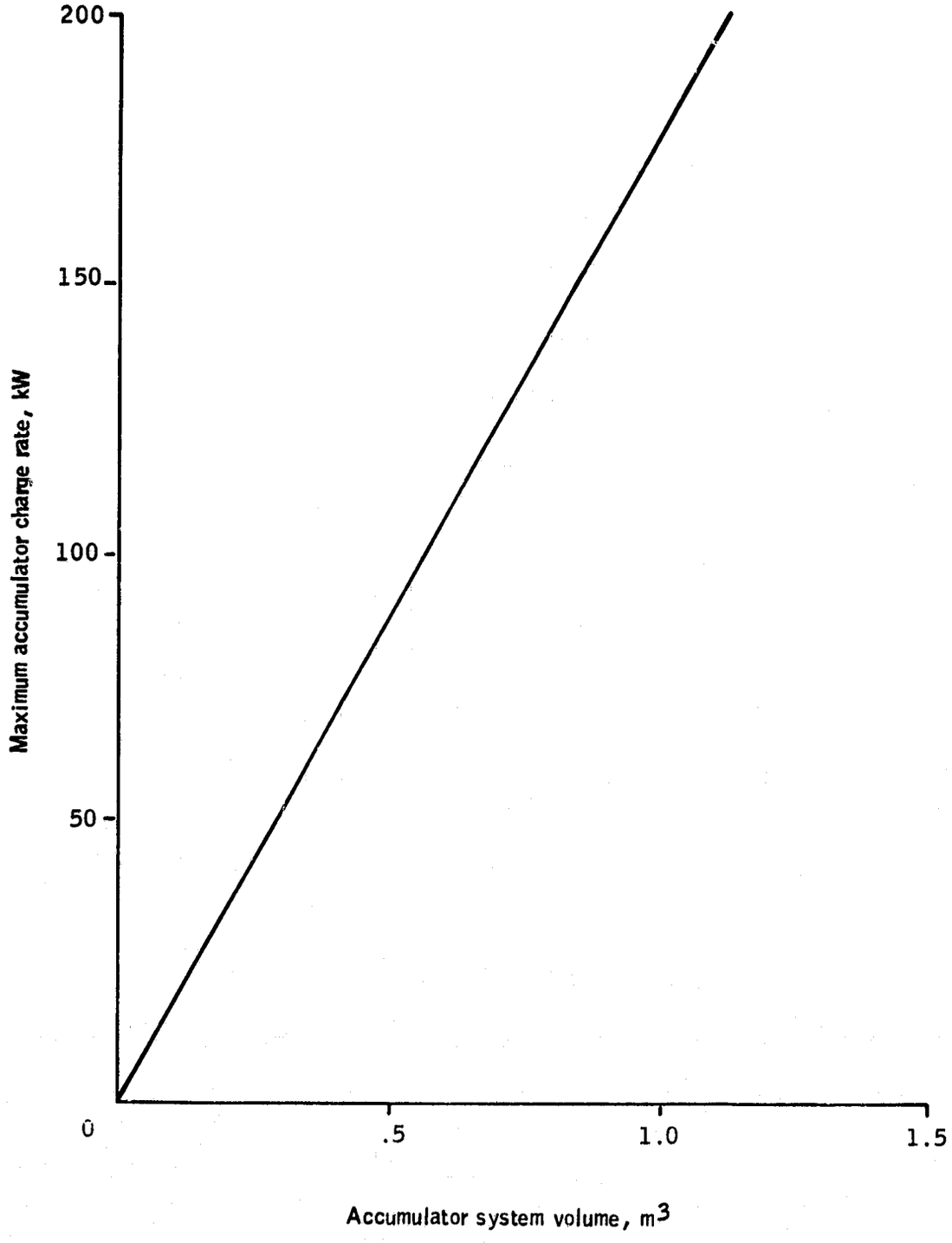

Figure 26.-Pneumatic accumulator system charge rate as a function of accumulator volume.

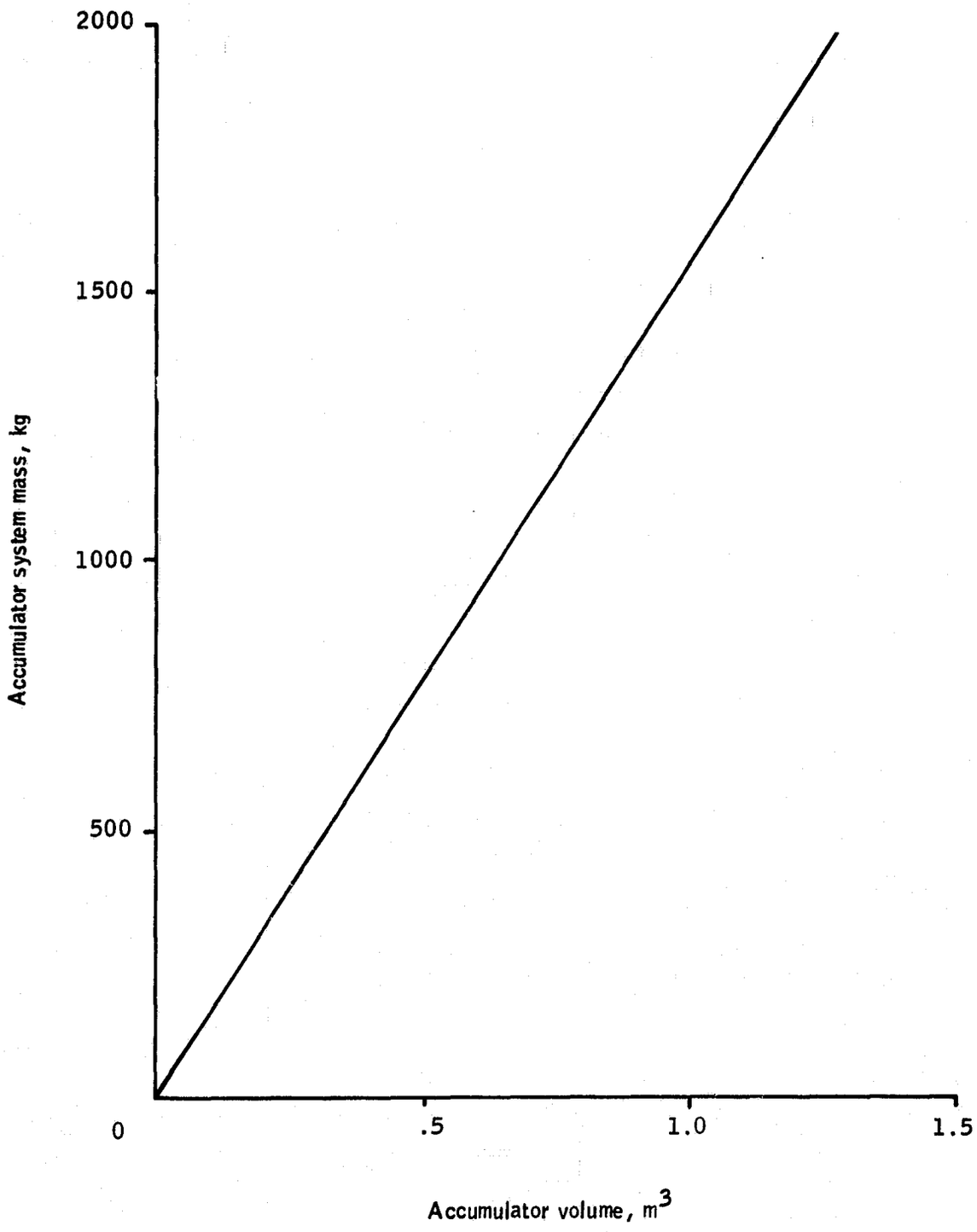

Figure 27.-Pneumatic accumulator system mass as a function of accumulator system volume.

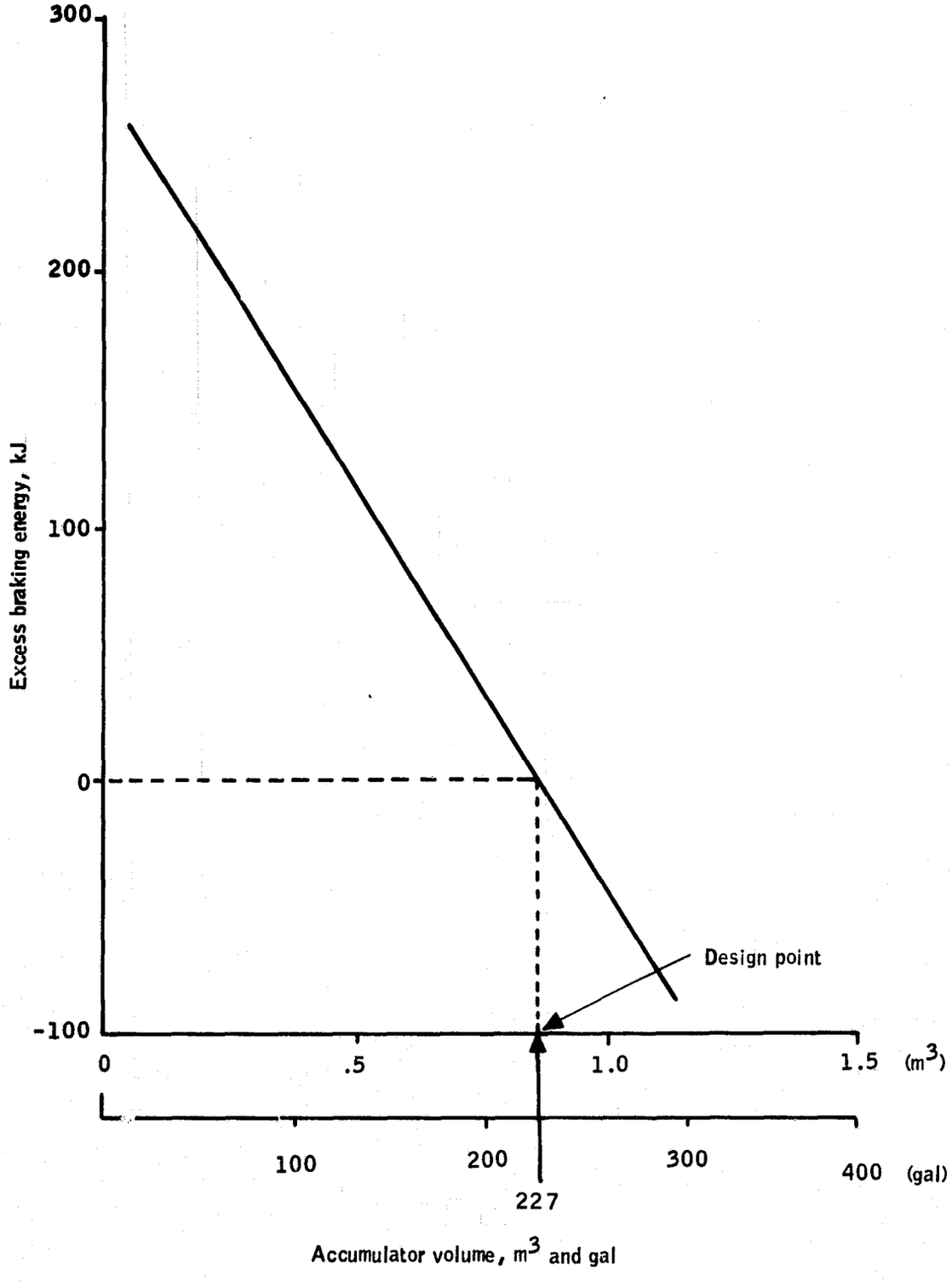

Figure 28.-Excess braking energy versus accumulator volume for the pneumatic accumulator system.

The resulting buffer system weighs 1332 kg (2937 lb) (nearly the same as the baseline vehicle), can store 676 kJ, and has a maximum charge rate of 151 kW (at 88 km/h). By contrast, the hydropneumatic buffer system had a weight of 111 kg, a maximum storage capacity of 368 kJ, and a maximum charge rate of 81 kW. The large capacity and charge rate of the pneumatic accumulator is a direct result of the requirement that the buffer be capable of accepting all of the braking energy from an 88-km/h (55 mi/h) stop. Putting a buffer in the vehicle increases the vehicle weight, thus increasing the recoverable braking energy. The buffer size must then be increased to accept the extra braking energy. The results of the pneumatic buffered vehicle are shown in Table 10.

TABLE 10.-BUFFERED VEHICLE PERFORMANCE - PNEUMATIC BUFFER (80% BATTERY DISCHARGE)

Parameter	Electric vehicle with regenerative braking	Hydropneumatic buffer vehicle	Pneumatic buffer vehicle
Range,[a] km	80.6[b], 89.0[c]	83.5	44.5
Buffer charge rate, kW	66.0	81.0	151.0
Buffer discharge rate, kW	32.0	13.8	23.8
Buffer weight, kg	0	111.3	1332.0
Maximum battery discharge, kW	32.0	16.1	29.7

[a] Straight electric vehicle range = 68.5 km
[b] Regeneration fraction = 0.7
[c] Regeneration fraction = 1.067

Electric Vehicle With Spring Buffer

This concept was modeled as shown in Figure 29 which is a simplified version of Figure 10. In this system, hydraulic fluid is stored under pressure generated by a spring-loaded hydraulic cylinder. The fluid is pumped into or taken out of the cylinder by a hydraulic motor/pump as with the hydropneumatic buffer concept.

The spring buffer system thus consists of an accumulator (a nested set of metallic springs), a hydraulically operated piston, and a variable-displacement hydraulic motor/pump. The energy is

stored in the potential energy of the springs in torsion. The defining equation for the springs is:

$$W = 5.5 \times 10^{-4} \frac{M}{G} (T_2^2 - T_1^2) \qquad (38)$$

where

W = energy of expansion from T_1 to T_2, J

M = spring mass, kg

G = spring modulus of elasticity, Pa

T_2 = shear stress at state 2, Pa

T_1 = shear stress at state 1, Pa

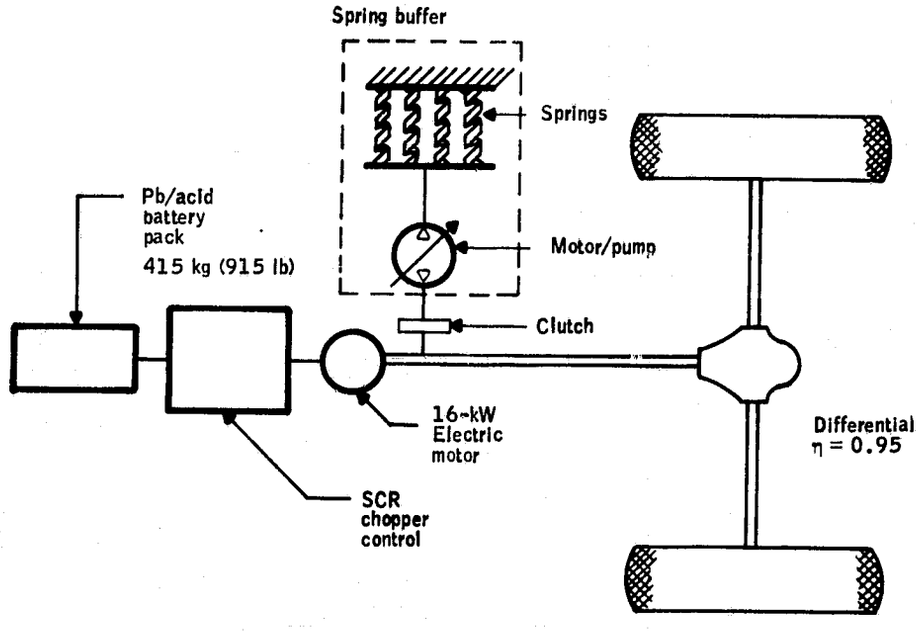

Figure 29.-Model of electric vehicle with a spring buffer.

The value of T was assumed to be 30 times the pressure in the piston. As in the two previous systems, the energy content of the buffer was chosen to follow the change in kinetic energy of the vehicle. The resulting equation for the pressure schedule of the piston therefore becomes:

$$p = \left[p_0^2 - \frac{v^2}{v_{88}^2} \left(p_0^2 - p_{88}^2 \right) \right]^{1/2} \qquad (39)$$

where

p = pressure at velocity v

p_0 = pressure at zero velocity

v = vehicle velocity

v_{88} = maximum vehicle velocity, 88 km/h (55 mi/h)

p_{88} = pressure at v_{88}

The displacement of the motor/pump is calculated from:

$$D = Pow/Sp_{88} \qquad (40)$$

where

D = motor pump maximum displacement

S = motor pump speed at 88 km/h (55 mi/h)

p_{88} = piston pressure at 88 km/h (55 mi/h)

Pow = braking power at 88 km/h (55 mi/h)

The value of p_0 was set at 20.7×10^6 Pa (3000 psi) based on the limitations of available motor/pumps. The pressure p_{88} was a tradeoff between motor/pump size and spring mass. Based on analysis similar to that performed for the pneumatic buffer system, and using a mass of 6500 kg/m^3 displacement for the motor/pump, the minimum value of accumulator storage capacity per unit mass occurs at a value for p_{88} of 7.5×10^6 Pa (1100 psi). These results are shown graphically in Figure 30.

Using a value of p_0 of 20.7×10^6 Pa (3000 psi), p_{88} of 7.5×10^6 Pa (1100 psi), Equation (39) allows computation of piston pressure as a function of vehicle velocity. The results are plotted in Figure 31. The accumulator capacity, accumulator maximum discharge rate (at 88 km/h), and buffer system mass are plotted as a function of spring mass for the selected design in Figures 32 through 34.

The motor/pump model includes leakage losses, friction losses, viscous losses, and compression losses. For a motor/pump rated at 7.5×10^6 Pa (1100 psi) and 3600 rpm, these losses are computed with the following equations as:

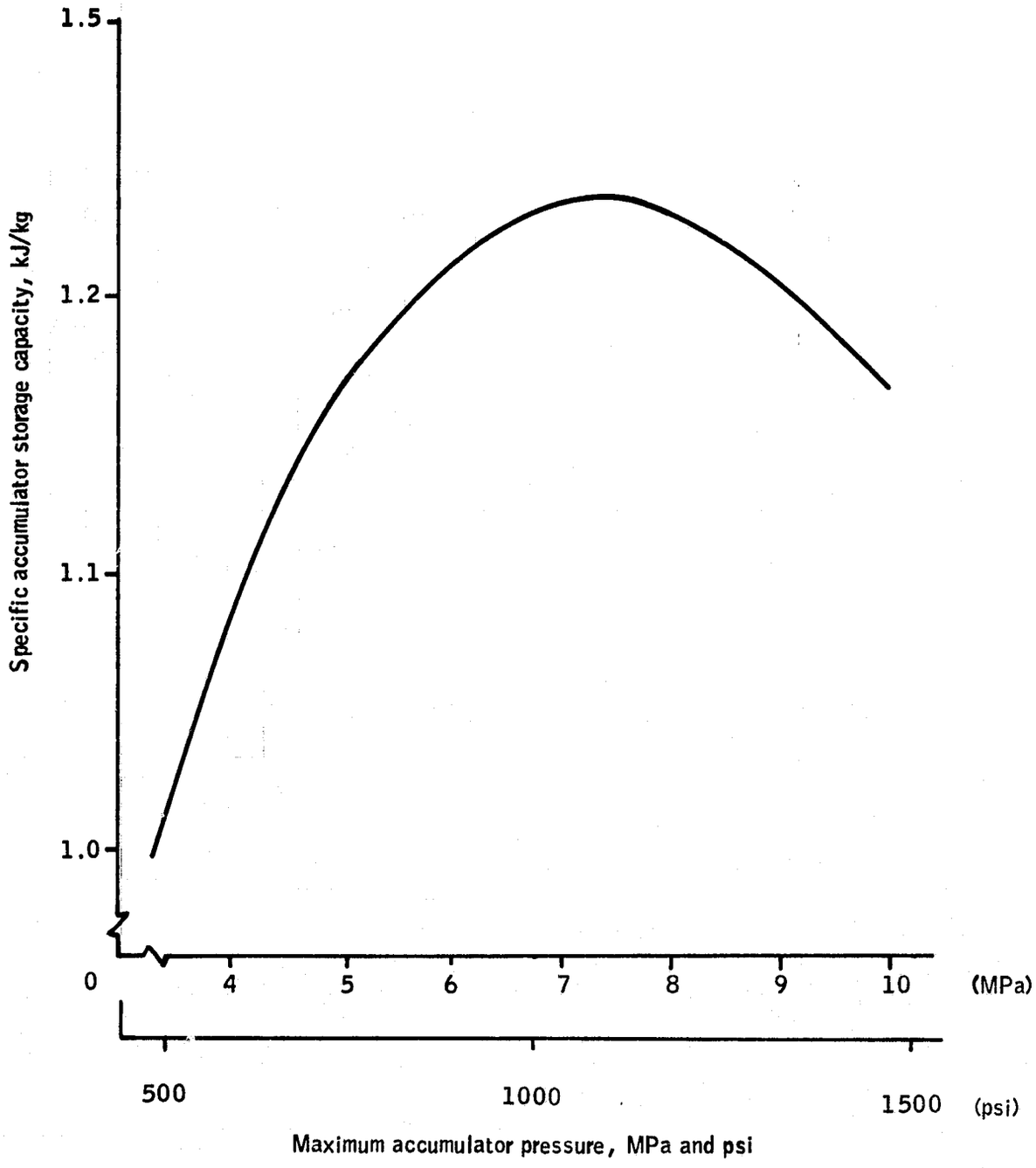

Figure 30.-Specific accumulator energy capacity as a function of maximum accumulator pressure for the spring/electric vehicle.

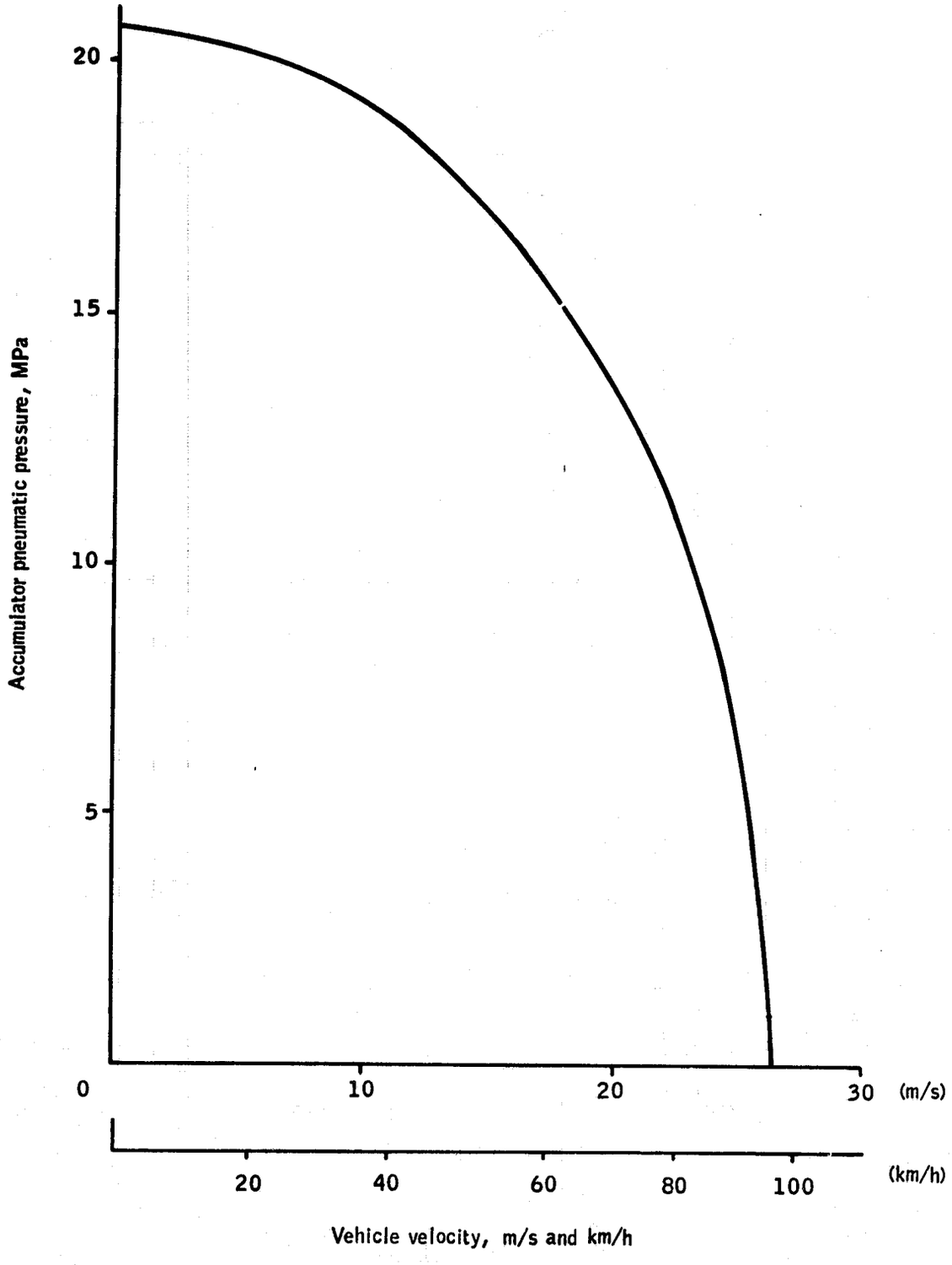

Figure 31.-Spring accumulator system pressure as a function of velocity for the spring/ electric vehicle.

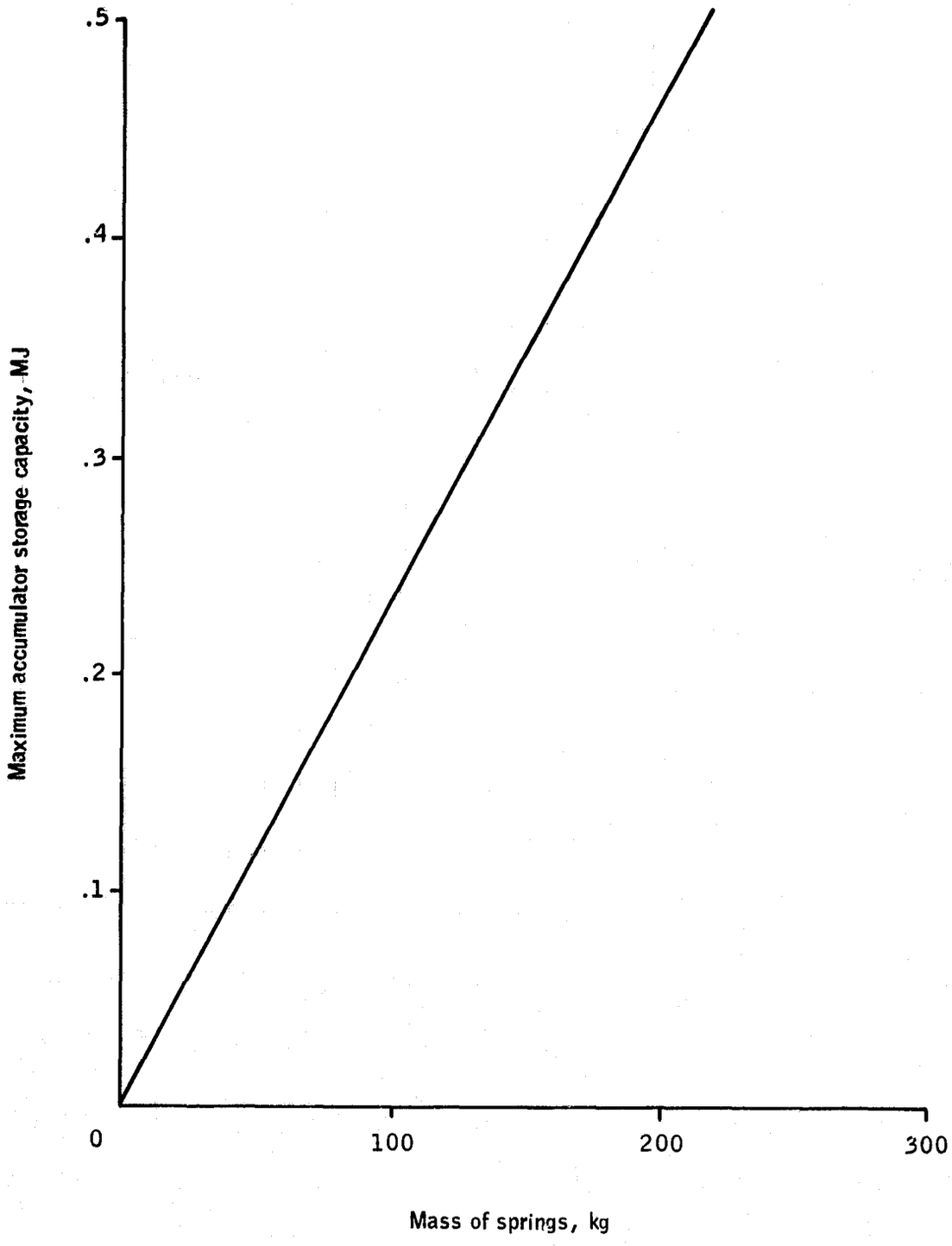

Figure 32.-Accumulator storage capacity versus spring system mass for the spring/electric vehicle.

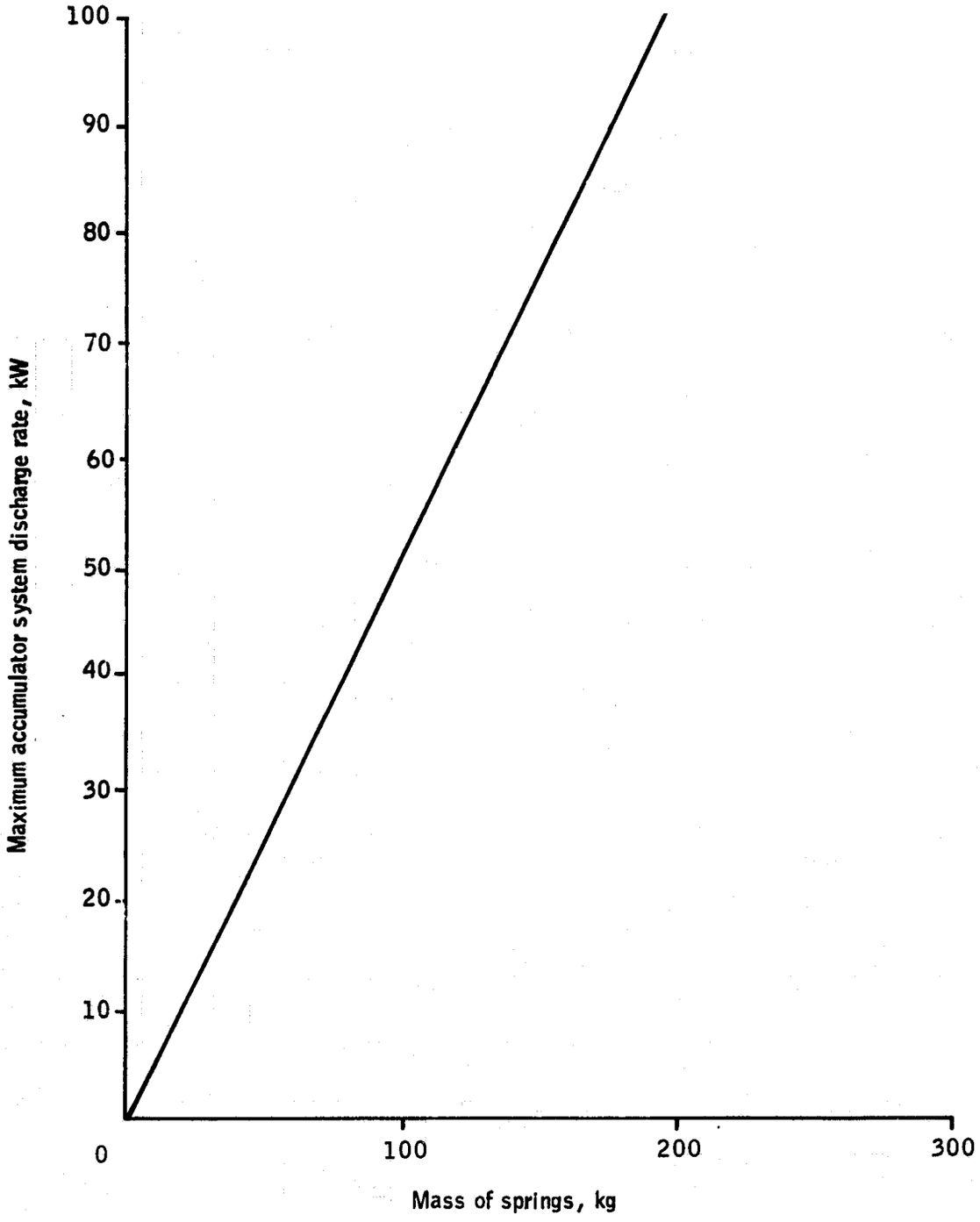

Figure 33.-Maximum accumulator discharge/charge rate versus spring system mass for the spring/electric vehicle.

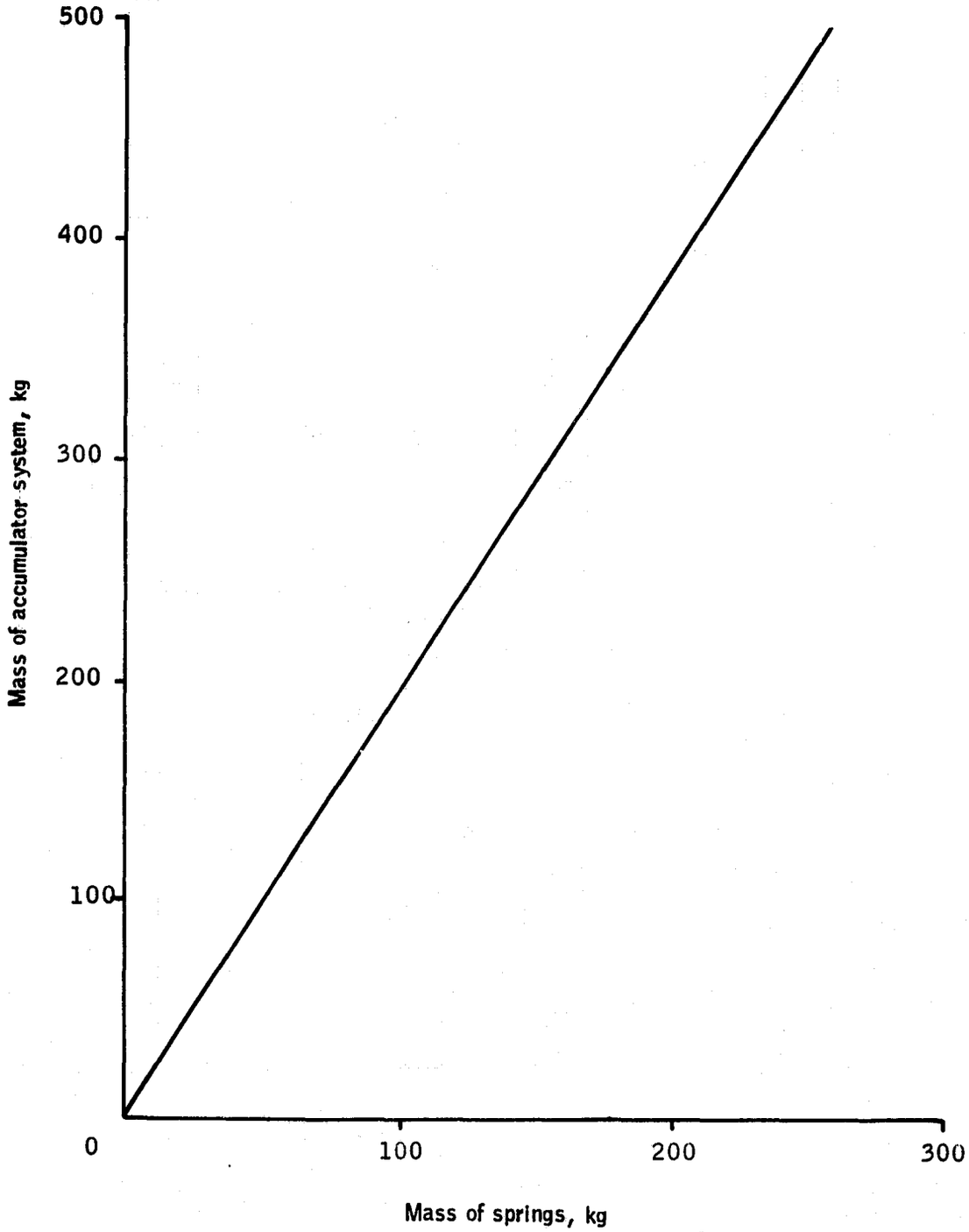

Figure 34.-Accumulator system mass as a function of spring mass for the spring/electric vehicle.

$$\text{Leakage loss} = 3.24 \times 10^{-6}\ P_r p^{1/2},\ \text{(watts)} \quad (41)$$

$$\text{Friction loss} = 6.54 \times 10^{-13}\ P_r p(\omega),\ \text{(watts)} \quad (42)$$

$$\text{Viscous loss} = 3.43 \times 10^{-9}\ P_r(\omega^2),\ \text{(watts)} \quad (43)$$

$$\text{Compression loss} = 5.84 \times 10^{-12}\ p(\omega^2)\ P_0/P_r,\ \text{(watts)} \quad (44)$$

where

P_r = rated output of the motor/pump at 7.5×10^6 Pa (1100 psi) and 3600 rpm, W

p = piston pressure, Pa

ω = motor/pump speed, rpm

P_0 = instantaneous power output of the motor/pump, W

The above set of equations, along with the family of buffer designs defined by Figures 32 through 34 can be used to determine which design meets the braking requirement. Figure 35 gives the results of such an analysis, and shows that a buffer consisting of 178 kg (392 lb) of springs is required. The results of the spring-buffered vehicle performance are given in Table 11.

TABLE 11.-BUFFERED VEHICLE PERFORMANCE - SPRING BUFFER (80% BATTERY DISCHARGE)

Parameter	Electric vehicle with regenerative braking	Hydropneumatic buffer vehicle	Pneumatic buffer vehicle	Spring buffer vehicle
Range,[a] km	80.6[b], 89.0[c]	83.5	44.5	63.5
Buffer charge rate, kW	66.0	81.0	151.0	89.5
Buffer discharge rate, kW	32.0	13.8	23.8	19.9
Buffer weight, kg	0	111.3	1332.0	337.0
Maximum battery discharge, kW	32.0	16.1	29.7	21.2

[a] Straight electric vehicle range = 68.5 km
[b] Regeneration fraction = 0.7
[c] Regeneration fraction = 1.067

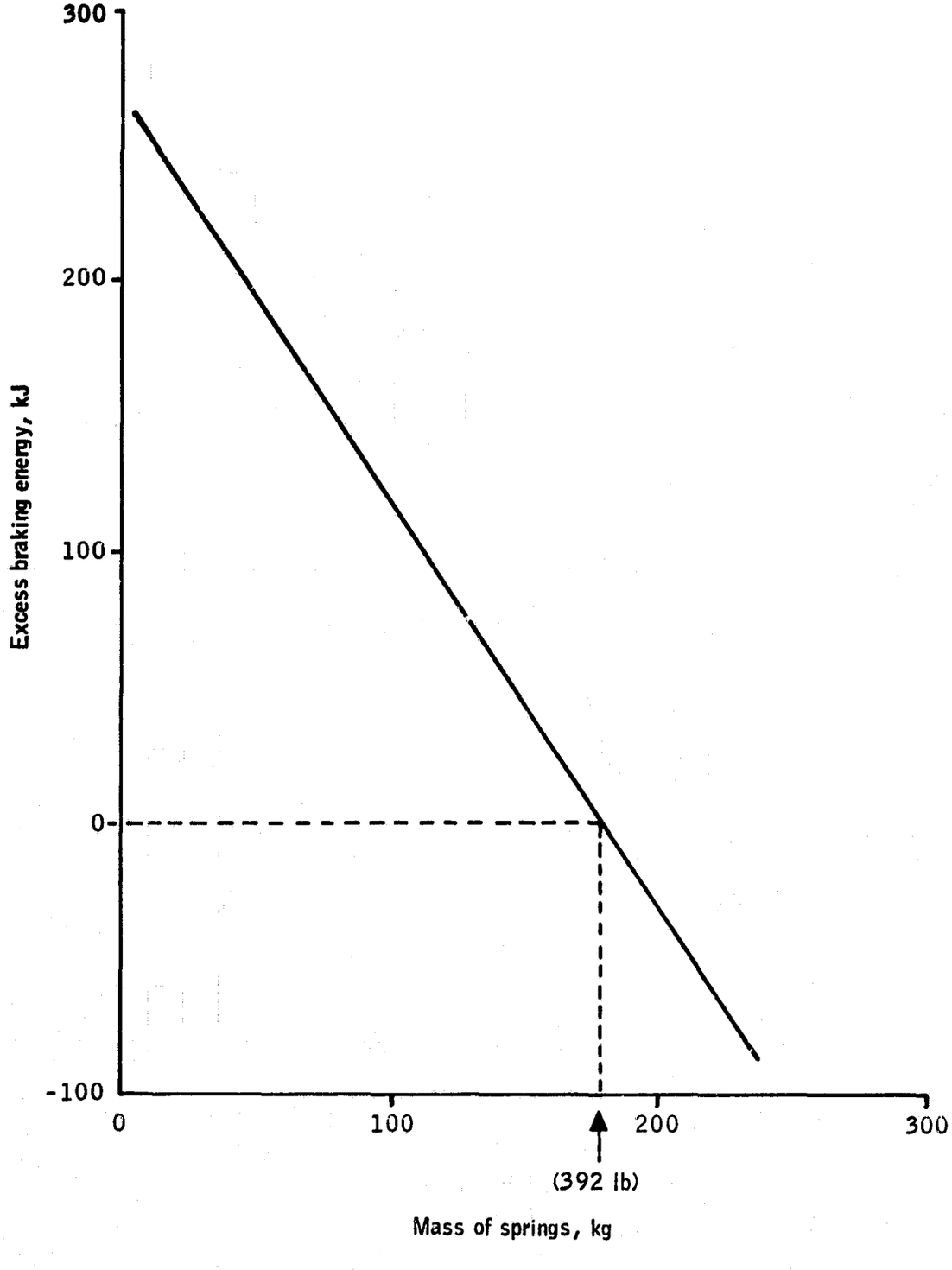

Figure 35.-Excess braking energy versus spring system mass for the spring/electric vehicle.

Electric Vehicle With Flywheel Buffer

This concept is modeled as shown in Figure 36 which is a simplified version of Figure 11.

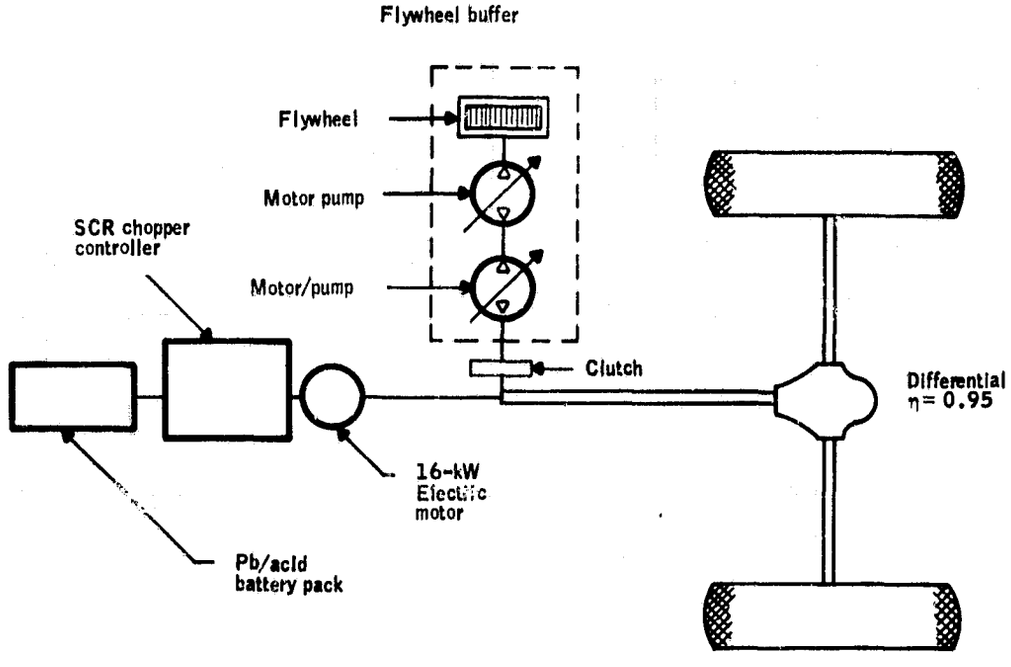

Figure 36.-Model of electric vehicle with flywheel buffer.

The flywheel buffer system consists of a flywheel and a continual variable-transmission (CVT) consisting of two hydraulic motor/pumps. The defining equation for the flywheel system is:

$$\omega = (1/2)\ I\ (\omega_f^{\ 2} - \omega_i^{\ 2}) \qquad (45)$$

where

ω = instantaneous angular velocity of the flywheel, rad/s

I = moment of inertia of the flywheel (kg-m^2)

ω_f = final angular velocity of the flywheel, rad/s

ω_i = initial angular velocity of the flywheel, rad/s

Like the other buffer systems, the flywheel speed was chosen as a function of vehicle velocity only and follws the kinetic energy profile of the vehicle. The resulting equation for the angular velocity schedule of the flywheel is:

$$\omega = \left[\omega_0^2 - \left(\frac{v}{v_{88}}\right)^2 (\omega_0^2 - \omega_{88}^2)\right]^{1/2} \quad (46)$$

where

ω = flywheel angular velocity at vehicle velocity V

ω_0 = flywheel angular velocity as zero vehicle velocity

v_{88} = maximum vehicle velocity (88 km/h) (55 mi/h)

ω_{88} = flywheel angular velocity at vehicle velocity V_{88}

v = instantaneous vehicle velocity, km/h

Representative values of ω_0 and ω_{88} are taken as 2618 rad/s (25 000 rpm) and 1047 rad/s (10 000 rpm) based on data presented by Garret Airesearch (ref. 14). Figure 37 gives the resulting flywheel schedule. The maximum pressure within the motor/pump system will be set at 20.7×10^6 Pa (3000 psi) based on the limitations of available motor/pumps. Using the above values, Figures 38 through 40 define a set of possible flywheel buffer system designs.

The dual motor/pump transmission losses consist of leakage losses, friction losses, inertial losses, and compression losses. The motor/pump maximum displacements are set by the following equations:

$$D = POW/(rps)\ (p_r) \quad (47)$$

where

D = motor pump maximum displacement, m^3

POW = rated transmission power handling ability, W

rps = motor/pump speed at rated power condition (60 rps for the pump on the differential, 83.33 rps for the pump on the flywheel)

p_r = hydraulic fluid pressure in the system at rated conditions (20.7×10^6 Pa) (3000 psi)

Once the displacement of the motor/pump was selected, Equation (47) was used to solve for the pressure in the transmission at anytime by substituting the current power value in place of the rated power and the current rps values in place of the rated rps values. The highest of the two resulting pressure values was used

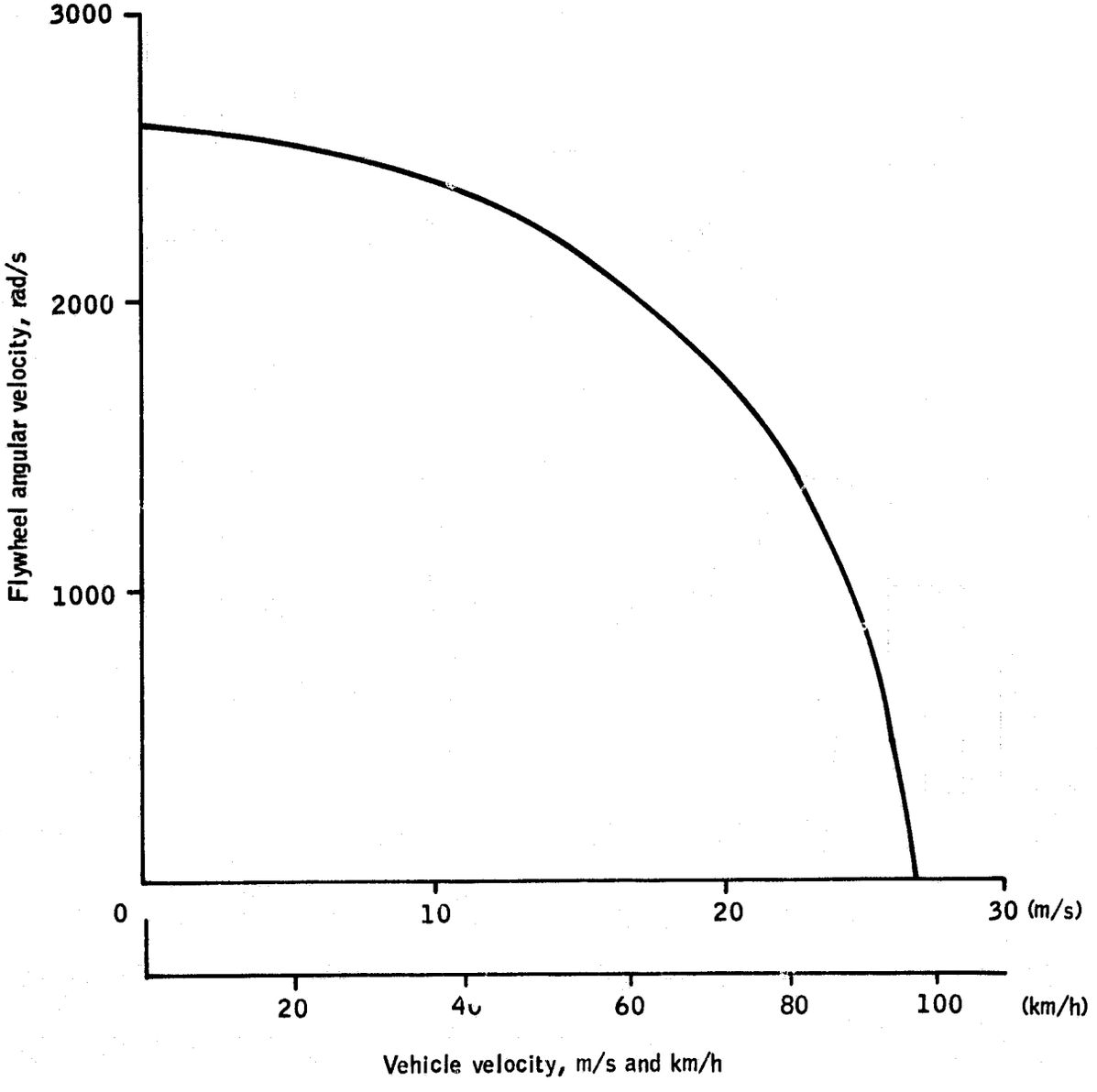

Figure 37.-Flywheel angular velocity as a function of vehicle velocity.

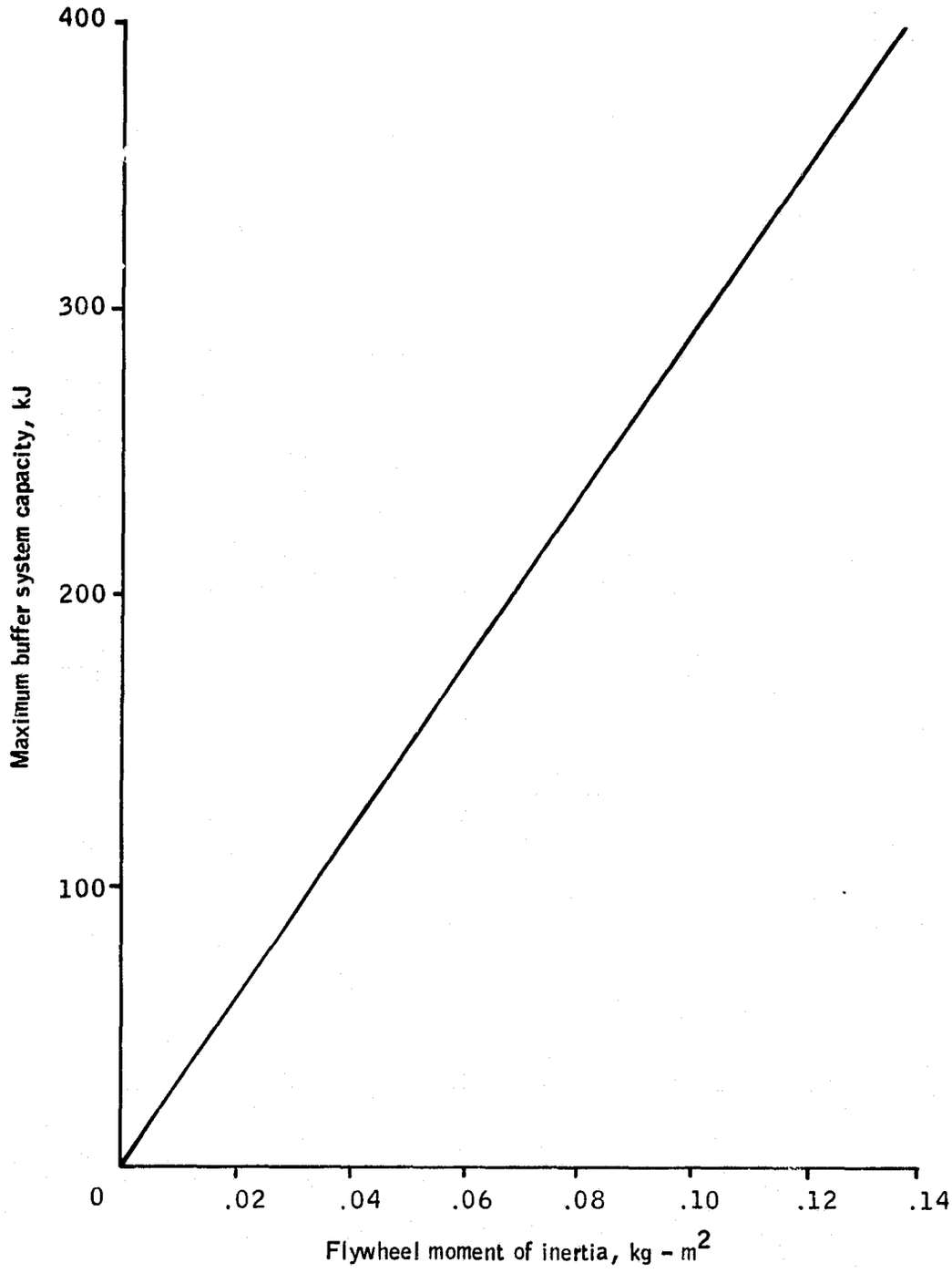

Figure 38.-Maximum buffer system storage capacity as a function of flywheel moment of inertia.

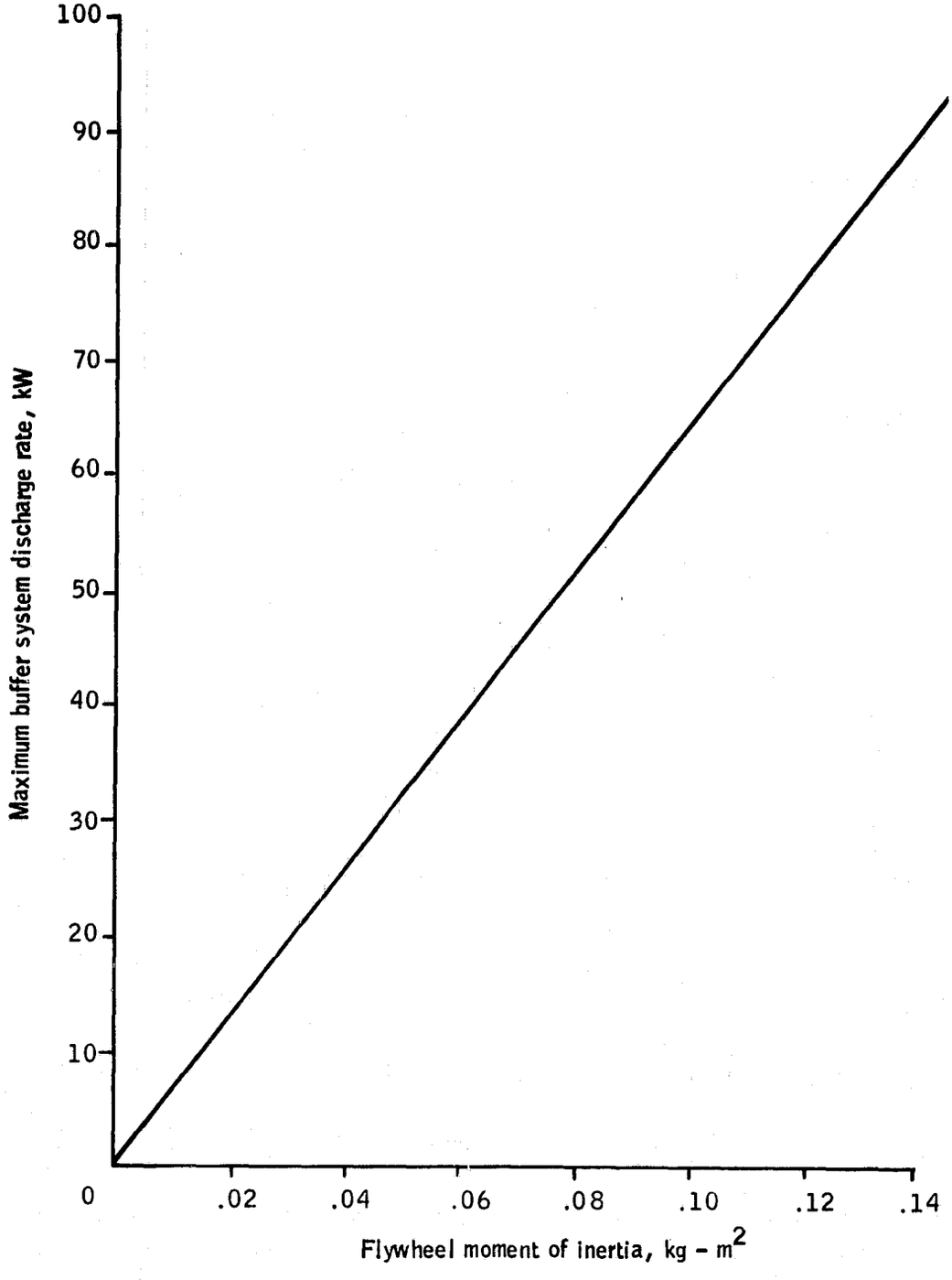

Figure 39.-Maximum buffer system discharge rate as a function of flywheel moment of inertia for the flywheel/ electric vehicle.

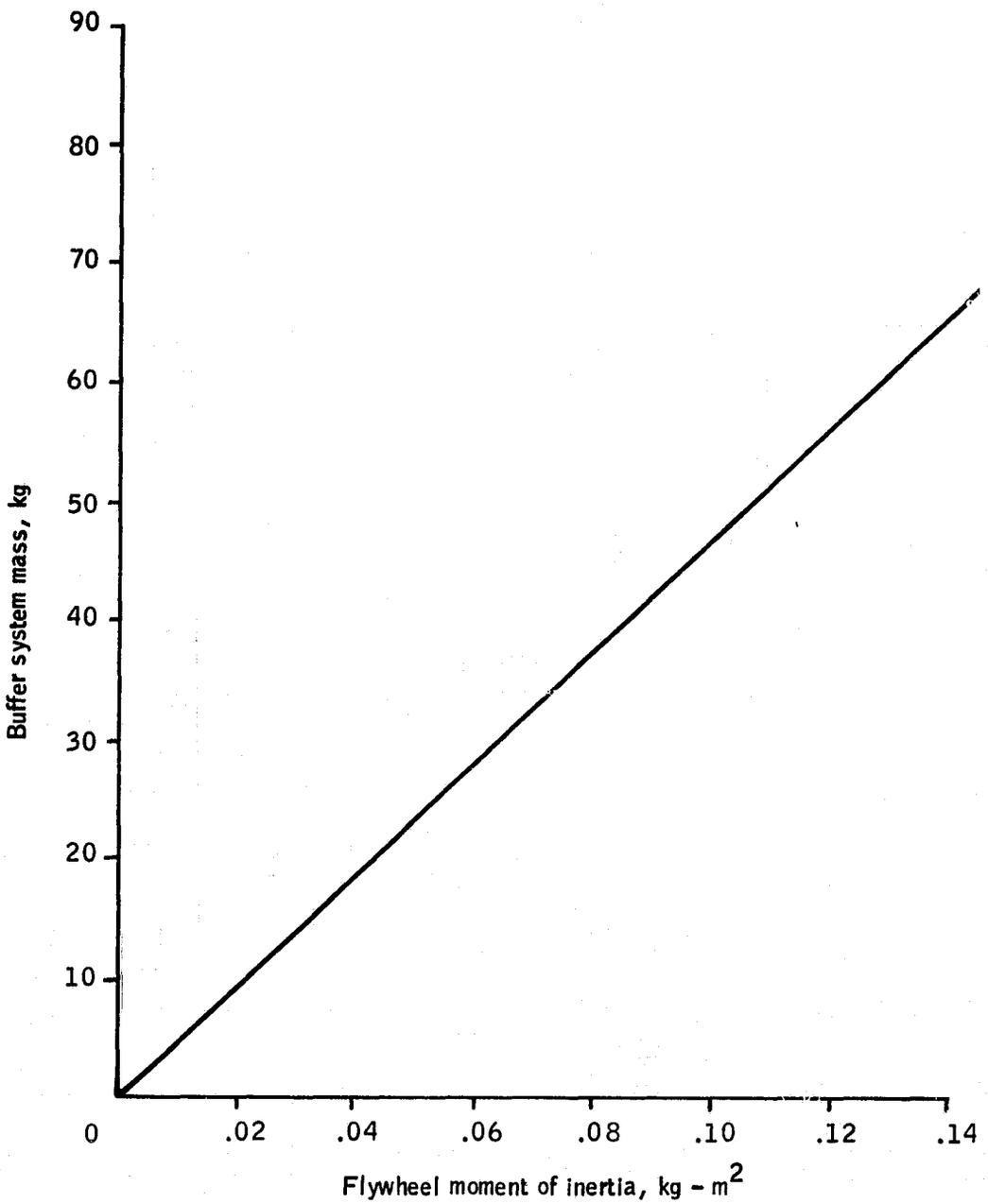

Figure 40.-Buffer system mass as a function of flywheel moment of inertia.

as the pressure in the transmission and the other motor/pump was operated at reduced displacement. The loss equations for the transmission then are:

$$\text{Leakage loss} = (1558\ D_1 + 2165\ D_2)p^{1/2}, \text{ (watts)} \quad (48)$$

$$\text{Friction loss} = 2.94 \times 10^{-4}\ (D_1\ rpm_1 + D_2\ rpm_2)P, \text{ (watts)} \quad (49)$$

$$\text{Viscous loss} = 1.54\ D_1\ rpm_1^2 + 1.11\ D_2\ rpm_2^2, \text{ (watts)} \quad (50)$$

$$\text{Compression loss} = (3.7 \times 10^{-12}\ rpm_1^2 + 1.92 \times 10^{12}\ rpm_2^2) * P * (POW/PRATED), \text{ (watts)} \quad (51)$$

where

D_1 = maximum displacement of motor/pump connected to the differential, m^3

D_2 = maximum displacement of motor/pump connected to the flywheel, m^3

rpm_1 = rpm of motor/pump no. 1 (88 km/h = 3600 rpm)

rpm_2 = rpm of motor/pump no. 2, one-half the rpm of the flywheel

PRATED = rated power carrying capacity of the transmission, W

POW = current power into the transmission, W

p = hydraulic pressure within the transmission, Pa

The above set of equations, along with the family of designs defined by Figures 38 through 40 can be used to determine which design meets the braking requirement. Figure 41 gives the results of the analysis, showing that a flywheel with a moment of inertia of 0.106 kg-m^2 is required. The results of the flywheel-buffered vehicle performance are compared with other buffers in Table 12.

Vehicle Range for Selected Buffers

The range of the vehicles equipped with the five different buffers with the three battery models is shown in Table 13.

Use of all three models results in the same range ranking for the add-on buffer concepts--hydropneumatic, flywheel, spring, pneumatic.

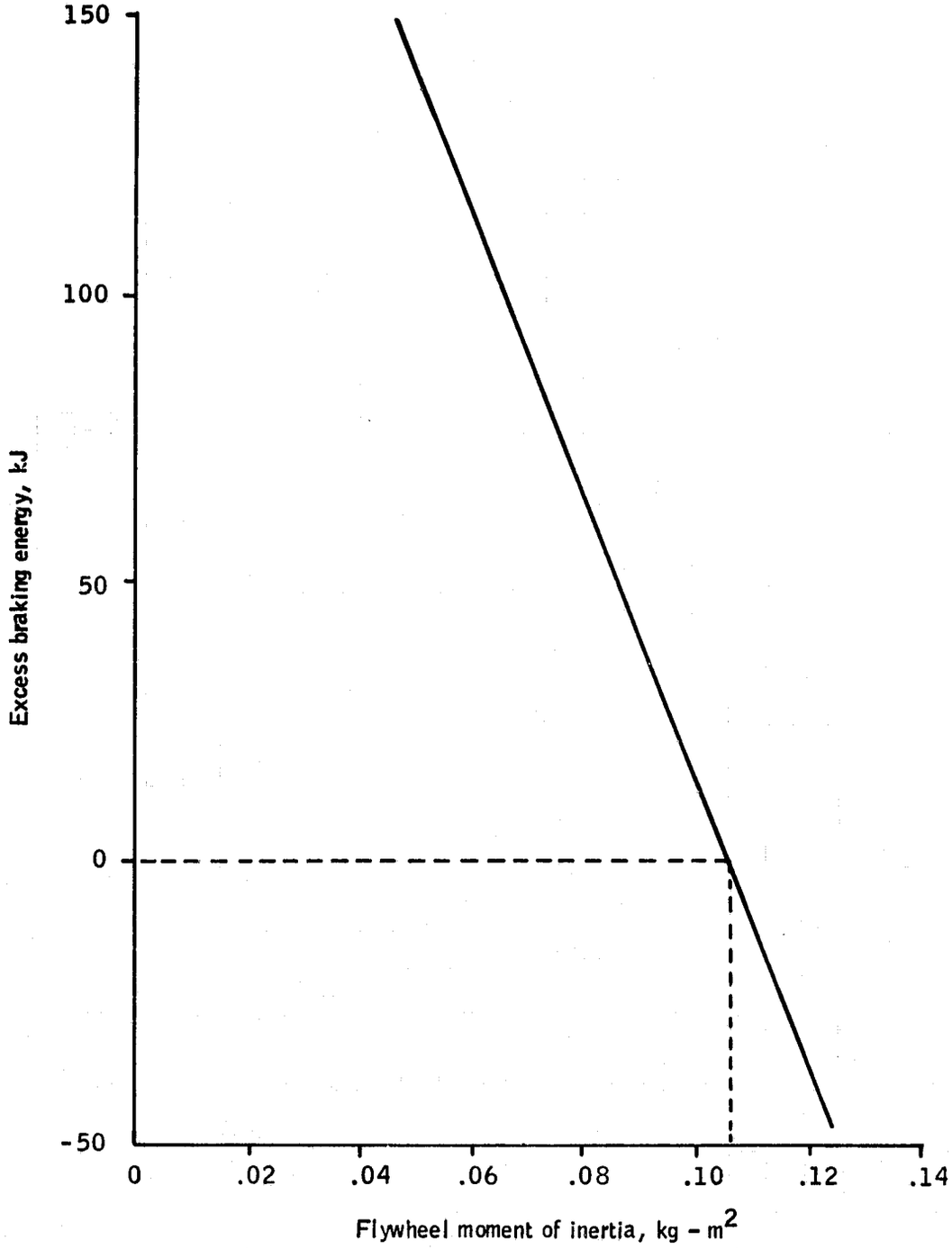

Figure 41.-Excess braking energy as a function of flywheel moment of inertia for a flywheel/electric vehicle.

TABLE 12.-BUFFERED VEHICLE PERFORMANCE - FLYWHEEL BUFFER (80% BATTERY DISCHARGE)

Parameter	Electric vehicle with regenerative braking	Hydropneumatic buffer vehicle	Pneumatic buffer vehicle	Spring buffer vehicle	Flywheel buffer vehicle
Range,[a] km	80.6[b], 89.0[c]	83.5	44.5	63.5	74.3
Buffer charge rate, kW	66.0	81.0	151.0	89.5	68.0
Buffer discharge rate, kW	32.0	13.8	23.8	19.9	11.3
Buffer weight, kg	0	111.3	1332.0	337.0	49.3
Maximum battery discharge, kW	32.0	16.1	29.7	21.2	18.1

[a] Straight electric vehicle range = 68.5 km
[b] Regeneration fraction = 0.7
[c] Regeneration fraction = 1.067

TABLE 13.-PREDICTED RANGE FOR THE VARIOUS VEHICLE SYSTEM (100% BATTERY DISCHARGE)

Vehicle	Vehicle range (km)		
	Battery model no. 1	Battery model no. 2	Battery model no. 3
Electric	66.4	68.5	85.6
Motor/generator (regenerative braking)	68.3	-	100.8[a] 111.2[a]
Hydropneumatic	133.2	103.0	104.4
Flywheel	116.8	91.6	92.9
Spring	93.4	76.1	79.4
Pneumatic	55.0	50.8	55.6

[a] Corresponds to regeneration fractions of 0.7 and 1.067, respectively.

Model no. 3, the NASA EV106 battery model, projects better relative performance for the two electric vehicles, predicting that the motor/generator vehicle will outperform all of the buffer concepts except hydropneumatic using a regeneration fraction of 0.7, and will outperform all of the buffer system using a regeneration fraction of 1.067.

Tradeoffs and Buffer Rankings

Tradeoff information for each type vehicle considered was developed. The objective was to use this tradeoff information in conjunction with the simulation results from the analytic evaluation to make a recommendation for a buffer to be designed and developed.

A general list of tradeoff parameters was identified and is shown in Table 14. Many of these parameters are in themselves subsets of more general and pertinent parameters referred to as decision factors. For example, vehicle efficiency and buffer weight can be considered to be part of the overall vehicle range factor and, while these factors will be exhibited, they will not be part of the final rating.

TABLE 14.-TRADEOFF PARAMETERS

No.	Description
1	Range
2	Vehicle efficiency
3	Total buffer energy capacity
4	Maximum buffer charge rate
5	Maximum buffer discharge rate
6	Buffer weight
7	Maximum battery discharge rate
8	Initial cost
9	Life-cycle cost
10	Safety
11	Special vehicle requirements
12	Maintenance
13	Durability and reliability
14	Driveability
15	Development time
16	Special controls
17	Special maintenance equipment

The breakdown of the tradeoff parameters grouped under each decision factor is shown in Table 15.

TABLE 15.-DECISION FACTORS

Decision factor	Parameter
Range	Vehicle efficiency Maximum buffer charge rate Maximum buffer discharge rate Buffer weight Maximum battery discharge rate
Consumer acceptance	Initial cost Safety (perceived) Driveability Life-cycle cost: - Maintenance - Repair - Durability and reliability
Potential for improvement in range	Buffer efficiency Buffer weight reduction Optimal integrated design
Development risk	Development time Special maintenance equipment Special vehicle requirements

The parameters under each decision factor were in turn considered separately for each of the five vehicle concepts except for those parameters considered to be a direct factor in determining the range and therefore redundant.

The steps involved in preparing this particular rating scheme were not always based solely on factors which were mathematically representable, but rather on factors which sometimes required an experienced assessment for which it was difficult to assign numerical values; for example, safety. The comparisons stated herein were the result of comparing the candidate buffer concepts on the basis of the factors listed, using data and experience that were available.

The four evaluation criteria or decision factors -- range, consumer acceptance, development risk, and potential for improvement in range -- are numerically weighted according to their relative subjective importance in determining overall ratings. In turn each parameter which makes up these factors is numerically weighted for each vehicle. These numerical scores are then summed for each vehicle to determine its final score for comparison.

Buffer ranking within parameter classification is done by distributing 20 points among the five buffer candidates. This allows a weight to be placed on the relative value that one candidate has over another in a particular performance area.

The key tradeoff parameters listed in Table 15 are briefly described as follows:

- Range -- Range is considered to be the most important of the criteria shown in Table 15. Since electric vehicles are of limited range, any increase in range improves vehicle acceptability considerably.

  The subset of parameters under range in Table 15 is a function of the vehicle design and each in turn affects the range directly. Therefore, they were not scored separately, which avoids including them twice in the rating matrix. Further, since one of the vehicles actually has less range than the baseline electric vehicle, change in range from the baseline vehicle was used as a scoring factor. Table 16 shows the values for each parameter under range, and Table 17 shows the actual scoring for the Δ-range factor.

- Consumer acceptance -- As with any product used by the general public, consumer acceptance plays a strong role in its success. The parameters considered to be part of this decision factor were initial buffer cost, safety, driveability, and life-cycle cost (LCC), which includes maintenance cost, repair cost, durability, and reliability considerations.

- Initial cost -- This is the sum of the cost of the components, cost of assembling the components, and the dealer mark up (17%). These costs are broken out in Tables 18 through 21 for each of the buffers considered except the electric vehicle with regenerative braking. For this concept, the replacement of the motor by a motor/generator was estimated to add 100 dollars to the cost of the vehicle.

TABLE 16.-VEHICLE RANGE PARAMETER VALUES (80% BATTERY DISCHARGE)

Parameter	Electric vehicle with regenerative braking	Hydropneumatic buffer vehicle	Pneumatic buffer vehicle	Spring buffer vehicle	Flywheel buffer vehicle
Range,[a] km	80.6[b], 89.0[c]	83.5	44.5	63.5	74.3
Buffer charge rate, kW	66.0	81.0	151.0	89.5	68.0
Buffer discharge rate, kW	32.0	13.8	23.8	19.9	11.3
Buffer weight, kg	0	111.3	1332.0	337.0	49.3
Maximum battery discharge, kW	32.0	16.1	29.7	21.2	18.1

[a] Straight electric vehicle range = 68.5 km
[b] Regeneration fraction = 0.7
[c] Regeneration fraction = 1.067

TABLE 17.-RANGE SCORING FOR THE FIVE BUFFER CONCEPTS (80% BATTERY DISCHARGE)

Parameter	Electric vehicle with regenerative braking	Hydropneumatic buffer vehicle	Pneumatic buffer vehicle	Spring buffer vehicle	Flywheel buffer vehicle
Range,[a] km	80.6	83.5	44.5	63.5	74.3
Normalized range, km	36.1	39.0	0	19.0	29.8
(Score)	5.8	6.3	0	3.1	4.8
Range,[b] km	89.0	83.5	44.5	63.5	74.3
Normalized range, km	44.5	39.0	0	19.0	29.8
(Score)	6.7	5.9	0	2.9	4.5

[a] Regeneration fraction = 0.7
[b] Regeneration fraction = 1.067

TABLE 18.-HYDROPNEUMATIC BUFFER SYSTEM ESTIMATED COST BREAKDOWN

Hydropneumatic buffer system components	Quantity	
	10K	100K
Variable-displacement motor-pump with built-in servocylinder C_1	175	125
Servovalve (V_4) -- single-stage, spool type	35	26
Solenoid valves V_1, V_3, V_5 -- cartridge types	48	36
Check valve V_2 -- cartridge type	3	2
Relief valve V_6 -- cartridge type	6	4
Filter -- screw-in	6	4
Manifold -- die-cast aluminum	21	16
Reservoir -- die-cast aluminum	9	7
Accumulator -- moulded FRP	45	35
Transducers: T_1 - selector switch	7	5
T_2 - brake RVDT	20	15
T_3 - accelerator RVDT	20	15
T_4 - C_1 LVDT	30	22
T_5 - 5000-psi pressure transducer	18	14
T_6 - rotary-pulse generator	4	3
S_1/K solenoid-actuated clutch	21	16
Control system: μp with in-out, inventory, drivers, clock	18	10
Total, $	468	355
Assembly, test, and installation labor	37	27
Total, $	505	382
Total (with 17% markup), $	591	447

TABLE 19.-SPRING BUFFER SYSTEM ESTIMATED COST BREAKDOWN

Spring-storage buffer system components		Quantity	
		10K	100K
Variable-displacement motor pump w/built-in servocylinder C_1		175	125
Servovalve (V_4) -- single-stage, spool type		35	26
Solenoid valves V_1, V_3, V_5 -- cartridge type		48	36
Check valve V_2, cartridge type		3	2
Relief valve V_6, cartridge type		6	4
Filter -- screw-in		6	4
Manifold -- die-cast aluminum		21	16
Reservoir -- die-cast aluminum		9	7
Spring storage:	Cylinder	45	35
	Spring system	360	280
	Housing	63	48
Transducers:	T_1 - selector	7	5
	T_2 - brake RVDT	20	15
	T_3 - accelerator RVDT	20	15
	T_4 - C_1 LVDT	30	22
	T_5 - 5000 psi pressure transducer	18	14
	T_6 - rotary-pulse generator	4	3
S_1-K; solenoid-actuated clutch		21	16
Control system: μP with in-out, memory, drives, clock		18	10
Total, $		909	683
Assembly, test, and installation labor		39	30
Total, $		948	713
Total (with 17% markup), $		1109	834

TABLE 20.-PNEUMATIC BUFFER SYSTEM ESTIMATED COST BREAKDOWN

Pneumatic buffer system storage	Quantity	
	10K	100K
Variable-displacement expander-compressor with servocylinder and lube oil pump	230	190
Servovalve (V_4) -- poppet type	30	22
Solenoid valves V_1, V_3, V_5, V_{7A}, V_{7B} -- cartridge type	75	55
Check valves V_2, V_8	2	2
Relief valve V_6	6	4
Filter F_1	3	2
Filter, lube oil	1	1
Muffler	4	3
Manifold -- die-cast aluminum	18	14
Receivers -- drawn steel	220	170
Transducers: T_1 - selector switch	7	5
T_2 - brake RVDT	20	15
T_3 - accelerator RVDT	20	15
T_4 - C_1 LVDT	30	22
T_5 - 200-psi pressure transducer	18	14
T_6 - rotary-pulse generator	4	3
S_1 -K Solenoid-operated clutch	21	16
Control system: μP with in-out, memories, drives, clock	18	10
Total, $	727	563
Assembly, test, and installation data	47	35
Total, $	774	598
Total (with 17% markup), $	906	700

TABLE 21.-FLYWHEEL BUFFER SYSTEM ESTIMATED COST BREAKDOWN

Flywheel buffer system components	Quantity	
	10K	100K
Variable-displacement motor/pump A	170	120
Variable-displacement motor/pump B	140	105
Electromechanical servomotors SMA, SMB (2)	84	62
Replenishing pump system	28	21
Reservoirs and interconnect -- die-cast aluminum	16	13
Flywheel and housing with seal	73	52
Transducers: T_1 - selector switch	7	5
T_2 - brake RVDT	20	15
T_3 - accelerator pedal	20	15
T_4 - SMB LVDT	30	22
T_5 - SMA LVDT	30	22
T_6 - ΔP sensor	19	15
T_7 - flywheel counter	4	3
T_8 - SMA counter	4	3
S_1/K solenoid-actuated clutch	21	16
Control system: μP with in-out, memories, drives, clock	19	11
Total ($)	685	500
Assembly, test, and installation labor	39	31
Total, $	724	531
Total (with 17% markup), $	847	621

- Perceived safety -- Safety is shown with consumer acceptance because it was considered in terms of safety from injury to the occupants of the vehicle as well as occupants of other vehicles during a collision, and maintenance personnel during maintenance.

  Even though all the vehicles would be built safely, energy stored in any manner could be viewed as a potential hazard; even the lead/acid battery common to all the candidate systems could be viewed as a safety hazard. In an accident, all concepts constitute a possible source of trouble, but each has somewhat different characteristics.

  The pressure vessels on the hydropneumatic buffer constitutes a hazard to all persons in a high-speed collision should they be ruptured and release the energy instaneously.

  The pneumatic buffer, although having the advantage of low pressure, has the disadvantages of higher temperatures and generation of a freezable condensate which constitutes a hazard.

  The spring buffer, in addition to being a fairly small high-density vehicle component, contains a high concentration of energy. Any sudden release of this energy from a collision or other accident could become unsafe.

  The flywheel buffer, although lightweight and relatively small in size, contains a spinning rotor at all vehicle velocities. As with the spring system, a sudden release of this energy could become unsafe.

- Driveability -- This is a measure of how the vehicle handles under ordinary driving conditions. The consumer must be able to make the transition to these vehicles with minimum retraining.

- Life-cycle cost -- This is defined to be the cost per kilometer of mass-produced hardware over its operating life.

  The LCC was computed, for electric vehicle with each of the candidate buffer systems, based on the guidelines developed during the course of the contract for life-cycle cost calculations shown in Table 22.

TABLE 22.-GUIDELINES FOR LIFE-CYCLE COST CALCULATIONS

No.	
1.	Costs are calculated only for the propulsion system plus the battery. Other vehicle costs, insurance, taxes, etc., are not included.
2.	Calculations are in 1978 dollars. A 2% discount factor is used.
3.	Acquisition cost is the sum of the Original Equipment Manufacturer (OEM) cost (manufacturing cost plus corporate level costs such as general and administrative, required return on investments of facilities and tooling, cost of sales, ...) of components plus the cost of assembling the components plus the dealer markup (17%).
4.	Annual production is 100,000 units.
5.	Operating costs are the sum of maintenance costs, repair costs, electricity costs, fuel cost, and primary battery storage replacement costs.
6.	The repair costs are estimates.
7.	Electricity cost is 4 cents/kWh from the wall plug.
8.	Vehicle lifetime is 10 years and 160,000 kilometers (100,000 miles).
9.	No inflation factor is included in the discount rate, since it is assumed that personal disposable income tracks inflation.
10.	Cost of finance is not included in this procedure since it is assumed that the discounted present value of the sequence of total payments would approximately equal the original purchase price.
11.	All expenses are assumed to be costed at the end of each year. Year "Zero" is reserved for those costs which must be incurred before the vehicle is operated.
12.	Scrap/salvage value is 10%.
13.	In determining the life of propulsion system components (such as a primary energy storage system, etc.), it is assumed that the "vehicle" is driven 16,000 km (10,000 miles) per year.

The LCC computed for each vehicle is shown in Table 18. The operating cost worksheet for the expected 10-year lifetime for each vehicle is shown in Tables 23 through 28. Maintenance and repair costs were also included in computing the costs.

- Durability and reliability -- It is expected, as with safety, that all buffer systems would be built with the most durable and reliable components that current state of the art permits.

  Table 29 shows the individual scoring for the parameters under consumer acceptance. The proportionate average score was obtained by summing scores for each vehicle and using that sum to score the vehicle over all parameters under consumer acceptance.

- Development risk -- This includes consideration for development time of the various buffers, special maintenance equipment which may have to be developed to maintain the vehicle over its life cycle, and special vehicle requirements or modifications which may be necessary to the baseline vehicle to fit the various buffers as to the vehicle.

  Development time is the estimated time between prototype testing and production packaging. The first row of Table 30 shows the estimates for each of the vehicles and the relative score for each type of buffer.

- Special maintenance equipment -- This results from the periodic service of the unusual components in each buffer system. For example, the hydropneumatic buffer system may require the charging of the accumulator for servicing; the flywheel may need to be evacuated, requiring vacuum equipment in the service center; pneumatic system dewatering requires special tools, etc. The second row of Table 30 shows briefly what each system may require along with scores for each in this category. The list, however, is not all-inclusive and may include maintenance equipment not easily identified in such a study as conducted on this task.

  All buffered vehicles, except the electric vehicle with regenerative braking, require some modifications to accommodate the buffers -- some, however, more than others. The third row of Table 30 shows a subjective

TABLE 23.-LIFE-CYCLE COST WORKSHEET - ELECTRIC VEHICLE WITH REGENERATIVE BRAKING (REGENERATION FRACTION = 1.067)

Parameter	Year									
	1	2	3	4	5	6	7	8	9	10
Maintenance, ¢/km										
Electric										
Battery				5.72				5.72		
Buffer										
Maintenance total										
Repair, ¢/km										
Electric (motor brush Δ)		0.18		0.18		0.18		0.18		0.18
Auxiliaries (brakes)			0.69			0.69			0.69	
Transmission										
Repair total	0	0.18	0.69	0.18	0	0.87	0	0.18	0.69	0.18
Electricity, ¢/km	0.66	0.66	0.66	0.66	0.66	0.66	0.66	0.66	0.66	0.66
Total, ¢/km	0.66	0.84	1.35	6.56	0.66	1.53	0.66	6.56	1.35	0.84
Total, $/yr	105.60	134.40	216.00	1049.60	105.60	244.80	105.60	1049.60	216.00	134.40
Life-cycle cost, $/yr										
Initial cost										
Operating cost, $/yr	105.60	134.40	216.00	1049.60	105.60	244.80	105.60	1049.60	216.00	134.40
Chassis salvage (-)										
Battery salvage (-)				-91.50				-91.50		
Totals, $/yr	105.60	134.40	216.00	958.10	105.60	244.80	105.60	958.10	216.00	134.40
Discount factor	0.980	0.961	0.942	0.924	0.906	0.888	0.871	0.853	0.837	0.820
Present value, $	103.49	129.16	203.47	885.28	95.67	217.38	91.98	817.26	180.79	110.21
Total cost, $	2834.69									
Life-cycle cost, ¢/km	1.77									

TABLE 24.-LIFE-CYCLE COST WORKSHEET - ELECTRIC VEHICLE WITH REGENERATIVE BRAKING (REGENERATION FRACTION = 0.7)

Parameter	Year									
	1	2	3	4	5	6	7	8	9	10
Maintenance, ¢/km										
Electric										
Battery				5.72				5.72		
Buffer										
Maintenance total										
Repair, ¢/km										
Electric (motor brush Δ)		0.18		0.18		0.18		0.18		0.18
Auxiliaries (brakes)			0.69			0.69			0.69	
Transmission										
Repair total	0	0.18	0.69	0.18	0	0.87	0	0.18	0.69	0.18
Electricity, ¢/km	0.72	0.72	0.72	0.72	0.72	0.72	0.72	0.72	0.72	0.72
Total, ¢/km	0.72	0.90	1.41	6.62	0.72	1.59	0.72	6.62	1.41	0.90
Total, $/yr	115.20	144.00	225.60	1059.20	115.20	254.40	115.20	1059.20	225.60	144.00
Life-cycle cost, $/yr										
Initial cost										
Operating cost, $/yr	115.20	144.00	225.60	1059.20	115.20	254.40	115.20	1059.20	225.60	144.00
Chassis salvage (-)										
Battery salvage (-)				-91.50				-91.50		
Total, $/yr	115.20	144.00	225.60	967.70	115.20	254.40	115.20	967.70	225.60	144.00
Discount factor	0.980	0.961	0.942	0.924	0.906	0.888	0.871	0.853	0.837	0.820
Present value, $	112.90	138.38	212.52	894.15	104.37	225.91	100.34	825.45	188.83	118.08
Total cost, $	2920.93									
Life-cycle cost, ¢/km	1.83									

TABLE 25.-LIFE-CYCLE COST WORKSHEET - ELECTRIC VEHICLE WITH A HYDROPNEUMATIC BUFFER SYSTEM

Parameter	Year									
	1	2	3	4	5	6	7	8	9	10
Maintenance, ¢/km										
Electric										
Battery				5.72						
Buffer	0.10	0.25	0.10	0.25	0.10	0.25	0.10	0.25	0.10	0.25
Maintenance total	0.10	0.25	0.10	5.97	0.10	0.25	0.10	0.25	0.10	0.25
Repair, ¢/km										
Control components						0.15				
Energy buffer			0.125			0.375			0.125	
Repair total	0	0	0.125	0	0	0.525	0	0	0.125	0
Electricity, ¢/km	0.70	0.70	0.70	0.70	0.70	0.70	0.70	0.70	0.70	0.70
Total, ¢/km	0.80	0.95	0.80	6.67	0.80	0.95	0.80	6.67	0.80	0.95
Total, $/yr	128.00	152.00	128.00	1067.20	128.00	152.00	128.00	1067.20	128.00	152.00
Life-cycle cost, $/yr										
Initial cost (446.94)										
Operating cost, $/yr	128.00	152.00	128.00	1067.20	128.00	152.00	128.00	1067.20	128.00	152.00
Chassis salvage (-)										
Battery salvage (-)				-91.50				-91.50		-44.60
Total, $/yr 446.94	128.00	152.00	128.00	975.70	128.00	152.00	128.00	975.70	128.00	107.40
Discount factor 1.0	0.980	0.961	0.942	0.924	0.906	0.888	0.871	0.853	0.837	0.820
Present value, $ 446.94	125.44	146.07	120.58	901.55	115.97	134.98	111.49	832.27	107.14	88.07
Total cost, $	3130.50									
Life-cycle cost, ¢/km	1.96									

TABLE 26.-LIFE-CYCLE COST WORKSHEET - ELECTRIC VEHICLE WITH A FLYWHEEL BUFFER SYSTEM

Parameter	Year									
	1	2	3	4	5	6	7	8	9	10
Maintenance, ¢/km										
Electric										
Battery			5.72				5.72			
Buffer	0.10	0.25	0.10	0.25	0.10	0.25	0.10	0.25	0.10	0.25
Maintenance total	0.10	0.25	5.82	0.25	0.10	0.25	5.82	0.25	0.10	0.25
Repair, ¢/km										
Control components						0.31				
Buffer			0.31			0.31			0.31	
Repair total	0	0	0.31	0	0	0.62	0	0	0.31	0
Electricity, ¢/km	0.79	0.79	0.79	0.79	0.79	0.79	0.79	0.79	0.79	0.79
Total, ¢/km	0.89	1.04	6.92	1.04	0.89	1.66	6.61	1.04	1.20	1.04
Total, $/yr	142.40	166.40	1107.20	166.40	142.40	265.60	1057.60	166.40	192.00	166.40
Life-cycle cost, $/yr										
Initial cost (621.27)										
Operating cost, $/yr	142.40	166.40	1107.20	166.40	142.40	265.60	1057.60	166.40	192.00	166.40
Chassis salvage (-)										-62.13
Battery salvage (-)			-91.50				-91.50			
Total, $/yr 621.27	142.40	166.40	1015.70	166.40	142.40	265.60	966.10	166.40	192.00	104.27
Discount factor 1.0	0.980	0.961	0.942	0.924	0.906	0.888	0.871	0.853	0.837	0.820
Present value, $ 621.27	139.55	159.91	956.79	153.75	129.01	235.85	841.47	141.94	160.70	85.50
Total cost, $	3625.74									
Life-cycle cost, ¢/km	2.27									

TABLE 27.-LIFE-CYCLE COST WORKSHEET - ELECTRIC VEHICLE WITH A SPRING BUFFER SYSTEM

Parameter	Year									
	1	2	3	4	5	6	7	8	9	10
Maintenance, ¢/km										
Electric										
Battery			5.72			5.72			5.72	
Buffer	0.26	0.45	0.26	0.575	0.26	0.45	0.26	0.575	0.26	0.45
Maintenance total	0.26	0.45	5.98	0.575	0.26	6.17	0.26	0.575	4.98	0.45
Repair, ¢/km										
Control components						0.19				
Chassis				0.03				0.03		
Buffer			0.531			0.531			0.531	0
Repair total	0	0	0.531	0.03	0	0.72	0	0.03	0.531	0
Electricity, ¢/km	0.92	0.92	0.92	0.92	0.92	0.92	0.92	0.92	0.92	0.92
Total, ¢/km	1.18	1.37	7.43	1.53	1.18	7.81	1.18	1.53	7.43	1.37
Total, $/yr	188.80	219.20	1188.96	244.80	188.80	1249.60	188.80	244.80	1188.96	219.20
Life-cycle cost, $/yr										
Initital cost (834.21)										
Operating cost	188.80	219.20	1188.96	244.80	188.80	1249.60	188.80	244.80	1188.96	219.20
Chassis salvage (-)										-83.42
Battery salvage (-)			-91.50			-91.50			-91.50	
Total, $/yr 834.21	188.80	219.20	1097.46	244.80	188.80	1158.10	188.80	244.80	1097.46	135.78
Discount factor 1.0	0.980	0.961	0.942	0.924	0.906	0.888	0.871	0.853	0.837	0.820
Present value, $ 834.21	185.02	210.65	1033.81	226.20	171.05	1028.39	164.44	208.81	918.57	111.34
Total cost, $	5092.49									
Life-cycle cost, ¢/km	3.18									

TABLE 28.–LIFE-CYCLE COST WORKSHEET WITH A PNEUMATIC BUFFER SYSTEM

Parameter	Year									
	1	2	3	4	5	6	7	8	9	10
Maintenance, ¢/km										
Electric										
Battery		5.72		5.72		5.72		5.72		
Buffer	0.17	0.17	0.17	0.42	0.17	0.17	0.17	0.42	0.17	0.17
Maintenance total	0.17	5.89	0.17	6.14	0.17	5.89	0.17	6.14	0.17	0.17
Repair, ¢/km										
Control components						0.25				
Chassis			0.03	0.04		0.03		0.04	0.03	
Buffer				0.08		0.06	0.33	0.08		
Repair total	0	0	0.03	0.12	0	0.34	0.33	0.12	0.03	0
Electricity, ¢/km	1.31	1.31	1.31	1.31	1.31	1.31	1.31	1.31	1.31	1.31
Total, ¢/km	1.48	7.20	1.51	7.57	1.48	7.54	1.81	7.57	1.51	1.48
Total, $/yr	236.80	1152.00	241.60	1211.20	236.80	1206.40	289.60	1211.20	241.60	236.80
Life-cycle cost, $/yr										
Initial cost (699.66)										
Operating cost, $/yr	236.80	1152.00	241.60	1211.20	236.80	1206.40	289.60	1211.20	241.60	236.80
Chassis salvage (-)										
Battery salvage (-)		-91.50		-91.50		-91.50		-91.50		-69.97
Total, $/yr 699.66	236.80	1060.50	241.60	1119.70	236.80	1114.90	289.60	1119.70	241.60	166.83
Discount factor 1.0	0.980	0.961	0.942	0.924	0.906	0.888	0.871	0.853	0.837	0.820
Present value, $ 699.66	232.06	1019.14	227.59	1034.60	214.54	990.03	252.24	955.10	202.22	136.80
Total cost, $	5963.98									
Life-cycle cost, ¢/km	3.73									

TABLE 29.-CONSUMER ACCEPTANCE SCORING

Parameter	Electric vehicle with regenerating braking	Hydropneumatic buffer vehicle	Pneumatic buffer vehicle	Spring buffer vehicle	Flywheel buffer vehicle
Initial cost, $ (100,000 units/yr	100	446.94	699.66	834.21	621.27
(Score)	(12.1)	(2.7)	(1.7)	(1.5)	(2.0)
Life-cycle cost, ¢/km[a]	1.83[b], 1.77[c]	1.96	3.73	3.18	2.27
(Score)	(5.4)	(4.8)	(2.6)	(3.0)	(4.2)
Safety	← All can be built safe →				
(Score)	(4)	(4)	(4)	(4)	(4)
Driveability	Equivalent to electric	Equivalent to electric	Poor	Poor	Equivalent to electric
(Score)	(5)	(5)	(2)	(3)	(5)
Proportionate average score	(6.6)	(4.1)	(2.6)	(2.9)	(3.8)

[a]Based on production of 100K units per year.

[b]Regeneration fraction = 0.7.

[c]Regeneration fraction = 1.067.

judgment of the degree of modification along with relative scoring values.

The last row of Table 30 shows the proportionate average score for development risk for each vehicle.

- Potential for improvement in range -- This evaluation criterion is important for the ultimate success of a buffer system, in that any design change or improvement in the state of the art of any of the buffer components which results in an immediate improvement in range will increase consumer acceptability. An increase in buffer efficiency (percent improvement of braking energy recovered), buffer weight reduction, and optimal integrated design are examples for potential improvement in range. The estimated improvement expected in near term (1 to 3 years) for each of the buffers is shown in Table 31. Only increase in buffer efficiency is shown because a buffer weight reduction or an optimally integrated buffer system resulting in vehicle weight reduction has the effect of increasing buffer efficiency. The bottom row shows the scoring in this category.

- Rating matrix -- The rating matrix for each regeneration fraction of 0.7 and 1.067, respectively, that was used to select the buffer to recommend for design and development is shown in Tables 32 and 33. Weighting factors have been selected to define the relative importance of the four decision factors.

An example at the bottom of Tables 32 and 33 show how the total score for each buffer system was computed. Based on the scores the following buffer ranking is apparent:

a) With regeneration fraction = 0.7:

1. Hydropneumatic buffer vehicle
2. Electric vehicle regenerative braking
3. Flywheel buffer vehicle
4. Spring buffer vehicle
5. Pneumatic buffer vehicle

TABLE 30.-DEVELOPMENT RISK SCORING

Parameter	Electric vehicle with regenerative braking	Hydropneumatic buffer system	Pneumatic buffer system	Spring buffer system	Flywheel buffer system
Development time, yr	0 to 1	1	3	1.5	0 to 1
(Score)	(5)	(4)	(2)	(4)	(5)
Special maintenance equipment	None	Gas precharge equipment discharge capability	Dewatering and charge/discharge capability	Spring tension release	Flywheel evacuation
(Score)	(6)	(4)	(3)	(3)	(4)
Special vehicle requirements (modifications)	None	Slight	Considerable	Slight	Slight
(Score)	(6)	(4)	(2)	(4)	(4)
Score	5.7	4	2.3	3.7	4.3

TABLE 31.-POTENTIAL FOR IMPROVEMENT IN RANGE SCORING

Parameter	Electric vehicle with regenerative braking	Hydropneumatic buffer vehicle	Pneumatic buffer vehicle	Spring buffer vehicle	Flywheel buffer vehicle
Efficiency of buffer (percent improvement of braking energy recovered	10	10	20	15	20
Improvement due to:	Battery improvement	Motor pump efficiency	Motor pump	Elastomers	Drive train
		High-pressure vessels		Elastomers	Rotor materials
Score	2.7	2.7	5.3	4.0	5.3

TABLE 32.-RATING MATRIX (REGENERATION FRACTION = 0.7)

Parameter	Weight	Electric vehicle with regenerative braking	Hydropneumatic buffer vehicle	Pneumatic buffer vehicle	Spring buffer vehicle	Flywheel buffer vehicle
Range (normalized)	10	5.8	6.3	0	3.1	4.8
Consumer acceptance	6	6.6	4.1	2.6	2.9	3.8
Potential for improvement in range	3	2.7	2.7	5.3	4.0	5.3
Development risk	1	5.7	4.0	2.3	3.7	4.3
Total score (summation of parameter weight times the individual score)[a]	-	111.4	99.7	33.8	64.1	91.0

[a] For example: Hydropneumatic buffer =10 x 6.3 + 6 x 4.1 + 3 x 2.7 + 1 x 4.0 = 99.7.

TABLE 33.-RATING MATRIX (REGENERATION FRACTION = 1.067)

Parameter	Weight	Electric vehicle with regenerative braking	Hydropneumatic buffer vehicle	Pneumatic buffer vehicle	Spring buffer vehicle	Flywheel buffer vehicle
Range (normalized)	10	6.7	5.9	0	2.9	4.5
Consumer acceptance	6	6.6	4.1	2.6	2.9	3.8
Potential for improvement in range	3	2.7	2.7	5.3	4.0	5.3
Development risk	1	5.7	4.0	2.3	3.7	4.3
Total score (summation of parameter weight times the individual score)[a]	-	120.4	95.7	33.8	62.1	88.0

[a] For example: Hydropneumatic buffer = 10 x 5.9 + 6 x 3.7 + 3 x 2.7 + 1 x 4.0 = 95.7.

b) With regeneration fraction = 1.067:

1. Electric vehicle/regenerative braking
2. Hydropneumatic buffer vehicle
3. Flywheel buffer vehicle
4. Spring buffer vehicle
5. Pneumatic buffer vehicle

Even though the electric vehicle with regenerative braking ranks highest when using a battery regeneration fraction of 1.067, it was not selected for continued design on this program. Extensive effort is currently being devoted to this concept by other contractors. Thus, the hydropneumatic buffer system was selected as the buffer design for further consideration. The percent range increase over the straight electric vehicle was calculated to be 22% (see Table 13).

DISCUSSION OF RESULTS

Hydropneumatic Buffer Design

A layout schematic of an electric vehicle with the selected hydropneumatic energy buffer is shown in Figure 42. The arrangement is shown in this manner to show mechanical and hydraulic linkages and flow paths and not to depict any relative location of one component to another.

Drive command inputs are shown on the left; mode selection (reverse-park-neutral-drive) is via transducer T_1; acceleration commands are via a conventionally located pedal and transducer T_3. Braking commands are normally through the brake and transducer, T_2 -- emergency operation of the brakes is manually possible with the manual linkage from the pedal to the master cylinder (C_2, with reservoir R_2) connected to the conventional friction brakes. Overpressure is prevented by both normal control modes and by the relief valve, V_6.

These commands enable the control system to operate all of the thrust-control elements in the following manner:

- Normal cruise power and low-powered acceleration are provided by the electric motor, EM, supplied with battery current by the chopper.

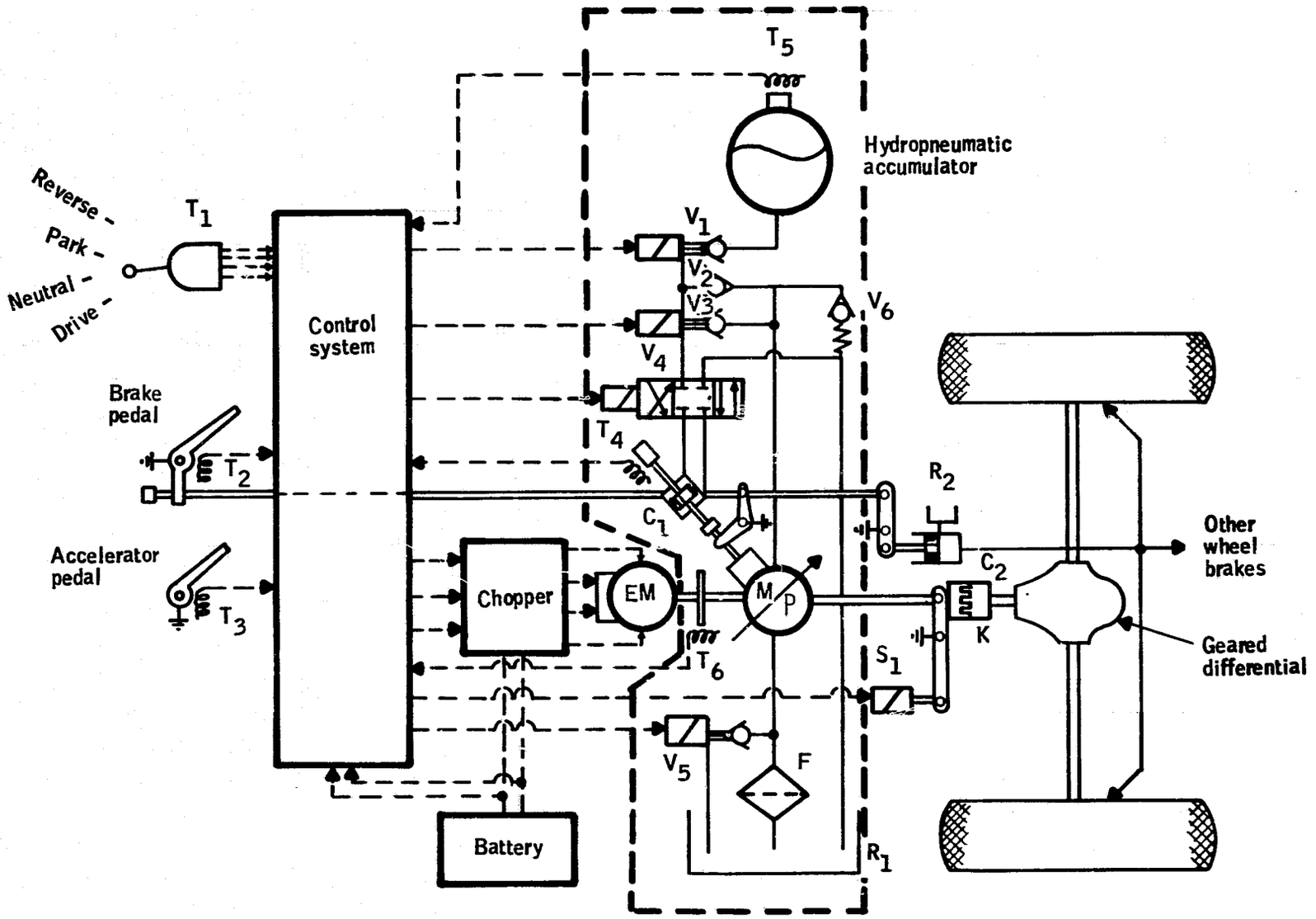

Figure 42.-Electric vehicle with the recommended energy buffer - hydropneumatic.

- High-rate acceleration is provided by the electric propulsion system aided by the hydraulic motor/pump, MP. Flow from the hydropneumatic accumulator is through the main shutoff solenoid valve, V_1, and the normal propulsion solenoid valve, V_3. Torque is controlled by the electro-hydraulic servo-valve, V_4, proportioning flow to the displacement servocylinder, C_1, whose loop is closed by transducer T_4. Fluid discharged from the motor/pump passes through the filter, F, and into the high-capacity reservoir, R_1.

- Regenerative braking is obtained by "stroking" the motor/pump with the V_4-C_1-T_4 servo into the pumping mode. The filter bypass valve, V_5, is energized to minimize pump cavitation, and the "no-back" check valve, V_2, prevents motoring of the pump once the vehicle comes to a complete stop. High-G stops -- above the capability of the hydraulic regeneration system -- are possible by overstroking the pump and operating the C_2-R_2 friction braking system.

- Proper operation of the hydropneumatic buffer system is provided by mixed commands to the V_4-C_1-T_4 displacement control and the chopper when provided with information from the accumulator pressure sensor, T_5, and vehicle speed sensor, T_6. If initial or additional accumulator charging is necessary, solenoid S_1 may be used to disengage the main drive clutch, K, and accomplish this by driving the motor pump directly with the electtic motor.

This configuration allows the buffer to be commanded in the most efficient manner; electric motor power can be minimized (and battery efficiency maximized) while maintaining buffer pressure balance on a time-sharing basis.

Of the components described in Figure 42, the major components that affect the performance and cost of the buffered vehicle include: battery, electric motor, hydraulic accumulator, and hydraulic motor/pump. Although the battery pack and electric motor are not integral parts of the selected buffer system, they must be considered in the optimization because their size affects the buffer component sizes. For the design analysis of the buffered vehicle, actual manufacturer's data were obtained for buffer components. The equations for electric motor and hydraulic pump/motor were updated. The design analysis of the hydropneumatic buffered vehicle with the updated parameters is described below.

Battery pack.-The battery pack size was optimized based on range and life-cycle cost. The following assumptions were made:

1) Use the previously defined buffer performance.

2) Select vehicle motor size of 11 kW.

3) Total vehicle mass consisted of:

- Base vehicle mass (chassis and passengers)
- Battery pack mass
- Electric motor mass
- Buffer system mass

Based on these assumptions, the battery pack mass was determined which would result in minimum battery life-cycle cost with maximum range. This was done by determining the vehicle range for various masses with the computer program and using those results to determine the appropriate life-cycle cost.

The mass of the total vehicle was assumed to consist of the mass of a base vehicle, the mass of the battery pack, the accumulator system, and the drive motor system, and is given by the equation:

$$M_V = M_{AC} + CP_m + M_{Bat} + M_{Body} \qquad (52)$$

where

M_V = vehicle mass, kg

M_{AC} = hydropneumatic buffer mass, kg

C = 6.67 $\frac{kg}{kW}$, an average of motor data shown in ref. 8

P_m = electric motor power, kW

M_{Bat} = battery mass, kg

M_{Body} = vehicle body mass, kg

The body mass was held constant at 836 kg (1844 lb), and the accumulator mass was set at 110 kg (244 lb).

The EV106 NASA battery model (model no. 3 in Figure 12) was used to estimate range of the vehicle per cycle. A polynomial curve fit of that battery model was used. The original data and the curve fit equation are shown in Figure 43.

The battery life used in the economic analysis was 800 cycles at an 80% depth of discharge based on data given in ref. 5 and Argonne National Lab goals for lead/acid batteries available in 1980. The cycle life was not varied due to differences in average power and peak power rates during the driving cycle, since no data were available to quantify these effects.

The variation of vehicle range with battery mass is shown in Figure 44. The resulting variation of battery life-cycle costs with the battery mass is shown in Figure 45. Initial battery cost of $2/kg (1978 dollars) and replacement after 800 charge/discharge cycles were used to determine the life-cycle cost. The optimal battery mass is between 400 and 450 kg (880 and 990 lb). The 415 kg (915 lb) was chosen to allow comparison with the preliminary analysis which had 415 kg (915 lb) of batteries.

The above analysis assumed both a constant charge/discharge efficiency for the battery pack at all average rates and a constant cycle life at all average power rates. However, the average power rate during the cycle varies significantly with battery mass as shown in Figure 46. Thus, it is likely that both the battery discharge efficiency and the battery cycle life decrease with increasing average cycle power, thereby increasing the life-cycle costs over those shown in Figure 45. It is possible that the actual optimal battery mass is slightly higher than the optimal given on Figure 45.

Electric motor.-The electric motor model was updated to include the effect of high torque at low vehicle velocity during acceleration. Previously, it was assumed that the current draw by the electric motor was a function of velocity only. The current draw was now modeled to be a function of both velocity and torque. Power losses were modified to reflect this updated model.

The losses in kW are:

$$\text{Armature power} = 3.00 \times 10^{-3} \left(P_{out} \frac{\omega_r}{\omega} \right)^2 \qquad (53)$$

$$\text{Field power} = 2.31 \times 10^{-3} \left(P_{out} \frac{\omega_r}{\omega} \right)^2 \qquad (54)$$

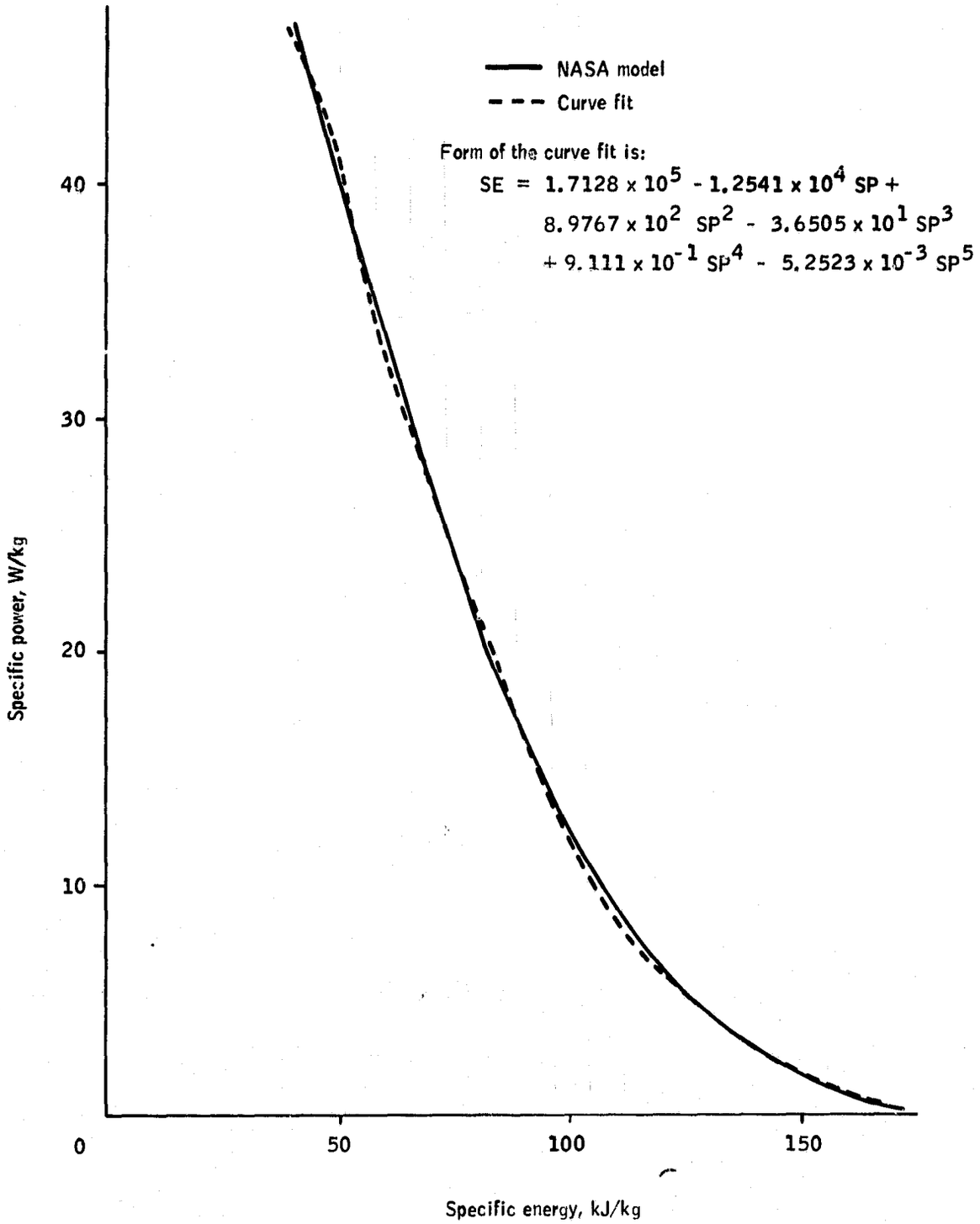

Figure 43.-EV106 battery model.

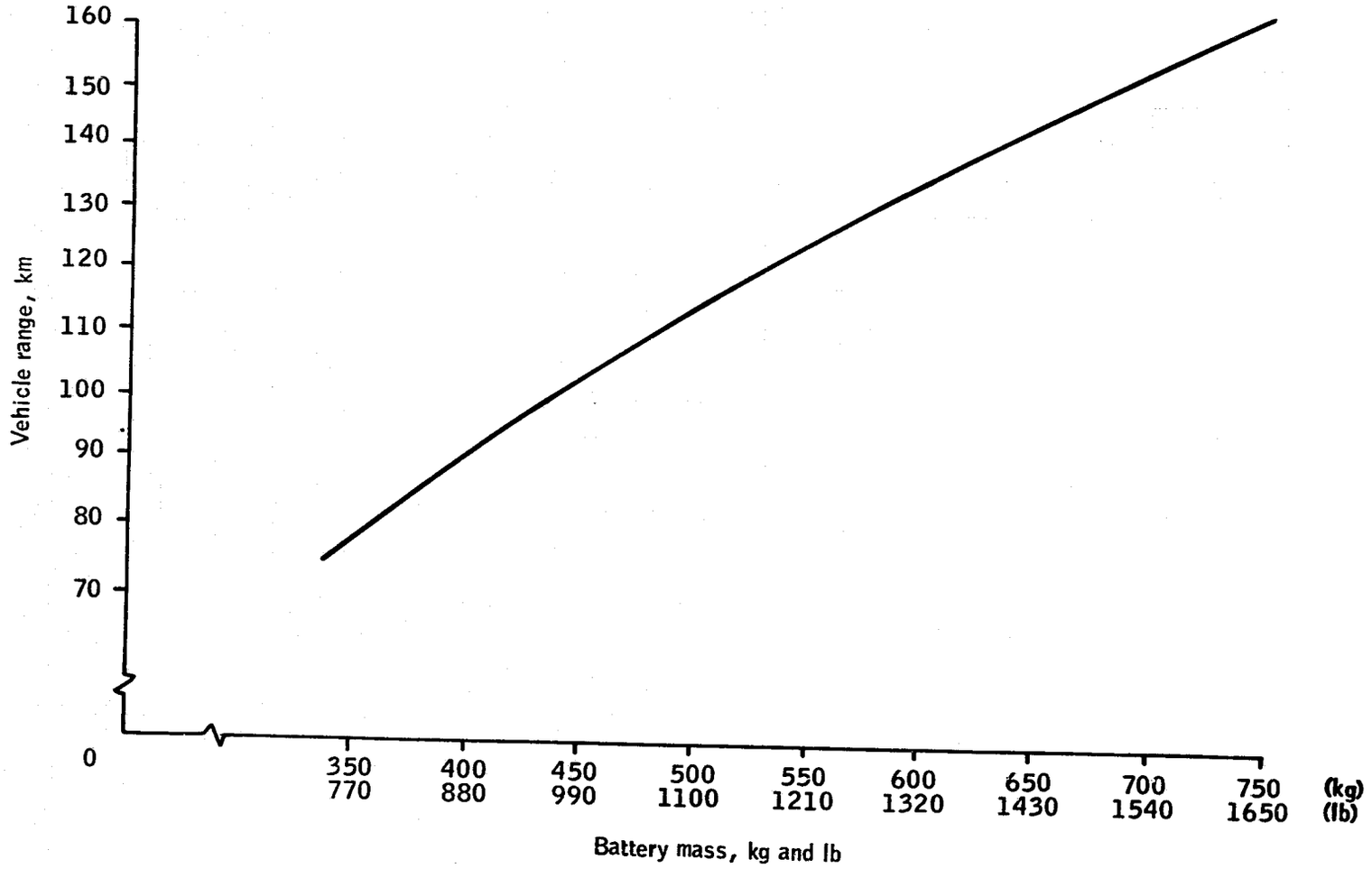

Figure 44.-Vehicle range versus battery mass.

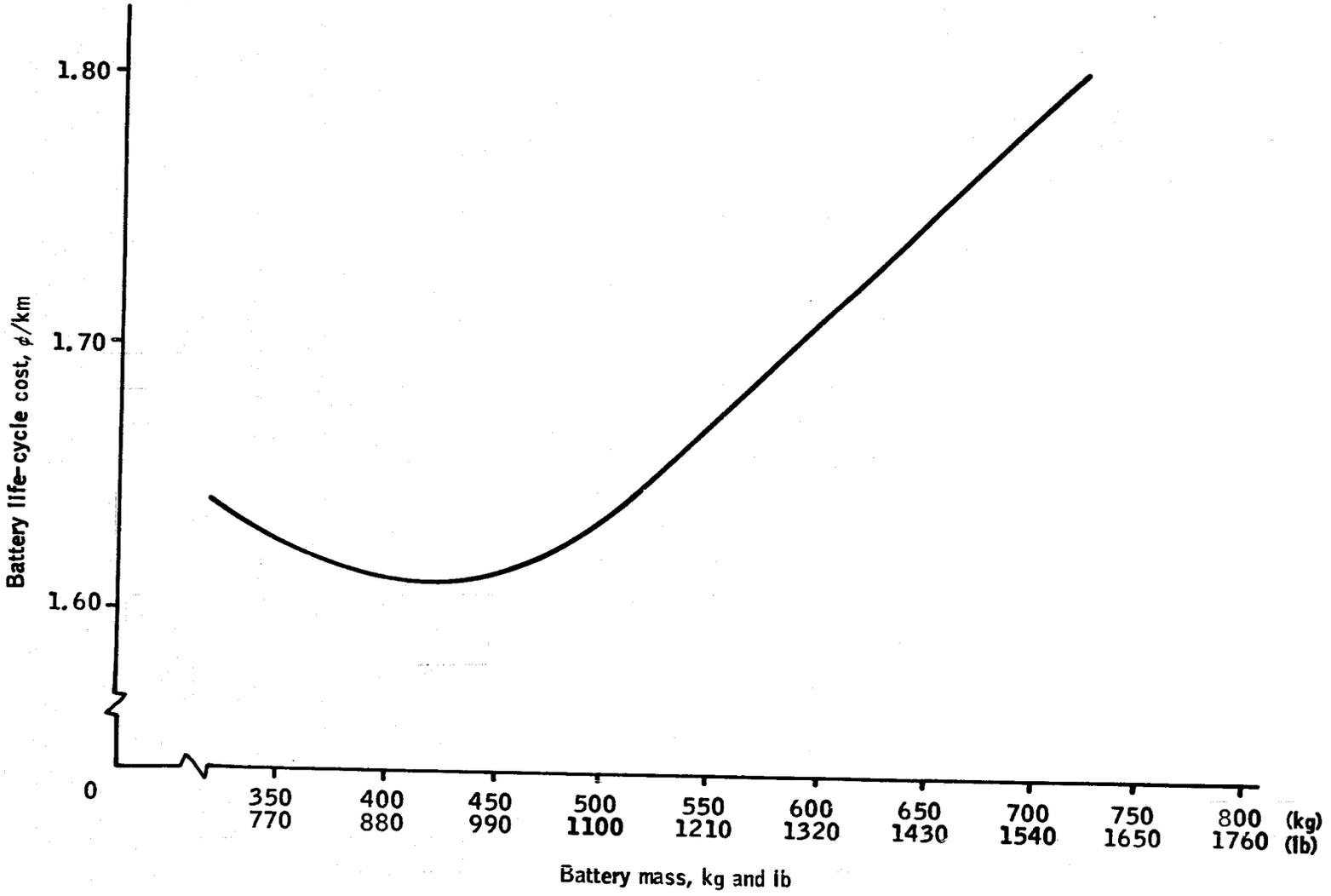

Figure 45.-Battery life-cycle costs versus battery mass.

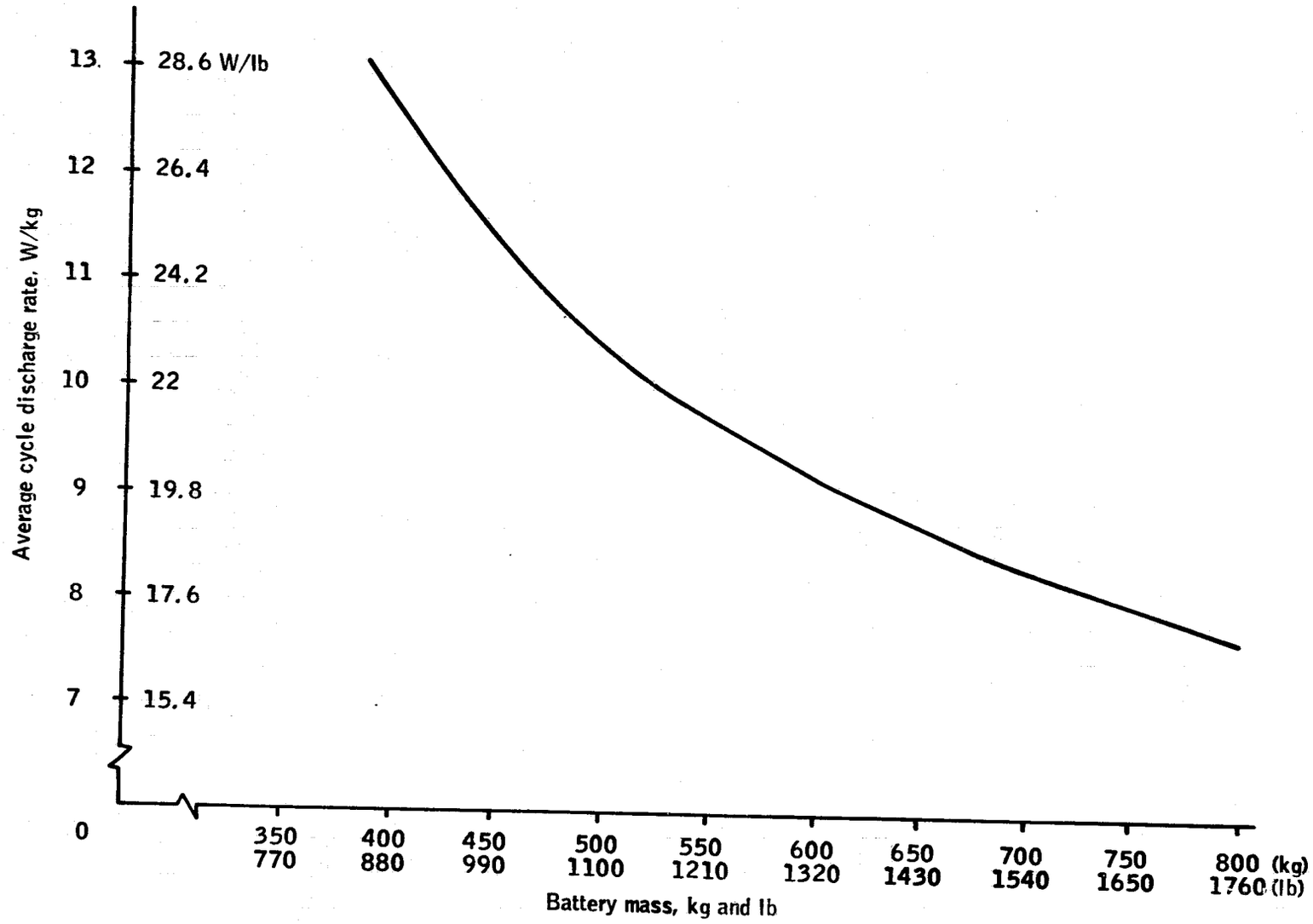

Figure 46.-Average cycle discharge rate versus vehicle battery mass.

$$\text{Eddy current power} = 5.00 \times 10^{-3} \, P_{out} \frac{\omega_r^2}{\omega} \quad (55)$$

$$\text{Hysteresis power} = 4.44 \times 10^{-5} \, \omega \quad (56)$$

$$\text{Friction power} = 2.67 \times 10^{-5} \, \omega \quad (57)$$

$$\text{Windage power} = 1.73 \times 10^{-8} \, \omega^2 \quad (58)$$

where

P_{out} = motor output power (kW)
ω_r = rated rpm
ω = instantaneous rpm

A 16-kW motor was used for the design analysis. The results of the analysis for the straight electric vehicle and the buffered vehicle with the updated motor model are shown in Table 34. The straight electric vehicle range has dropped from 85.6 km to 77.4 km and the buffered vehicle range from 104.4 km to 94.4 km because of the new electric motor model.

TABLE 34.-ELECTRIC AND BUFFERED VEHICLE PERFORMANCE
(UPDATED ELECTRIC MOTOR MODEL)

Parameter	Straight electric vehicle	EV-Hydropneumatic buffer (estimated data)
Battery size, kg	415	415
Electric motor size, kW	16	16
Accumulator size, gal	-	20.2
Motor/pump size, in^3/rev	-	5.5
Vehicle weight, lb	3000	3244
Range, km	77.4	94.4
Percent increase in range	-	22
Buffer initial cost, $[a]	-	394
Life-cycle cost, ¢/km[a]	-	1.83

[a]100K units - based on manufacturer's estimated cost.

Through contacts with various hydraulic motor/pump and accumulator manufacturers, actual motor/pump efficiencies and weights were obtained. Based on the data supplied by vendors the motor/pump model was updated. The updated equations for different motor/pump power losses and other buffer losses are given below:

1) Hydraulic motor/pump power losses, [W]:

a) Leakage losses = $2.874 \times 10^{-3} D_M \left(\frac{D}{D_M}\right)^{-0.0797}$

$$\left[7.662 \times 10^{-9} p^{1.3643} + 7.97 \times 10^{-11} p^{1.257} \omega\right] \quad (59)$$

b) Friction losses = $2.35 \times 10^{-4} D_M p(\omega) + 6000 D_M(\omega)$ (60)

c) Viscous losses = $6.35 \times 10^{-4} D_M(\omega)^3$ (61)

d) Compression losses = $1.6 D(\omega)^2$ (62)

2) Other losses, [W]:

e) Piping friction losses = $0.01 \left(\frac{Wp}{W_r p_r}\right)^3$ (63)

f) Accumulator expansion losses = 0.01 Wp (64)

where

D_M = maximum motor/pump displacement, m^3/rev
D = instantaneous motor/pump displacement, m^3/rev
p = buffer pressure, Pa
ω = speed of motor/pump, rev/min
W = fluid flow rate, m^3/s
p_r = maximum buffer pressure, Pa
w_r = fluid flow rate at rated conditions, m^3/s

Various buffer component sizes were computed by varying accumulator pressure schedules and volumes. For each pressure schedule and accumulator volume, the corresponding motor/pump size in turn was determined from the deceleration rate schedule (J227a a Schedule Driving cycle) 1 vehicle energy. Life-cycle costs were then determined for each set of buffer component sizes. Minimum life-cycle cost was the basis for selecting the component sizes.

Since maximum accumulator pressure is set at 20.7 MPa (3000 psi), and maximum energy to be stored is fixed (kinetic energy of the vehicle at 88 km/h), the accumulator volume can be changed only by varying the minimum pressure. This in turn effects the weight (wall thickness of a cylinder) and maximum vehicle kinetic energy. Thus, life-cycle costs were computed for various minimum accumulator pressures.

The results of the analysis with the updated electric motor model and buffer model are shown in Table 35. Also given in this table are the performance characteristics of the buffered vehicle with the buffered vehicle range dropped from 94.4 km to 81.2 km. The new range represents only a 5% increase in range over the straight electric vehicle. Also, the buffer weight increased from 111 kg (244 lb) to 158 kg (348 lb) based on vendor data.

TABLE 35.-ELECTRIC VEHICLE WITH HYDROPNEUMATIC BUFFER PERFORMANCE (ESTIMATED DATA VERSUS ACTUAL DATA)

Parameter	Straight electric vehicle	EV-Hydropneumatic buffer	
		Estimated data	Actual data
Battery size, kg	415	415	415
Electric motor size, kW	16	16	16
Accumulator size, gal	-	20.2	19.5
Motor/pump size, in^3/rev	-	5.5	5.9
Vehicle weight, lb	3000	3244	3348
Range, km	77.4	94.4	81.2
Percent increase in range	-	22	5
Buffer initial cost, $[a]	-	394	350
Life-cycle cost, ¢/km[a]	-	1.83	1.53

[a]100K units - based on manufacturer's estimated cost.

The reasons for this substantial difference in performance between using estimated data and vendor data were investigated. The problem areas were identified and are discussed below.

Problem Areas

Through contact with various hydraulic motor/pump and accumulator manufacturers it was determined that several problems existed in obtaining off-the-shelf components to meet the defined buffer requirements. Actual motor/pump efficiencies were less than previously estimated and weighed more than previously estimated, causing predicted range increases to be unacceptably low. Also, motor/pumps with the combination of size and maximum speed required were unavailable, and lightweight accumulators in the required size did not exist.

Motor/pump.-The motor/pump problems referred to are primarily due to the fact that available off-the-shelf hydraulic motor/pumps do not operate efficiently as motors at low displacements. The low displacement was caused by the mismatch of acceleration and deceleration in the J227a schedule D driving cycle and the requirement to store all the braking energy in the buffer from an 88 km/h (55 mi/h) stop after a 10-s coast. Since the motor/pump displacement was sized by the deceleration (0.25 g), the motor/pump in the motor (acceleration) mode was operated at low displacement to match the relatively slow acceleration (0.073 g) requirement. The mismatch of acceleration to deceleration was such that the selected motor/pump operates as a motor during acceleration between 11 and 21% displacement. Typical manufacturer's data for axial-piston motor/pumps shows efficiency to be very low at this low displacement (see Figure 47). The efficiency previously estimated is also shown.

Also, an increase in weight in our buffer system was recommended by the manufacturer to more closely approximate the actual weight. Thus, the weight was increased from 110 kg (244 lb) to 158 kg (348 lb). This caused a decrease in predicted range. The results of this additional data, including initial and life-cycle costs were given in Table 35. The percent range increase over the straight electric vehicle using this data was only 5%.

Accumulators.- It was expected that lightweight, fiber-wrapped aluminum pressure vessels would be available. However, the large sizes required were not anticipated and could not be obtained as off-the-shelf hardware.

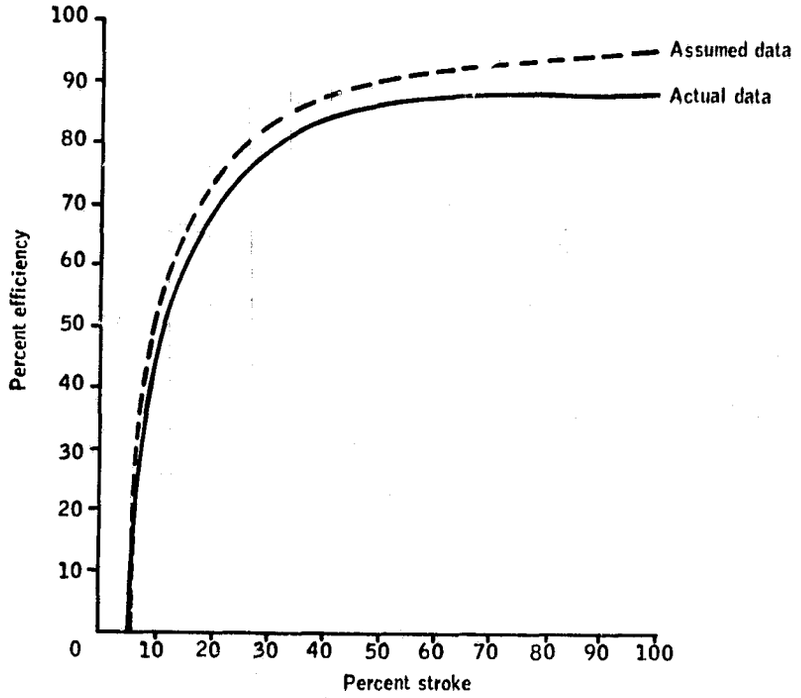

Figure 47.-Typical axial-piston motor/pump efficiencies as a function of % full stroke.

The problem areas discussed are summarized below:

1) Lightweight accumulators in the size range for this buffer were not available.

2) Motor/pump efficiencies were overestimated.

3) Motor/pump weight was underestimated.

4) Maximum motor/pump speeds were underestimated.

Subsequently, the fabrication and testing of the buffer initially intended in the contract title was not carried out. Emphasis was shifted to a renewed design analysis and a vendor survey to determine if specialized components or newly developed components could result in acceptably lightweight and efficient hardware.

Renewed Design Analysis

In view of the circumstances with the actual hardware performance and availability, it was not appropriate to fabricate and test to prove the principle. Thus, the design analysis and optimization were renewed and the following steps were taken in an attempt to improve vehicle range and determine to what extent buffer component hardware must be developed to meet the requirements of the selected hydropneumatic energy buffer:

- Buffer performance criteria were redefined.
- A modification to the driving cycle was considered.
- The original accumulator concept was reinvestigated.
- An in-depth accumulator and motor/pump vendor survey was conducted.
- Specialized buffer components were determined.

Buffer performance criteria.-Originally, the buffer system was to be capable of accepting all the available energy from an 88 km/h (55 mi/h) stop in 9 s after a 10-s coast. Refer to Figure 2. This requirement sets the maximum motor/pump operating speed, the motor/pump size (maximum power occurs at initial deceleration), and accumulator volume (within the constraints of ΔP in the accumulator).

This criteria was changed so that the buffer would be capable of accepting the kinetic energy from 88 km/h (55 mi/h) but only retain the energy available from a 72-km/h (45-mi/h) stop in 9 s after coasting for 10 s. The new criterion reduces the size of the motor/pump and accumulator. Since the acceleration requirement is the same up to 72 km/h (45 mi/h) in 28 s , the motor/pump must operate at higher swashplate angles than before and thus operate more efficiently.

Driving cycle modification.-Studies conducted by the Environmental Protection Agency for actual urban driving in the Los Angeles area indicate that the deceleration part of the J227a Schedule D driving cycle represents typical urban driving. However, typical average accelerations from these studies infer that an acceleration to 72 km/h (45 mi/h) in 15 s is more realistic for internal-combusion engine automobiles. Since the addition of a buffer to an electric vehicle makes it capable of acceleration similar to that of internal-combustion engine vehicles, a modified

driving cycle was considered. A modified driving cycle with the J227a Schedule D cycle superimposed is shown in Figure 48. The acceleration portion was changed to 72 km/h (45 mi/h) in 15 s instead of 28 s.

The results of the new buffer performance criteria for both 15-s and 28-s acceleration are shown in Table 36. The most profound effect was caused by changing the buffer performance criteria from 88 km/h (55 mi/h) to 72 km/h (45 mi/h). Comparing old criteria vehicle performance with new criteria vehicle performance, the predicted increase in range over a straight electric vehicle was changed from 5% to 19%. With a 15-s acceleration, the range was increased by 23%.

Accumulator concept analysis.-The energy available during braking is stored as potential energy in the accumulator. In a hydropneumatic accumulator, a hydraulic fluid is pumped from a reservoir to an accumulator as during deceleration of the vehicle, which compresses a gas. The compressed gas acts like a spring. During discharge of this stored energy, as during acceleration of the vehicle, the gas expands, discharging the fluid. The two thermodynamic processes generally considered describing this type of expansion and compression of the gas are isothermal and adiabatic. Those two concepts will be reconsidered in detail here to determine if the original assumption of an adiabatic process to store the energy was indeed correct.

Therefore, the objective of this analysis was to consider these two individual processes in the design of hydropneumatic accumulator and the performance of the hybrid vehicle system.

Isothermal versus adiabatic process: An isothermal process is one in which the pressure and volume changes at constant temperature. Thus, the energy of an ideal gas cannot change for an isothermal process. For example, in a compression process, all the heat of compression is dissipated. This happens when there is sufficient time for heat exchange with the surroundings (i.e., if the process is slow).

An adiabatic process is one in which there is no heat transfer between the system and its surroundings. For example, in an adiabatic compression process, the heat of compression is retained within the gas. This happens, if the process happens quickly.

Between two given pressures or for a given pressure ratio, the work done per unit mole of gas is more for an isothermal process than an adiabatic process. In other words, for a given amount

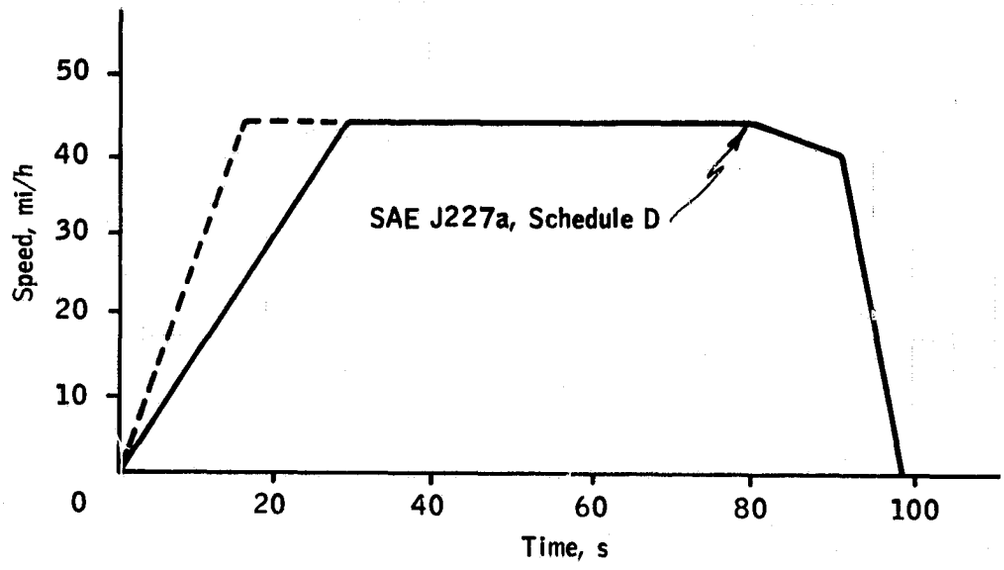

Figure 48.-Modified J227a (D) driving schedule.

TABLE 36.-PERFORMANCE OF ELECTRIC VEHICLE WITH HYDROPNEUMATIC BUFFER (MODIFIED CRITERIA AND 28-s VERSUS 15-s ACCELERATION TIME)

Parameter	Acceleration time	
	28 s	15 s
Battery size, kg (lb)	415 (915)	415 (915)
Electric motor size, kW	16	16
Accumulator size, m^3 (gal)	0.055 (14.4)	0.055 (14.4)
Motor/pump size, cm^3/rev (in^3/rev)	72 (4.4)	72 (4.4)
Vehicle weight, kg (lb)	1518 (3348)	1518 (3348)
Range, km	92.1	95.4
Percent increase	19	23

of energy to be stored in a given volume of accumulator, an isothermal process will operate at a lower pressure ratio than an adiabatic process. This can be shown from the equations of work for these two processes:

$$\text{Isothermal:} \quad W = RT \ln \left(\frac{p_1}{p_2}\right) \tag{65}$$

$$\text{Adiabatic:} \quad W = \frac{RT_1}{\gamma - 1} \left[1 - \left(\frac{p_2}{p_1}\right)^{\frac{\gamma-1}{\gamma}}\right] \tag{66}$$

where

p_1, p_2 = initial and final pressures
T_1 = initial temperature
γ = specific heat ratio (γ = 1.4 for N_2)
R = gas constant

Also, as γ approaches unity the work done for an adiabatic process approaches isothermal.

The operating pressure ratio affects the performance and sizing of other buffer and vehicle components as well.

Effect on the overall system design: The assumption of an isothermal or adiabatic process in the accumulator not only affects the sizing of the accumulator but also the sizing and performance of other components in the buffer system.

For the SAE J227a Schedule D driving cycle under consideration, the maximum power at which the motor/pump will operate occurs at the start of the braking cycle. At this point the pressure in the accumulator is minimum. The motor/pump power is given by:

$$\text{Power} = \text{displacement} \times \text{speed} \times \Delta\text{-pressure} \tag{67}$$

or

$$\text{Displacement} = \text{power}/(\text{speed} \times \Delta\text{-pressure}) \tag{68}$$

For a given power and speed or with a given braking cycle, motor/pump displacement is inversely proportional to the pressure differential it is pumping to. The displacement of a motor/pump essentially determines its size and cost. Therefore, the higher the Δ-pressure or higher the minimum pressure in the accumulator, the smaller the motor/pump size. With the isothermal process

assumption, it was shown that the minimum pressure will be higher in the accumulator than with adiabatic. Therefore, for a given maximum pressure, the motor/pump size with an isothermal accumulator will be smaller. The motor/pump size not only affects the initial cost of the buffer but also the performance of the buffer but also the performance of the buffer system and the battery system in the electric hybrid vehicle.

The motor/pump efficiency decreases with swashplate angle or displacement ratio (see Figure 47). For a given rate of discharge of energy from the buffer system, as during the acceleration cycle, the displacement ratio at each time point during the acceleration cycle will be greater with a smaller-sized motor/pump than with a larger one. Therefore, with the isothermal assumption, the efficiency of the buffer will be higher than with adiabatic assumption. This higher efficiency of the buffer system not only provides more energy to be used for vehicle propulsion but also decreases the average energy and power to be discharged from the battery. The specific energy of a battery increases with decrease in rate of battery discharge or power. The net effect is an increase in range.

The effect of the component sizes on the cost and range and the results of the isothermal accumulator analysis are described below.

The following assumptions and data were used for the analysis:

1) SAE J227a Schedule D driving cycle and specifications.

2) Ideal gas behavior in the accumulator.

3) Actual motor/pump performance data.

4) Maximum pressure set at 20.7 MPa (3000 psia).

5) For the charge and discharge of the buffer, a control strategy was assumed such that the energy in the buffer or the pressure in the accumulator is strictly a function of the velocity of the vehicle. A maximum pressure of 20.7 MPa (3000 psia) was set at zero vehicle velocity. The minimum pressure occurs at the beginning of the coast phase. The pressure-velocity schedule during coast cycle was maintained by charging the buffer from the battery.

6) The motor/pump is assumed to be declutched during the cruise phase and have a top speed of 3600 rpm.

7) Battery cost was assumed at \$2/kg and battery life as 800 cycles at 80% discharge. Recharge efficiency is 0.8 with electric costs of 4.5 ¢/kWh. Battery scrap value is 10% of initial value.

8) Motor/pump initial costs are \$2.37/(cm^3/rev). Accumulator initial costs are \$1583/m^3. Motor/pump maintenance costs are \$0.365/(cm^3/rev) in years 3 & 9 and \$1.095 (cm^3/rev) in year 6. Accumulator maintenance costs are \$250/m^3 in years 3 & 9 and \$750/m^3 in year 6.

9) The net discount factor is 2%.

10) Vehicle is driven 16 000 km/year and has a life of 10 years.

The accumulator volume increases as the minimum buffer pressure (pressure at start of coast cycle) increases for a given maximum pressure of 20.7 MPa (3000 psia) as shown in Figure 49. With a decrease in accumulator volume, the moles of gas charged decreases; therefore, with small accumulators, to store a given amount of energy, the pressure ratio will be high (i.e., the minimum buffer pressure will be small). The required maximum motor/pump displacement decreases as the minimum buffer pressure increases as shown in Figure 50. The maximum displacement is required at the start of the braking phase when the power is maximum. For a given speed, the maximum displacement is inversely proportional to the pressure. The average battery discharge rate and electric energy consumption versus minimum buffer pressure is shown in Figure 51. With an increase in minimum buffer pressure, buffer efficiency increases and therefore energy consumption and hence average battery discharge rate decreases as shown. The vehicle mass and vehicle range as a function of minimum buffer pressure are shown in Figure 52. At very low minimum buffer pressure, the accumulator size is small but the motor/pump size is large. As the minimum pressure increases, the motor/pump size decreases and accumulator size increases. Therefore, vehicle mass shows a minimum. The vehicle range increases because of an increase in buffer efficiency. It levels off, however, because the range decrease due to increase in vehicle mass compensates for the increase in range due to increase in efficiency at high minimum buffer pressures.

The results of the economic analysis for the various design points or minimum buffer pressures are given in Table 37. The

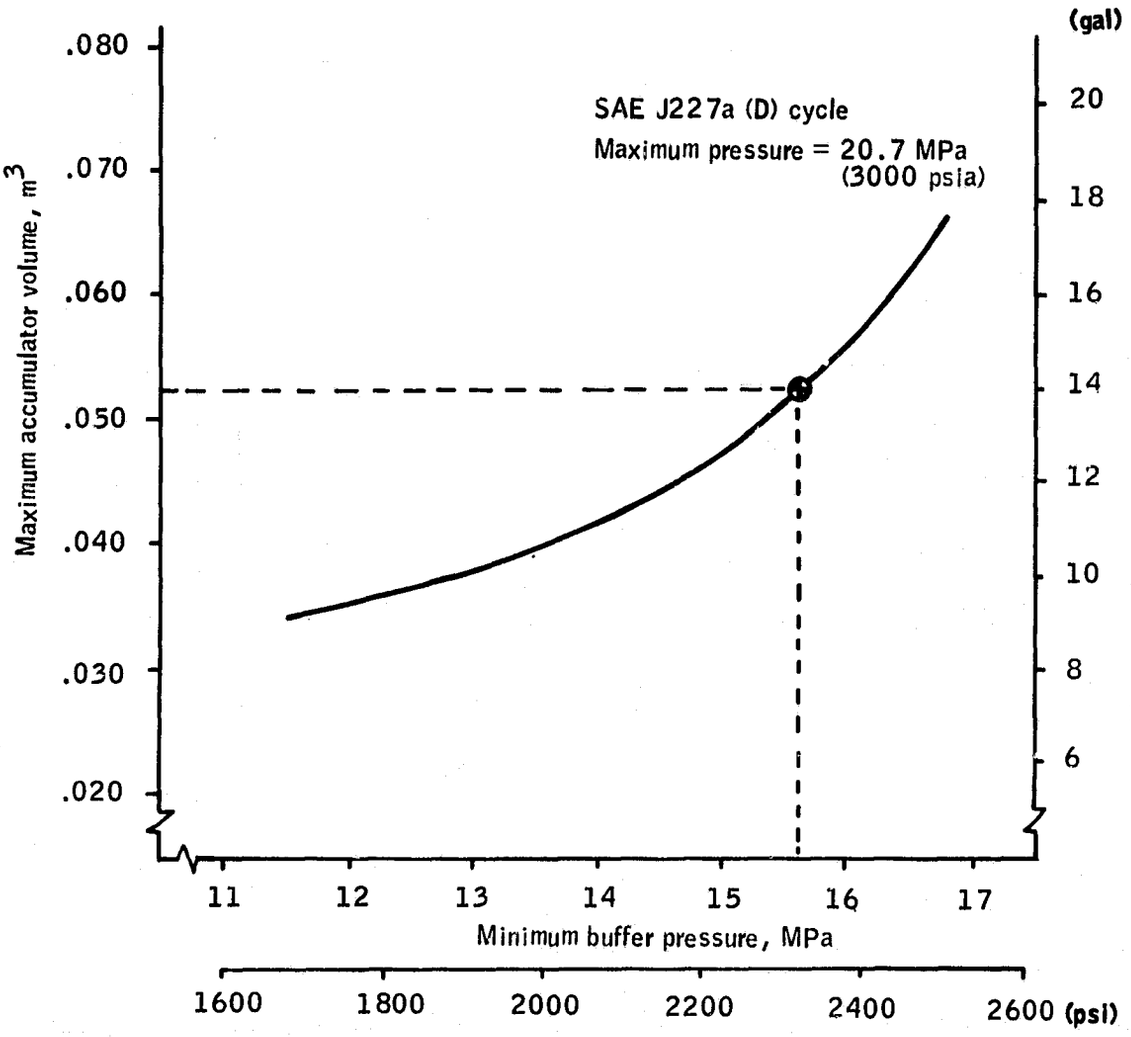

Figure 49.- Isothermal accumulator--accumulator volume versus minimum buffer pressure.

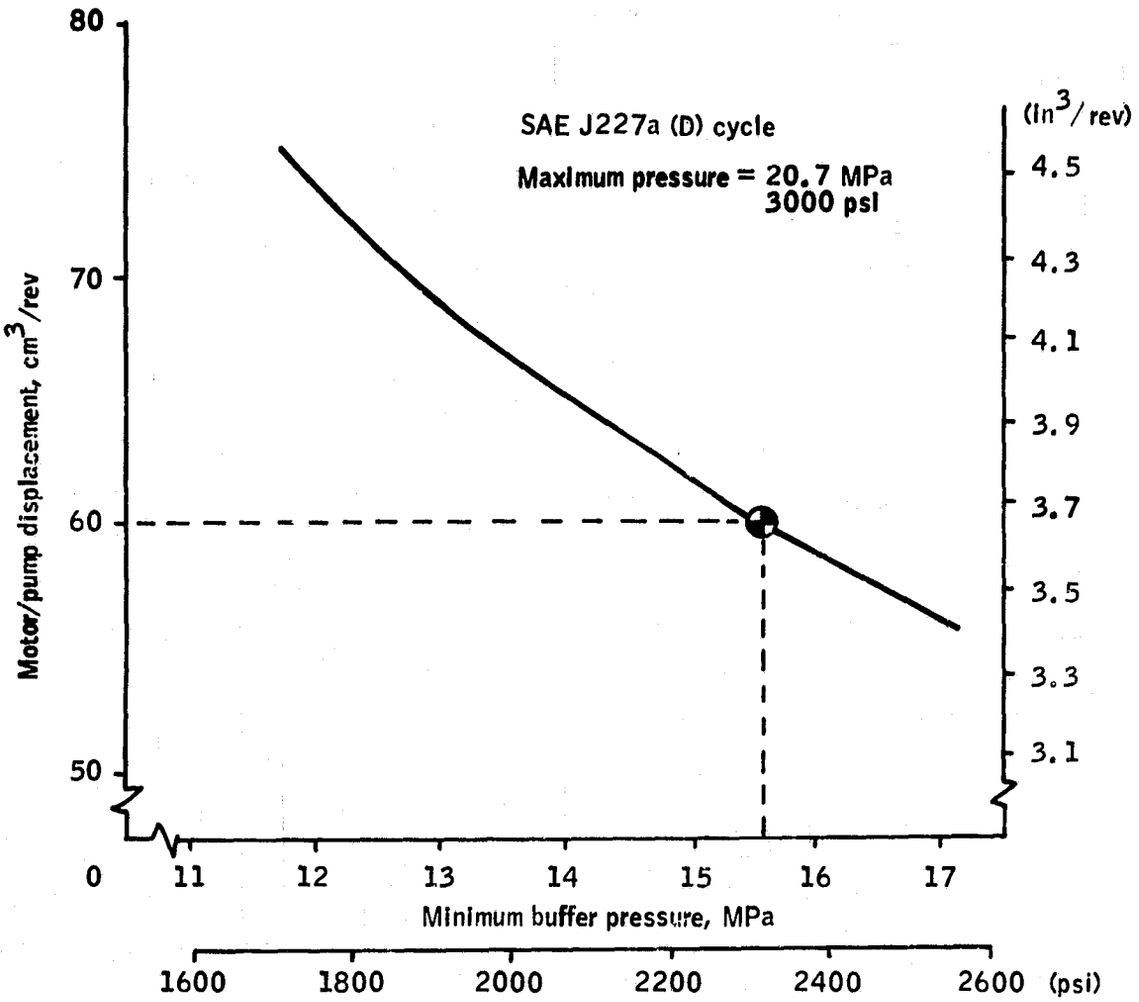

Figure 50.-Isothermal accumulator--motor/pump displacement versus minimum buffer pressure.

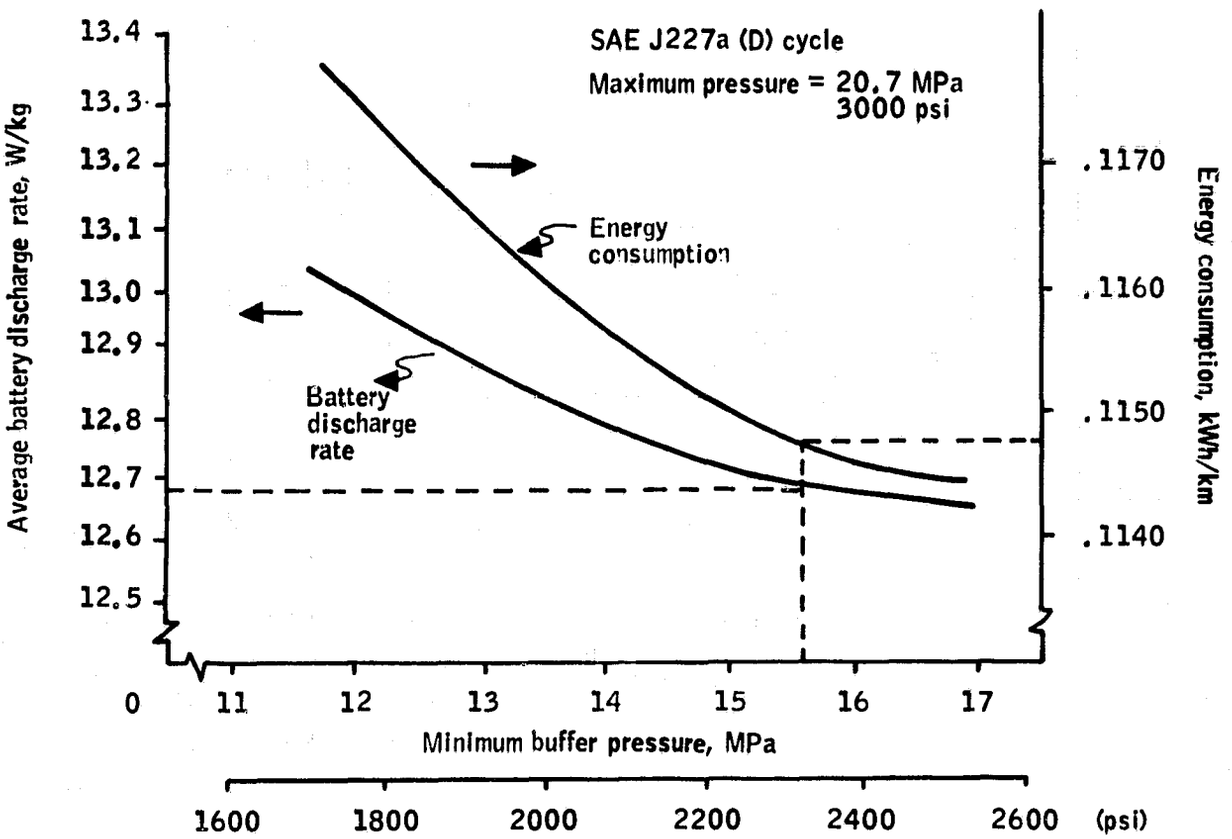

Figure 51.-Isothermal accumulator--energy consumption and battery discharge rate versus minimum buffer pressure.

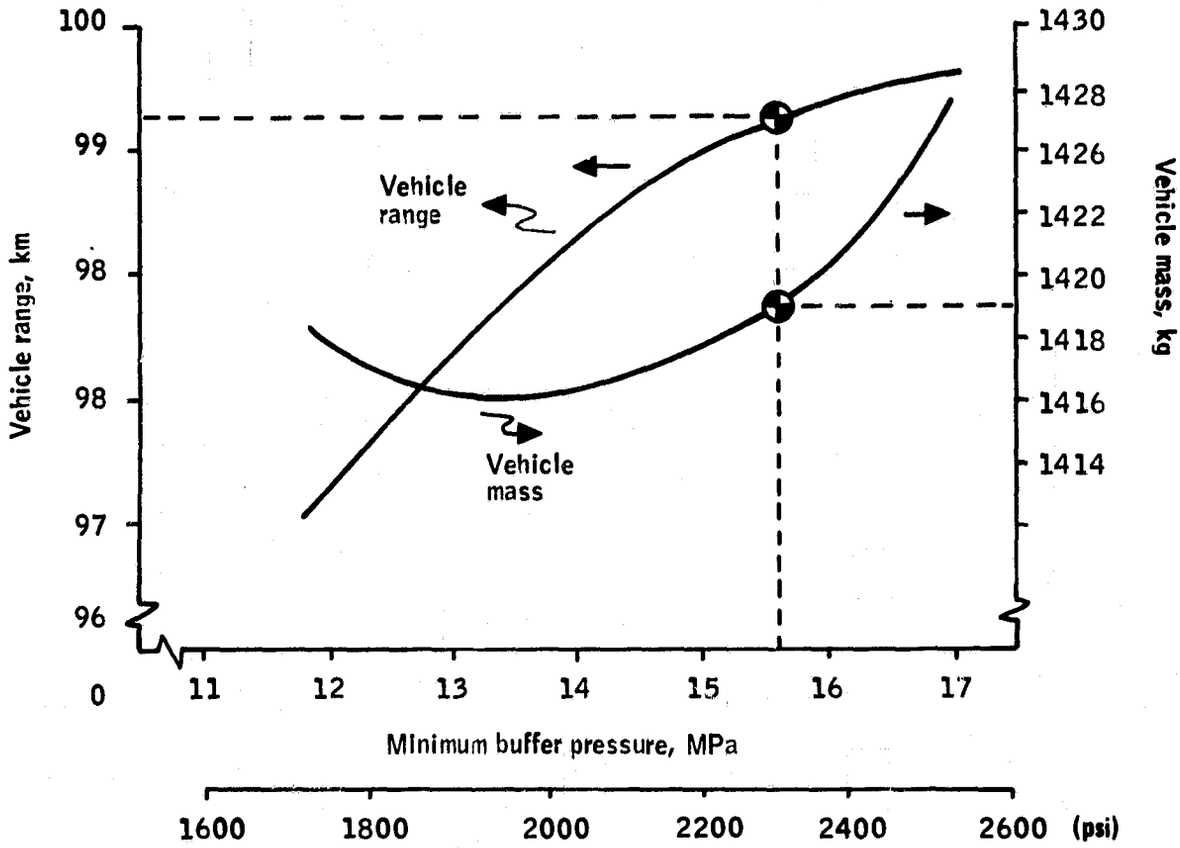

Figure 52.-Isothermal accumulator--vehicle range and vehicle mass versus minimum buffer pressure.

results are plotted in Figure 53 which shows a minimum in cost occurs at a minimum buffer pressure of 15.6 MPa (2265 psia). The actual energy consumptions and efficiencies of the buffer and battery system during each phase of the driving cycle are given in Table 38. The total energy available during the braking cycle is 214 kJ. The net energy charged to the accumulator during this phase is 194 kJ. For a braking period of 9 s, this represents an average rate of about 22 kW. In an isothermal process, since the energy of a gas does not change, an equal amount of heat has to be transferred to the surroundings at this same average rate of heat transfer. In the acceleration phase, the amount of energy available for vehicle propulsion is about 177 kJ. For the process to be isothermal, the same amount of heat should be gained from the environment in the 28-s acceleration phase. This represents an average rate of heat transfer of 6.5 kW.

TABLE 37.-ECONOMIC ANALYSIS OF ELECTRIC VEHICLE WITH ISOTHERMAL BUFFER SYSTEM

Parameter	Minimum volume, m^3					
	0.020	0.030	0.035	0.040	0.050	0.060
Battery cost, $ = 255.72 + $\frac{152\,575}{\text{Range}}$	1842.40	1804.80	1797.61	1792.23	1788.69	1787.14
Energy cost, $ = 8064 x kWh/km	948.33	931.39	927.36	924.94	923.33	922.52
Buffer cost, $ = 2691.25 x V	93.66	117.07	129.72	142.37	168.47	194.85
Motor/pump cost, $ = 3.99 x displacement	296.58	256.32	246.78	238.48	230.34	223.80
Cost:						
Initial, $	3180.97	3109.58	3101.47	3098.02	3110.83	3128.31
Life-cycle, ¢/km	1.998	1.943	1.938	1.936	1.944	1.955

The analysis shows that at the optimum design of an isothermal accumulator, the maximum volume of the accumulator is 0.0529 m^3 (14 gal). The maximum and minimum pressures are 20.7 mPa (3000 psia) and 15.6 mPa (2265 psia). The motor/pump has a maximum

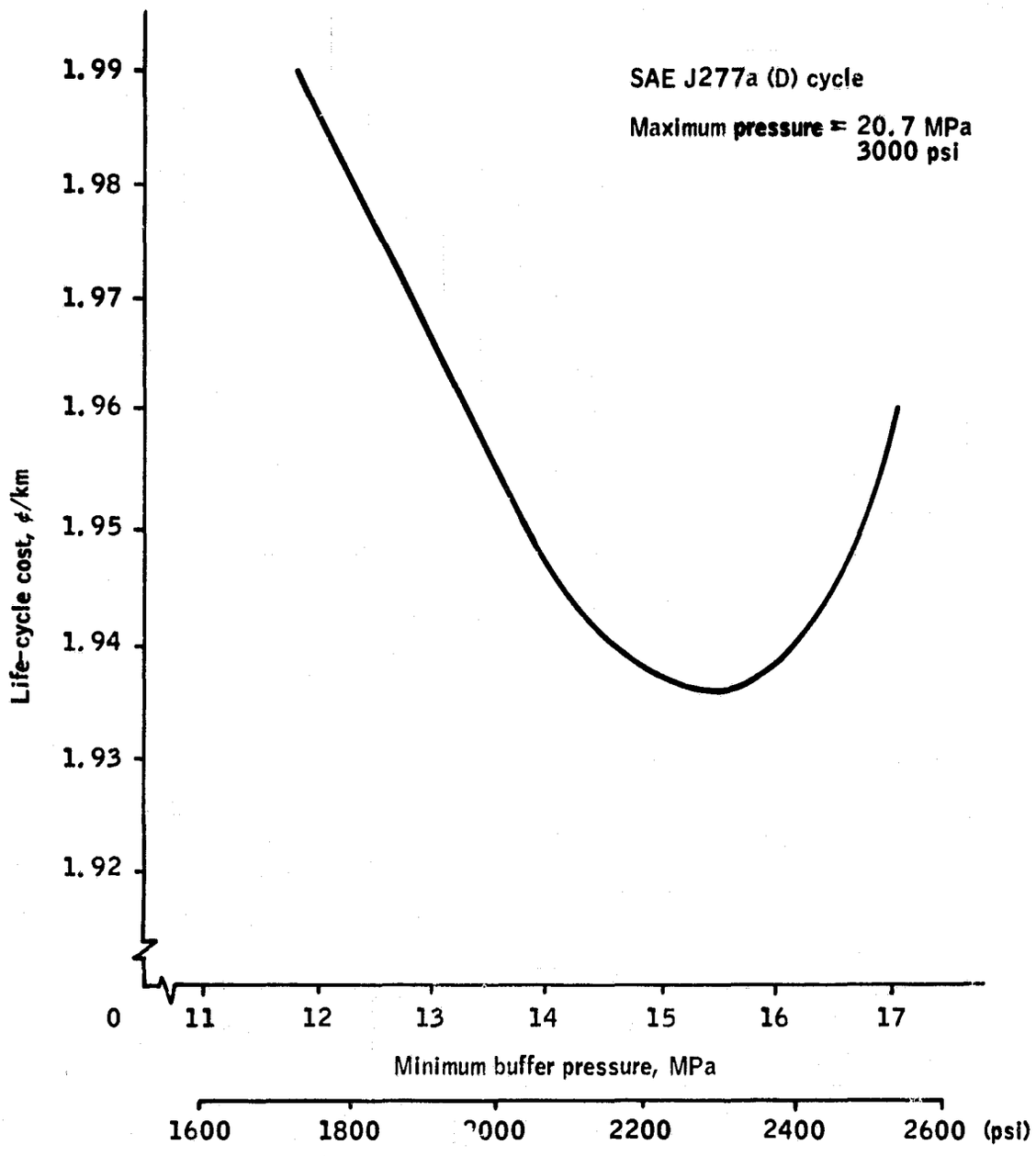

Figure 53.-Isothermal accumulator--economic tradeoff.

TABLE 38.-PERFORMANCE OF ELECTRIC VEHICLE WITH HYDROPNEUMATIC ACCUMULATOR (ISOTHERMAL)

Parameter	Acceleration phase, 28 s	Cruise phase, 50 s	Coast phase, 10 s	Brake phase, 9 sec	Total
Energy Requirement:					
Required at wheels, kJ	316	232	0	-225	-
Required at shaft, kJ	352	258	0	-214	-
From battery, kJ	236	319	87	0	642
From buffer, kJ	229	0	-36	-193	0
Efficiencies:					
Electric system	0.770	0.810	0.833	-	-
Buffer system	0.746	-	0.501	0.902	0.626
Drive train	0.950	0.950	-	0.950	-
Overall system	0.680	0.727	0.417	0.857	-

Vehicle Characteristics:

Vehicle range = 99.4 km

Vehicle mass = 1420 kg

Electric energy consumption = 0.1147 kWh/km

Average battery discharge = 12.67 W/km

Buffer Characteristics:

Buffer mass = 60 kg

Buffer pressures, max/min = 20.7 MPa/15.7 MPa

Motor/pump displacement = 59 cm^3/rev

Accumulator volume = 0.053 m^3

displacement of 59.8 cm^3/rev (3.65 in^3/rev) and a top speed of 3600 rpm. The vehicle range is 99.3 km, representing a 28% increase over the baseline electric vehicle range of 77.4 km.

Feasibility of an ideal isothermal accumulator: For the system to operate under isothermal conditions, the rates of heat transfer with the surroundings should be high, specifically, over 22 kW during braking phase and over 6 kW during acceleration phase. For heat transfer of these magnitudes with ambient surroundings, a very high surface area is required. Even by finning, the accumulator cannot achieve an isothermal process. Therefore, it was concluded even though an ideal isothermal accumulator will perform better than an adiabatic accumulator, as will be seen later in this section, the operation of the accumulator for the SAE cycle under consideration was far from isothermal because of high heat transfer rates. It was further concluded that because of the rapidity of the process, it would be close to an adiabatic process. The actual process may be somewhere between isothermal and adiabatic, but closer to adiabatic.

However, an accumulator could be designed to approach near-isothermal conditions. The design of a near-isothermal accumulator and its performance compared with adiabatic and ideal-isothermal are discussed below.

Design of a near-isothermal accumulator: A system could be designed to approach isothermal by storing the heat of compression in a high specific heat material incorporated in the accumulator. The heat is stored as sensible heat and, therefore, the larger the mass of material added the smaller the temperature swing. For example, for a quantity of heat stored at 200 kJ with a temperature change of 4°C, the amount of material with a specific heat of say 1 kJ/kg-°C required is about 50 kg. With 25 kg of this material, the temperature change will be 8°C. To achieve high heat transfer rates, the material should have a high thermal conductivity and high specific surface area. Assuming a heat transfer coefficient of 50 W/m^2-K, the specific area required is over 2 m^2/g. A material with these desired properties could be an aluminum mesh.

Assuming that such an accumulator design can be accomplished, vehicle performance analysis was conducted with 25 kg of added aluminum and 50 kg of aluminum.

Results of analysis: The performance and economics of the four accumulator designs--adiabatic, ideal isothermal, and near-isothermal each with 25 kg aluminum and 50 kg aluminum added--are given in Table 39. Notice the increase in vehicle range from

TABLE 39.-COMPARISON OF HYDROPNEUMATIC BUFFER SYSTEMS

Parameter	Adiabatic accumulator, optimum	Isothermal accumulator, optimum	Near-isothermal accumulator, 25 kg added	Near-isothermal accumulator, 50 kg added
Buffer:				
Min. volume, m^3	0.040 (10.6 gal)	0.040 (10.6 gal)	0.040 (10.6 gal)	0.040 (10.6 gal)
Max. volume, m^3	0.054 (14.2 gal)	0.053 (14.0 gal)	0.053 (14.0 gal)	0.053 (14.0 gal)
Min. pressure, MPa	13.8 (1996 psia)	15.6 (2267 psia)	15.6 (2267 psia)	15.6 (2267 psia)
Max. pressure, MPa	20.7 (3000 psia)	20.7 (3000 psia)	20.7 (3000 psia)	20.7 (3000 psia)
Motor pump:				
Displacement, cm^3/rev	65.2 (4.0 in^3/rev)	59.8 (3.6 in^3/rev)	59.8 (3.6 in^3/rev)	59.8 (3.6 in^3/rev)
Vehicle:				
Range, km	97.8 (60.8 mi)	99.3 (61.7 mi)	97.8 (60.8 mi)	96.2 (59.8 mi)
Mass, kg	1423.6 (3138 lb)	1420.5 (3132 lb)	1445.5 (3187 lb)	1470.5 (3242 lb)
Energy, kWh/km	0.1160 (0.1867 kWh/mi)	0.1147 (0.1846 kWh/mi)	0.1161 (0.1868 kWh/mi)	0.1176 (0.1893 kWh/mi)
Battery:				
Avg. discharge rate, W/kg	12.82 (5.82 W/lb)	12.68 (5.75 W/lb)	12.84 (5.82 W/lb)	13.00 (5.90 W/lb)
Battery life, yr at 16 000 km/yr	3.92	3.97	3.91	3.85
Economics:				
Initial cost, $	3154	3098	3190	3227
Life cycle cost, ¢/km	1.97 (3.17 ¢/mi)	1.94 (3.12 ¢/mi)	1.99 (3.21 ¢/mi)	2.02 (3.25 ¢/mi)

adiabatic to isothermal case. Also notice the decrease in the range as more weight is added to the vehicle mass, to make the process near isothermal. The motor/pump displacement for an isothermal accumulator is lower than that of an adiabatic accumulator for about the same energy transferred. This is because the work per unit mole is higher for an isothermal process and hence results in a lower operating pressure ratio as discussed in prior sections.

As shown in Table 39, the vehicle range with a near-isothermal accumulator containing 25 kg of aluminum mesh is the same for a vehicle with an adiabatic accumulator. The range decreases as more material is added to the near-isothermal accumulator (last column in the table). Also, in both the near-isothermal accumulator systems considered, the estimated initial cost and life cycle costs increased. Therefore, it was concluded that an isothermal accumulator should not replace the adiabatic accumulator being considered thus far.

Empirical equation for vehicle range: Using the results of computer runs with different buffer efficiencies and weights, an empirical equation was derived to calculate the vehicle range:

$$\frac{R}{R_1} = (1 - 0.345 \times \eta_B)^{-1.344} \times \left(\frac{M_1}{M} \times \frac{M_B}{M_{B1}}\right)^{1.28} \qquad (69)$$

where

R = range of hybrid vehicle, km

R_1 = range of straight electric vehicle, km

η_B = overall buffer efficiency

$$= \frac{\text{Net energy delivered for vehicle propulsion}}{\text{Total shaft energy charged to the buffer}}$$

M_1 = mass of straight electric vehicle, kg

M = mass of hybrid vehicle, kg

M_B = battery mass in hybrid vehicle, kg

M_{B1} = battery mass in straight vehicle, kg

The equation is valid only for the SAE J227a Schedule D driving cycle. The equation has been tested for validity for battery masses between 350 and 550 kg and vehicle masses between 1300 and 1600 kg.

For the baseline vehicle described in this report (i.e., M_{B1} = 415 kg, M_1 = 1360 kg), the equation for range is

$$R = 353.6\ (1 - 0.345 \times \eta_B)^{-1.344} \times \left|\frac{1}{M} \times M_B\right|^{1.28}$$

Examples:

1) Isothermal accumulator:

a) M_B = 415 kg, M = 1420 kg (see Table 39)

η_B = 0.626 (see Table 38)

From equation, R = 101.6 km
From computer calculations, R = 99.4
} 2.2% error

2) Adiabatic accumulator:

a) M_B = 415 kg, M = 1424 kg (see Table 39)

η_B = 0.579 (calculated)

From equation, R = 98.4 km
From computer calculation, R = 97.9
} 0.5% error

b) η_B = 0.579, M_B = 415 kg, M = 1518 kg (see Table 36)

From equation, R = 90.7
From computer calculation, R = 92.1
} 1.5% error

An interesting example of how this empirical form can be used is shown in Figure 54. It is a plot of range ratio (hydropneumatic buffered vehicle to straight electric) for a 1360-kg (3000-lb) vehicle versus various buffer masses of constant efficiency. This plot shows the effect of replacing batteries from a 1360-kg (3000-lb) vehicle by constant efficiency buffers of various weights. For the 158-kg (348-lb) buffer considered to be near-term state of the art in this report, only a 55.7-km range could be achieved if that buffer were substituted for 158 kg of batteries. The plot shows it would take an 87-kg (192-lb) buffer replacing 87 kg (192-lb) of batteries to achieve the same range as a 1360-kg (3000-lb) straight electric vehicle with 415 kg (915-lb) of batteries. A buffer whose mass is less than 87 kg (192-lb) could increase the range of the 1360 kg (3000-lb) vehicle without increasing its mass.

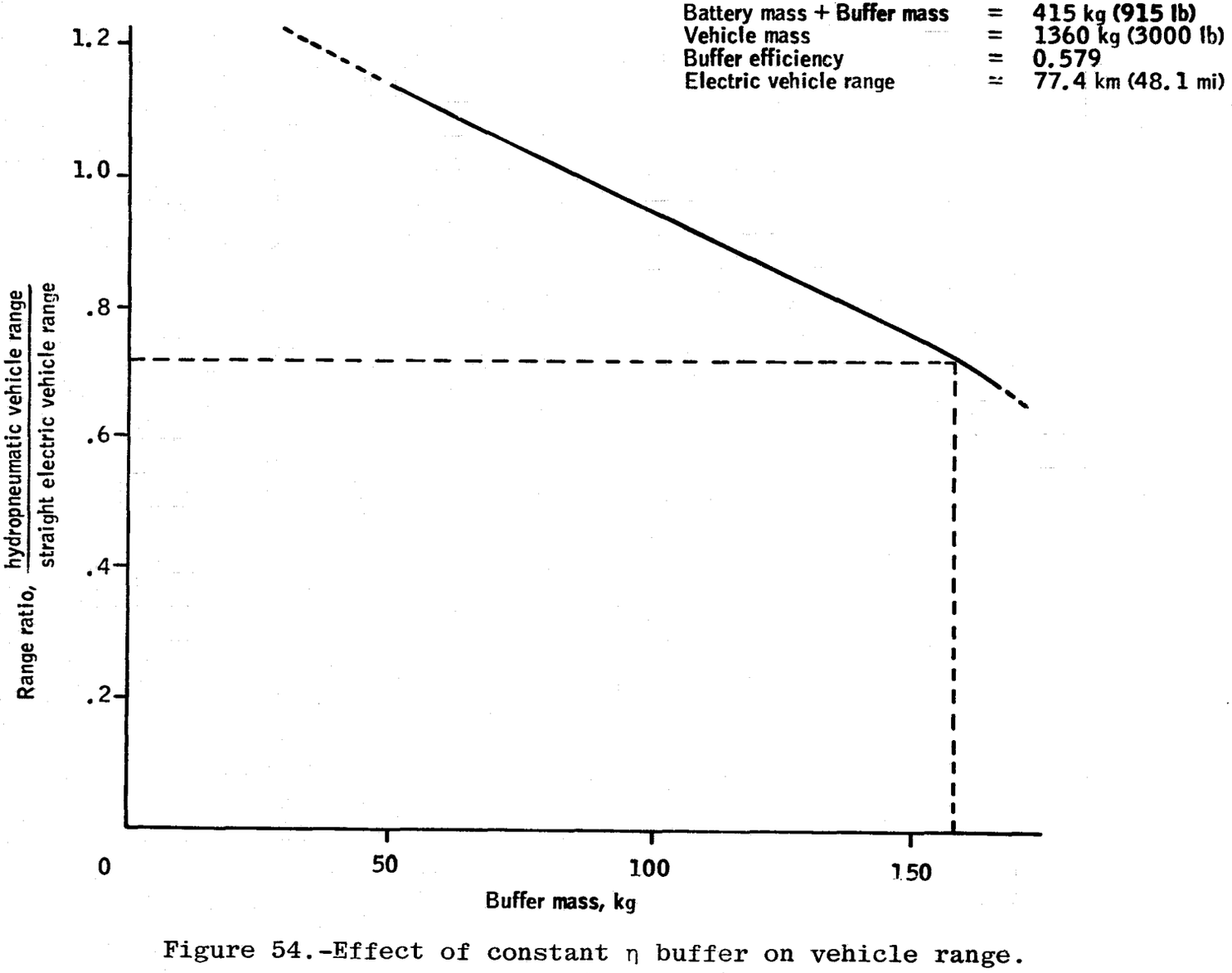

Figure 54.-Effect of constant η buffer on vehicle range.

Vendor surveys.-A survey of pressure vessel and accumulator manufacturers and hydraulic motor and pump manufacturers was conducted.

Pressure vessel and accumulators vendor survey: Letters requesting information were sent to the pressure vessel and accumulator manufacturers. The following characteristics were specified in the request:

- Volume: (0.054 m^3) 14.2 gal
- Maximum pressure: 20.7 MPa (3000 psi)
- Weight: < 45 kg (100 lb)

The manufacturers were asked:

"If you do not manufacture an accumulator with characteristics similar to those required by our design, are there modifications to existing hardware which would be worth investigating?"

Approximately 50% of those queried responded and only two responded positively. Table 40 summarizes their response.

TABLE 40.-SUMMARY OF RESPONSES FROM ACCUMULATOR MANUFACTURERS

Description	Vendor A	Vendor B
Component	Pressure vessel only	Complete accumulator
Material	Kevlar-wrapped aluminum	E-glass or S-glass wrapped aluminum
Volume, in^3	3280, 14.2 gal	3280, 14.2 gal
Weight, lb	≈75	≈100
Schedule	10 months	6 to 9 months
Cost	200 units minimum order with D.O.T. approval 120K nonrecurring, $1200 each	250 units minimum order with D.O.T. approval 75-100K nonrecurring, $550 to 600 without bladder

Motor/pump manufacturers: Letters requesting information were sent to the motor/pump manufacturers. Each manufacturer was specifically asked:

1) Do you manufacture a hydraulic motor/pump which would meet our requirements?

2) If not, are there modifications to existing hardware which could be made to meet our requirements? Cost? Time?

3) How sensitive are suction characteristics in the pumping mode?

4) Is it possible to avoid supercharging?

5) What is the weight of the unit?

6) What is the overall (volumetric and mechanical) efficiency of the motor/pump?

Five of the manufacturers expressed initial interest.

Responses indicated off-the-shelf, axial-piston, in-line hydraulic motor/pumps share a common drawback: poor efficiency at small swashplate angles when the unit is operated as a motor. However, manufacturers tend not to test their units in such a manner and therefore very little data actually exists stating these efficiencies. All five of those listed market variable-type pumps. All with the exception of one market axial-piston, in-line, swashplate-type pumps. Only one markets a bent-axis piston pump. The examples of each type are shown in Figure 55.

All of the five motor/pump manufacturers contacted were reluctant to discuss modifications to existing off-the-shelf hardware or "all-new" design which could meet the energy buffer contract requirements. However, two have released brochures in advance of a new line of motor/pumps to be marketed in 1980. Table 41 compares present off-the-shelf units with the soon-to-be-marketed units from these vendors. The typical motor/pump efficiencies are shown in Figure 56. Overall efficiencies of the Vendor C unit are somewhat lower than those of the Vendor D unit at approximately 30% of full stroke or less, and appears to make Vendor D units the best choice for the buffer system. However, actual efficiency has not yet been received.

The other three companies do not market now, nor have they revealed plans to market in the near future, hydraulic motor/pumps which would meet the energy buffer requirements in terms of weight and efficiency.

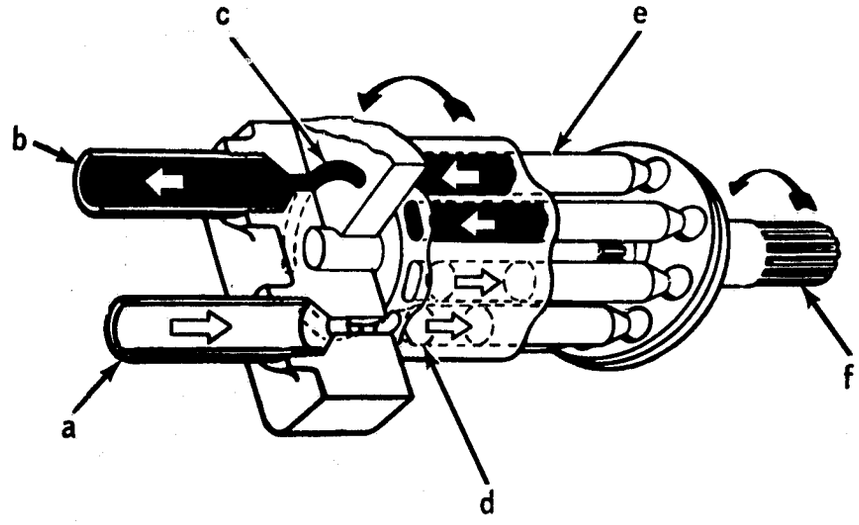

a) Axial-piston motor/pump

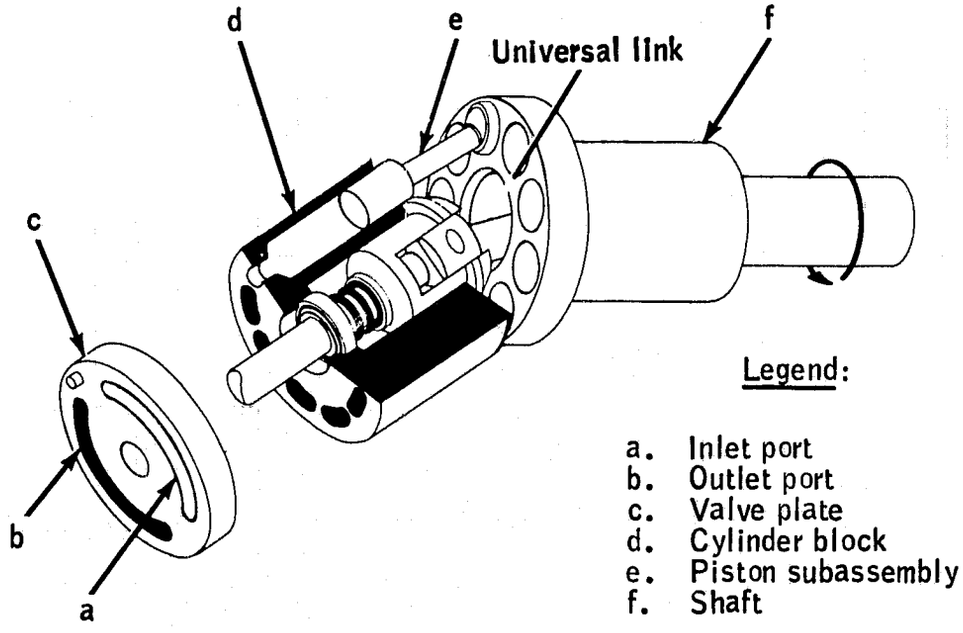

b) Bent-axis piston motor/pump

Figure 55.-Typical bent-axis and axial-piston-type motor/pumps.

TABLE 41.-VENDOR MOTOR/PUMP DATA

Parameter	Vendor C		Vendor D	
	Off the shelf	Near term	Off the shelf	Near term
Displacement, in^3/rev	4.26	4.00	6.72	4.70
Operating pressure, psi	3000	6000	5000	Equivalent or better
Maximum pressure, psi	5000	6000	6000	
Maximum speed, rpm:				
Full stroke	3200	4000	3300	
Partial stroke	3600	5000	5400	
Weight, lb	135	110	120	80 to 90

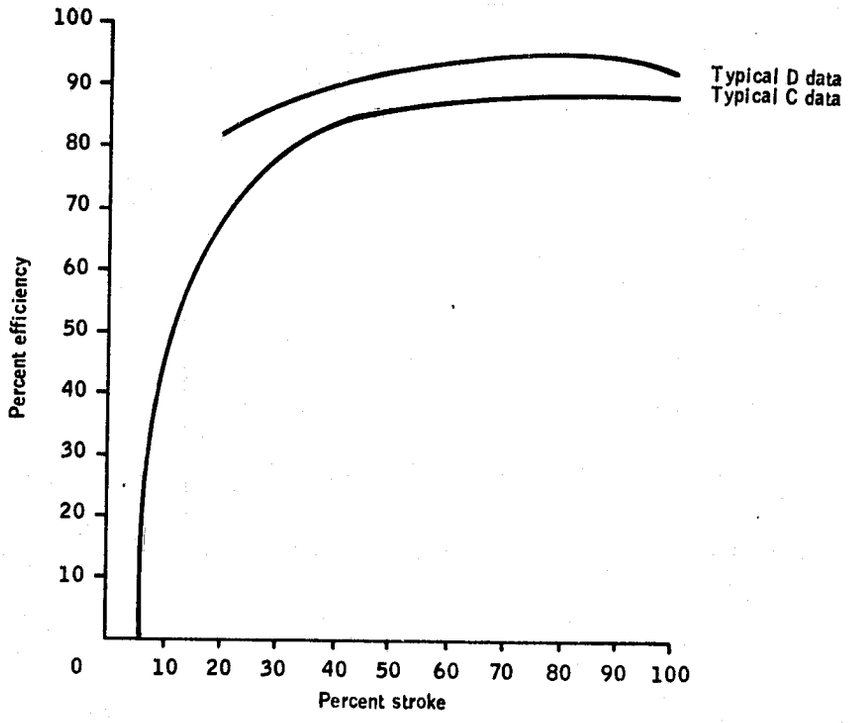

Figure 56.-Typical vendor motor/pump efficiencies as a function of % full stroke.

Table 42 summarizes buffer component weights to be most likely representative of a near-term hydropneumatic buffer described in this report. Buffer weights with both Vendors C and D motor/pumps are listed.

TABLE 42.-NEAR-TERM BUFFER COMPONENT WEIGHTS

Component	Size	Near-term component weight, lb
Motor/pump:		
Vendor C	4.00 (in^3/rev)	110
Vendor D	4.70 (in^3/rev)	90
Accumulator	14.2 gal	100
Fluid	-	35
Pipe and valves	-	55
Clutch and transmission	-	50
Total weight:		
Vendor C	-	350
Vendor D	-	330

CONCLUSIONS

The engineering assessment of energy buffers and subsequent tradeoff analysis showed that a hydropneumatic energy buffer could significantly extend the range and improve the performance of an electric vehicle. The baseline electric vehicle used in the analysis was a 1360 kg (3000 lb) vehicle containing 415 kg (915 lb) of lead/acid batteries exercised repeatedly over the SAE J227a schedule D electric vehicle driving cycle. The following observations were made:

1) A 5% increase in range over the baseline electric vehicle can be achieved using a hydropneumatic buffer with off-the-shelf components, with the buffer sized to store energy and accept power from 88 km/h (55 mi/h) deceleration in accordance with schedule D of the SAE J227a driving cycle.

2) A 19% increase in range over the baseline electric vehicle can be achieved using a hydropneumatic buffer with near-term components, with the buffer sized to accept power from 72 km/h (45 mi/h) and store energy from an 88 km/h (55 mi/h) deceleration (J227a sechedule D).

3) A 23% increase in range over the baseline electric vehicle with near-term buffer components can be obtained when the acceleration time is reduced from 28 s to 15 s due to higher efficiency of the motor/pump at higher swashplate angles.

4) The buffer operation is independent of the driving cycle because the energy state of the buffer is preprogrammed to be a function of the vehicle velocity only.

5) The isothermal process in the accumulator slightly improves the vehicle range over the adiabatic process.

The performance described in statements 2 and 3 can only be met with the use of lightweight, high-performance buffer components (hydraulic accumulator and hydraulic motor/pump). These components were not commercially available at time of writing this report. However, two accumulator vendors indicated that lightweight, fiber-wrapped accumulators could be developed and two motor/pump vendors indicated the near-term introduction of lightweight, higher-performance motor/pumps.

REFERENCES

1. Miller, J., Rasmussen, R.; Hydraulic Accumulators for Hybrid Automobiles and Transport Vehicles, University of California, Lawrence Livermore Laboratory, Report No. 10017 FR Revision A, 2 April 1978.

2. Davis, D.D., Renner, R.A., Younger, F.C., Epps, R.C., Lerner, S.S.: Determination of the Effectiveness and Feasibility of Regenerative Braking Systems on Electric and Other Automobiles. ERDA, UCRL-5230 6/1. September 9, 1977, Volume I, Summary, P. 50.

3. Behrin, E., et al.: Energy Storage Systems for Automobile Propulsion, Vol. 1, Overview and Findings, University of California, Lawrence Livermore Laboratory, Report No. UCRL-52303/1, 15 Dec 1978.

4. Anom.: Proceedings of the Third International Electric Vehicle Symposium, 19-21 Feb 1974. ERDA CONF. NO. 740215, Vols. 1 and 2.

5. Davis, D.D., et al.: Determination of the Effectiveness and Feasibility of Regenerative Braking Systems on Electric and Other Automobiles, Vols. 1 and 2, University of California, Lawrence Livermore Laboratory, Report No. UCRL-52306/1 and 2, 9 Sept 1977. pp 77-104.

6. Toland, R.H.: Current Status of Composite Flywheel Development. LLL, 17 January 1978, UCRL-80604.

7. Anom.: State of the Art of Lead/Acid Vehicle Batteries. Gould Laboratories, 26 August 1977, ANL-K-77-3639-1.

8. Anom.: State-of-the-Art Assessment of Electric and Hybrid Vehicles, CONS/1011-1, NASA TM 73756, Sept 1977, pp 299-324.

9. Anom.: Introduction to the ERDA Electric and Hybrid Vehicle Demonstration Project. ERHQ-0008, 1 March 1977.

10. Anom.: Near-Term Electric Vehicle Program, SAN/1213-1, Phase I, Final Report, August 1977, (AiResearch Mfg. Co.).

11. Anom.: Near-Term Electric Vehicle Program, SAN/1295-1, Phase I, Final Report, August 1977, (ASL Engineering Co.).

12. Anom.: Near-Term Electric Vehicle Program, SAN/1294-1, Phase I, Final Report, August 1977, (General Electric Co.).

13. Articles, A.F.: Vehicle Simulation Program (Rev. 1), Mechanical Technology Inc., Report No. MTI77TR79, Sept 1977.

14. Rowlett, B.H.: Electric-Powered Passenger Vehicle Design Study Program, Task 1 - Tradeoff Studies, AiResearch Mfg. Co., Report No. 76-13133 Rev. 1, 15 April 1977.

This page intentionally left blank.

(See reverse side.)

1. Report No.	2. Government Accession No.	3. Recipient's Catalog No.
NASA CR-159756		

4. Title and Subtitle	5. Report Date
ASSESSMENT AND PRELIMINARY DESIGN OF AN ENERGY BUFFER FOR REGENERATIVE BRAKING IN ELECTRIC VEHICLES	December 1979
	6. Performing Organization Code 5341-01-41658
7. Author(s) Robert Buchholz and Anoop K. Mathur	8. Performing Organization Report No. TSCI0082-FR
	10. Work Unit No.
9. Performing Organization Name and Address Honeywell Inc., Technology Strategy Center Rosedale Towers 1700 W. Highway 36 St. Paul, Minnesota 55113	11. Contract or Grant No. DEN3-48
	13. Type of Report and Period Covered Contractor Report
12. Sponsoring Agency Name and Address U.S. Department of Energy Office of Transportation Programs Washington, D.C. 20545	14. Sponsoring Agency Report No. DOE/NASA/0048-79/1

15. Supplementary Notes

Final Report. Prepared under Interagency Agreement EC-77-31-1044. Project Manager, A.C. Spagnuolo, Transportation Propulsion Division, NASA Research Center, Cleveland, Ohio 44135.

16. Abstract

Energy buffer systems, capable of storing the vehicle kinetic energy during braking and reusing this stored energy during acceleration, were examined. Some of these buffer systems when incorporated in an electric vehicle would result in an improvement in the performance and range under stop-and-go driving conditions. Buffer systems considered included flywheels, hydropneumatic, pneumatic, spring, and regenerative braking. Buffer ranking and rating criteria were established. Buffer systems were rated based on predicted range improvements, consumer acceptance, driveability, safety, reliability and durability, and initial and life-cycle costs. A hydropneumatic buffer system was selected.

An analysis and preliminary design of the hydropneumatic buffer in an electric vehicle with state-of-the-art off-the-shelf components was conducted. The SAE-J227a Schedule D driving cycle was used for the analysis. The analysis with vendor-supplied data showed that with currently available hydraulic accumulator and motor/pump components, only a 5% increase in an electric vehicle range can be expected. However, with modified sizing criteria and with components under development, a 19% increase in range can be expected over a straight electric vehicle without an energy buffer. A control strategy for buffer operation was planned to be independent of the driving cycle. An analysis also showed that the isothermal process in the accumulator results in a slightly better performance over the adiabatic process.

17. Key Words (Suggested by Author(s))	18. Distribution Statement
Electric vehicle Energy buffer Hydropneumatic buffer Regenerative braking Buffered vehicle	Unclassified - Unlimited STAR Category 37 and 85 DOE Category UC-96

19. Security Classif. (of this report)	20. Security Classif. (of this page)	21. No. of Pages	22. Price*
Unclassified	Unclassified	128	

* For sale by the National Technical Information Service, Springfield, Virginia 22151